DOKUZ EYLÜL UNIVERSITY

GRADUATE SCHOOL OF NATURAL AND APPLIED SCIENCES

INVESTIGATION OF THE EFFECTS OF COMBUSTION GASES AND EMISSION CHARACTERISTICS ON THERMAL PERFORMANCE

by

Semih YILMAZ

September, 2023

İZMİR

INVESTIGATION OF THE EFFECTS OF COMBUSTION GASES AND EMISSION CHARACTERISTICS ON THERMAL PERFORMANCE

A Thesis Submitted to the
Graduate School of Natural and Applied Sciences of Dokuz Eylül University
In Partial Fulfillment of the Requirements for the Degree of Doctor of Philosophy in Mechanical Engineering, Energy Program

by
Semih YILMAZ

September, 2023
İZMİR

Ph.D. THESIS EXAMINATION RESULT FORM

We have read the thesis entitled **"INVESTIGATION OF THE EFFECTS OF COMBUSTION GASES AND EMISSION CHARACTERISTICS ON THERMAL PERFORMANCE"** completed by **SEMİH YILMAZ** under supervision of **PROF.DR. DİLEK KUMLUTAŞ** and we certify that in our opinion it is fully adequate, in scope and in quality, as a thesis for the degree of Doctor of Philosophy.

Prof. Dr. Dilek KUMLUTAŞ

Supervisor

Prof. Dr. Yalçın ÇEBİ

Thesis Committee Member

Asst. Prof. Dr. Özay AKDEMİR

Thesis Committee Member

Assoc. Prof. Dr. M. Turhan ÇOBAN

Examining Committee Member

Prof. Dr. Aydoğan ÖZDAMAR

Examining Committee Member

Prof. Dr. Okan FISTIKOĞLU

Director

Graduate School of Natural and Applied Sciences

ACKNOWLEDGMENT

I would like to thank Prof. Dr. Dilek KUMLUTAŞ, my very valuable doctoral thesis supervisor and project executive, who provided all kinds of support in this thesis study and always showed the right path in my academic life, studies and work.

This thesis was supported by The Scientific and Technological Research Council of Turkey (TUBİTAK) and Demirdöküm Heating Company with the 5180092 encoded 1505 project. I would like to emphasize my appreciation for being a part of this effort on the project.

I want to convey my appreciation to my project team colleagues Dr. Özgün ÖZER, M.Sc. Utku Alp YÜCEKAYA, M.Sc. Ahmet Yakup CUMBUL and M.Sc. Hasan AVCI who have always supported me.

Also, I would like to express and show my gratitude to Assoc. Prof. Dr. M. Turhan ÇOBAN, Prof. Dr. Yalçın ÇEBİ and Asst. Prof. Dr. Özay AKDEMİR for their support while my research. I am grateful to my colleagues Dr. Kerim Deniz KAYA and Dr. Kubilay BAYRAMOĞLU for their unwavering support.

I offer my endless gratitude to my life partner Dr. Ece Sökmen YILMAZ, who has always been with me and supported me with endless love and patience. Special thanks to my father Recep YILMAZ, my mother Adile YILMAZ, my sister Sema YILMAZ and my whole family who never forgave their support from me and they made me come to this day.

Semih YILMAZ

INVESTIGATION OF THE EFFECTS OF COMBUSTION GASES AND EMISSION CHARACTERISTICS ON THERMAL PERFORMANCE

ABSTRACT

This doctoral thesis addresses the use of combustion models to investigate combustion and flow characteristics with theoretical and numerical methods. The main objective of the thesis is to investigate the effects of combustion flue gases and emission characteristics on thermal performance in a condensing boiler. Numerical codes have been developed on the basis of Gibbs energy minimization and equilibrium constant approaches. Theoretical investigations were implemented to obtain adiabatic flame temperatures and emissions with different equivalence ratios. CO and NO emissions reach peak values near ϕ = 0.9 and ϕ = 0.85, respectively. The model variations are obtained considerably below 1% in the range of ϕ= 0.6 - 0.9. Computational fluid dynamics (CFD) analyses were accomplished with Species transport (ST). The premixed gas inlet conditions effects on combustion and flow characteristics were examined parametrically. Variations of velocity and temperature along the combustion domain and CO and NO emissions were obtained. Variations in premixed gas inlet velocity directly affect the mean flue gas temperature and residence times, CO and NO emissions. The velocity profile is effective for flame and emissions. In terms of emissions, a substantial escalation occurs in outlet CO emissions with the increase in gas velocity. A rise in NO emissions was observed with the increase in average temperatures, and a decrease in NO emissions was observed with reducing residence time. The findings of this thesis suggest that the proposed methods can be used in design improvements and in reducing pollutant emissions by predicting flow and combustion characteristics.

Keywords: Combustion characteristics, computational fluid dynamics (CFD), premixed combustion, emission and flow, condensing boiler

YANMA GAZLARI VE EMİSYON KARAKTERİSTİKLERİNİN ISIL PERFORMANS ÜZERİNE ETKİLERİNİN İNCELENMESİ

ÖZ

Bu doktora tezi, emisyonlar ve alev sıcaklıkları gibi yanma ile ilgili parametreleri teorik ve sayısal yöntemlerle araştırmak için farklı yanma modellerinin kullanımını ele almaktadır. Tezin temel amacı, yoğuşmalı bir kazan ünitesinde yanma baca gazlarının ve emisyon özelliklerinin ısıl performans üzerindeki etkilerini incelemektir. Gibbs enerji minimizasyonu ve denge sabiti yöntemlerine dayalı olarak sayısal kodlar geliştirilmiştir. Adyabatik alev sıcaklıkları ve farklı eşdeğerlik oranlarındaki emisyonların elde edilmesi için teorik araştırmalar yapılmıştır. CO ve NO_x emisyonları sırasıyla $\phi = 0.9$ ve $\phi = 0.85$ değerleri civarında en yüksek değerlere ulaşmaktadır. $\phi = 0.6 – 0.9$ aralığında, modelde oluşan sapmalar %1'in oldukça altında olacak şekilde gerçekleşmiştir. Türlerin taşınımı (ST) yaklaşımı ile sayısal yanma bölgesi için HAD analizleri gerçekleştirilmiştir. Giriş hızı ve sıcaklığın akış ve yanma karakteristikleri üzerindeki etkileri parametrik olarak incelenmiştir. Yanma bölgesi boyunca hız ve sıcaklık değişimleri, çıkış bölgesinde ise CO ve NO emisyonları elde edilmiştir. Önkarışımlı gaz giriş hızındaki değişiklikler, baca gazlarının yanma odasında kalma süresini, ortalama sıcaklığını, CO ve NO emisyonlarını etkilediği görülmüştür. Hız profili alev ve emisyonlar için etkilidir. Emisyonlar açısından, gaz hızındaki artışla birlikte çıkış CO emisyonlarında önemli bir artış meydana gelmiştir. Ortalama sıcaklıklardaki artışla birlikte NO emisyonlarında artış gözlenmiştir. Baca gazlarının kalış süresinin kısalması ile NO emisyonları azalmıştır. Bu tezin bulguları, önerilen yöntemlerin akış ve yanma özelliklerini tahmin ederek tasarım iyileştirmelerinde ve kirletici emisyonları azaltmada kullanılabileceğini göstermektedir.

Anahtar kelimeler: Yanma karakteristikleri, hesaplamalı akışkanlar dinamiği (HAD), önkarışımlı yanma, emisyon ve akış, yoğuşmalı kazan

CONTENTS

Page

Ph.D. THESIS EXAMINATION RESULT FORM ii
ACKNOWLEDGMENT iii
ABSTRACT iiv
ÖZ ixv
LIST OF FIGURES ix
LIST OF TABLES xiii
LIST OF SYMBOLS xiv
ABBREVIATIONS xvii

CHAPTER - ONE INTRODUCTION 1

1.1 Literature Review 3
1.1.1 Literature Search on Condensing Boilers, Burners, Combustion and Emission Characteristics 3
1.1.2 Literature Search on Theoretical Combustion 13
1.2 Aim and Motivation 18

CHAPTER TWO - COMBUSTION IN CYLINDRICAL COMBUSTION REGION ON BOILERS 20

2.1 Development of Residential Boilers 20
2.1.1 Brief History 20
2.2 Boiler Characteristics 22
2.3 Burner Characteristics 25
2.3.1 Burner Types 25
2.3.2 Characteristics of Stability, Emission and Performance 31
2.3.3 Operating Parameters of the Burner 33
2.4 Standards and Regulations 34
2.5 Combustion in Condensing Boilers 37
2.5.1 Non-premixed (Diffusion) Flames 40
2.5.2 Premixed Flames 42
2.5.3 Physical Processes of Premixed Flames 44

2.5.4 Laminar Premixed Flames 45
2.5.5 Combustion with Premixed Flames in Condensing Boiler 48

CHAPTER THREE - THEORETICAL INVESTIGATION OF COMBUSTION IN CYLINDRICAL COMBUSTION REGION 51

3.1. Methodology 51
3.1.1 Gibbs Energy Minimization Method 53
3.1.2 Equilibrium Constants Method 59
3.1.3 Element Potential Method 70

3.2. Theoretical Investigation Parameters of the Study 71

3.3. Theoretical Investigation Results 72
3.3.1 The Variation of Adiabatic Flame Temperature with respect to Equivalence Ratio for G20, G25, and NG fuels 73
3.3.2 The Variation of Gaseous Emissions with respect to Equivalence Ratio for G20, G25, and NG fuels 75
3.3.3 Comparison and Reliability of Proposed Models 82

CHAPTER FOUR - NUMERICAL INVESTIGATION OF COMBUSTION IN CYLINDRICAL COMBUSTION REGION 85

4.1 Reacting Flow Modelling in Combustion Simulations 86
4.1.1 Generalized Three-Dimensional Navier-Stokes Equations for Reacting Flow Simulations 87
4.1.2 Reaction Mechanisms 89
4.1.2.1 Detailed Mechanisms 89
4.1.2.2 Reduction Mechanisms 90
4.1.3 Reacting Flow Models in CFD 91
4.1.3.1 Reacting Flow Models in Commercial CFD 91
4.1.3.2 Flamelet Model Approach and Flamelet Generation 93
4.1.3.3 Probability Density Function Approach 94

4.2 Modelling of Combustion Domain and Governing Equations of Numerical Study 96
4.2.1 Modelling with Species Transport (ST) and Finite-Rate Chemistry 96

4.2.1.1 Finite-Rate Kinetics without Turbulence-Chemistry Interaction (no TCI) 98

4.2.1.2 The Eddy-Dissipation Model 100

4.2.1.3 The Eddy-Dissipation-Concept (EDC) Model 101

4.2.1.4 The Relaxation to Chemical Equilibrium Model 102

4.3 Numerical Investigation Parameters of the Study 102

4.3.1 Combustion System Overview 102

4.3.2 Numerical Modelling of the Combustion Domain with Premixed Burner 104

4.3.3 Boundary Conditions and Simulation Setup 106

4.3.4 Mesh Generation 114

4.3.5 Mesh Independency 115

4.4 Validation of CFD Model with Numerical Results of the Study 118

4.5 Results 119

4.5.1 Effects of Premix Inlet Velocity and Temperature on the Velocity Distribution and Flow Characteristics along the Combustion Domain .120

4.5.2 Effects of Premix Inlet Velocity and Temperature on the Temperature Distribution along the Combustion Domain 123

4.5.3 Effects of Premix Inlet Velocity and Temperature on CO and NO Emissions along the Combustion Domain 131

CHAPTER FIVE - CONCLUSIONS 134

REFERENCES 138

LIST OF FIGURES

Page

Figure 2.1 Fundamental condensing boiler designs 23
Figure 2.2 Schematics of a) condensing regular and b) combination boilers 24
Figure 2.3 Types of gas burners 26
Figure 2.4 Power burner 27
Figure 2.5 A basic co-flow burner flame configuration 28
Figure 2.6 Flow field of a can type swirl combustor 28
Figure 2.7 A domestic burner in partially premixed mode 29
Figure 2.8 A cylindrical premixed burner with holes 29
Figure 2.9 Alterations of turndown ratio (TDR), the blowoff and flashback with respect to retention hole diameter 30
Figure 2.10 Alteration of heat load and equivalence ratio (ϕ) with suitable combustion range 31
Figure 2.11 Burner stable operation ranges depending on power input rate and first aeration 32
Figure 2.12 Diagram of a fan driven combustion system 33
Figure 2.13 Flame types from diffusion to premixed flame 38
Figure 2.14 Schematic of the Bunsen flame 40
Figure 2.15 Diffusion flame mechanism 41
Figure 2.16 A typical candle flame and associated physical processes 41
Figure 2.17 A non-premixed flame with a particular elevation with species alterations in jet fuel tube 42
Figure 2.18 The distribution of temperature a) non-premixed numerically calculated flame and laminar flames of b) ethylene, c) P-8 fuel, d) CH4 (methane) in the air 42
Figure 2.19 Premixed flame applications: a) Residential boiler, b) industrial low NOx combustor, c) residential lean premixed condensing boiler 43
Figure 2.20 Premixed flame mechanism 43
Figure 2.21 Schematic of a premixed flame flows through in a duct 44

Figure 2.22 a) Bunsen burner, b) normal and tangential component of unburned gas velocity 45
Figure 2.23 Schematic of an advanced residential cooktop burner 46
Figure 2.24 Schematic of a domestic cooktop burner 46
Figure 2.25 Cylindrical lean premixed burner with baffle plates 46
Figure 2.26 Stoichiometric methane-air flame mechanism at standard conditions 47
Figure 2.27 Cross sectional view of a cylindrical heating unit 49
Figure 2.28 a) Cylindrical perforated premixed burner and b) visual of the flame 49
Figure 3.1 Algorithm flowchart of Model 1 58
Figure 3.2 Algorithm flowchart of Model 2 69
Figure 3.3 Adiabatic flame temperature and equivalence ratio changes for G20, G25, and NG fuels 74
Figure 3.4 Mole fraction of CO with respect to equivalence ratio for G20, G25, and NG fuels 76
Figure 3.5 Mole fraction of NO with respect to equivalence ratio for G20, G25, and NG fuels 77
Figure 3.6 Mole fraction of N_2 with respect to equivalence ratio for G20, G25, and NG fuels 78
Figure 3.7 Mole fraction of O_2 with respect to equivalence ratio for G20, G25, and NG fuels 79
Figure 3.8 Mole fraction of CO_2 with respect to equivalence ratio for G20, G25, and NG fuels 80
Figure 3.9 Mole fraction of H_2O with respect to equivalence ratio for G20, G25, and NG fuels 81
Figure 4.1 Methane-air flame jet temperature contours on square ribbed plate 87
Figure 4.2 Turbulent flame modelling with CFD modelling 89
Figure 4.3 Main physical parameters in CFD modelling of combustion 92
Figure 4.4 Additional physics in CFD modelling of combustion 92
Figure 4.5 Chemistry parameters with respect to flow configuration in CFD modelling 93
Figure 4.6 Basic schematic of the laminar flamelet 94
Figure 4.7 Flame reaction progress and flame structure 94

Figure 4.8 Probability density function change in a jet flow 96
Figure 4.9 Schematic of a commercial condensing boiler 103
Figure 4.10 View of the burner as solid model: a) isometric and b) cross-sectional 104
Figure 4.11 a) Isometric view of the 2D combustion domain and b) sliced 60º sector 105
Figure 4.12 Two dimensional combustion region 106
Figure 4.13 Single hole combustion zone calculation area from the literature 107
Figure 4.14 Location of the double hole and 2D symmetrical combustion domain 107
Figure 4.15 Boundary conditions of the combustion domain 112
Figure 4.16 Dimensionless locations of data acquisition lines along the combustion domain.....113
Figure 4.17 The mesh structure: a) premixed gas inlet b) helical coil walls c) burnt gas outlet 114
Figure 4.18 Variation of the average velocity along the combustion domain for five different mesh cases.....117
Figure 4.19 Location of flue gas outlet planes in the combustion domain 118
Figure 4.20 Variation of the temperature along the combustion domain comparing current study with literature experimental study.....119
Figure 4.21 Velocity distributions at 500 K premixed gas inlet temperature for a) V_{in} = 0.5 m/s, b) V_{in} = 1.0 m/s, c) V_{in} = 1.5 m/s and d) V_{in} = 2.0 m/s premixed gas inlet velocities around the burner holes and surface.....121
Figure 4.22 Velocity distributions at 0.5 m/s premix gas inlet velocity for a) T_{in} = 300 K, b) T_{in} = 400 K and c) T_{in} = 500 K premix gas inlet temperatures around the burner surface 122
Figure 4.23 Variation of average velocities throughout the numerical domain for premixed gas inlet velocities of a) V_{in} = 0.5 m/s, b) V_{in} = 1.0 m/s, c) V_{in} = 1.5 m/s and d) V_{in} = 2.0 m/s 122
Figure 4.24 Temperature distributions at premixed gas inlet velocities a) V_{in} = 0.5 m/s, b) V_{in} = 1.0 m/s, c) V_{in} = 1.5 m/s and d) V_{in} = 2.0 m/s at 500K premixed gas inlet temperature around the burner surface 124

Figure 4.25 Variation of temperature throughout the numerical domain at 500 K premixed gas inlet temperature for premixed gas inlet velocities a) V_{in} = 0.5 m/s, b) V_{in} = 1.0 m/s, c) V_{in} = 1.5 m/s and d) V_{in} = 2.0 m/s.....125
Figure 4.26 Temperature distributions with velocity vectors at 500 K premixed gas inlet temperature for premixed gas inlet velocities a) V_{in} = 0.5 m/s, b) V_{in} = 1.0 m/s, c) V_{in} = 1.5 m/s and d) V_{in} = 2.0 m/s.....126
Figure 4.27 Temperature distributions at a) T_{in} = 300 K, b) T_{in} = 400 K and c) T_{in} = 500 K premix gas inlet temperatures for premixed gas inlet velocity of 0.5 m/s around the burner surface 128
Figure 4.28 Variation of temperature throughout the numerical domain at a) T_{in} = 300 K, b) T_{in} = 400 K and c) T_{in} = 500 K premix gas inlet temperatures for premixed gas inlet velocity of 0.5 m/s.....129
Figure 4.29 Temperature distributions with velocity vectors at a) T_{in} = 300 K, b) T_{in} = 400 K and c) T_{in} = 500 K premix gas inlet temperatures for premix gas inlet velocity of 0.5 m/s around the coils of the heat exchanger.....130
Figure 4.30 Calculated CO emissions versus premixed gas inlet velocities for 400 K and 500 K premixed gas inlet temperatures.....132
Figure 4.31 Calculated NO emissions versus premixed gas inlet velocities for 400 K and 500 K premixed gas inlet temperatures.....133

LIST OF TABLES

Page

Table 3.1 Curve fitting coefficients of equilibrium constants (K_i) 67
Table 3.2 Compositions of the standard gases G20, G25 and NG 72
Table 3.3 Mole fraction deviations of equilibrium products and adiabatic flame temperatures for G20, G25, and NG fuels (ϕ=0.65) 82
Table 3.4 Mole fraction deviations of equilibrium products and adiabatic flame temperatures for G20, G25, and NG fuels (ϕ = 0.7).....83
Table 3.5 Mole fraction deviations of equilibrium products and adiabatic flame temperatures for G20, G25, and NG fuels (ϕ = 0.75) 84
Table 4.1 Numerical setup parameters of the combustion domain 108
Table 4.2 Boundary condition parameters of the analyses.....113
Table 4.3 Mesh independency with average velocity on data acquisition lines.....117

LIST OF SYMBOLS

A	: Number of atoms in element species
A_m	: Model constant
A_r	: Pre-exponential factor
a_s	: Stoichiometric molar air-fuel ratio
b_i	: Number of atoms i^{th} element at the combustion products
$\bar{c}$	: Mean reaction progress variable
$C_{j,r}$	: Species molar concentration j^{th} species in reaction (kmol m^{-3})
C_p	: Heat capacity (kJ $kmol^{-1}$ K^{-1})
D	: Coefficient of the diffusion
E_S	: Calculated emission at the percentage standard oxygen conct.
E_r	: Reaction activation energy of the system (J $kmol^{-1}$)
E_M	: Measured emission concentration at premix gas outlet
f	: Mixture fraction of the gases
$\bar{f}$	: Mean mixture fraction of the gases
$\bar{f}'^2$	: The variance of mean gas mixture
F_ϕ	: Distribution function
G	: Gibbs energy (kJ)
$\bar{g}$	: Gibbs energy per mole (kJ $kmol^{-1}$)
$\vec{g}$	: Constant of the gravity, 9.81 (m s^{-2})
$\bar{G}$	: Mean flame position
H	: Total enthalpy (kJ)
H_{comb}	: Heat of the combustion per fuel (J kg^{-1})
K_P	: Equilibrium constant
k	: Kinetic energy of the turbulence (J kg^{-1})
k_t	: Coefficient of the thermal conductivity (W m^{-1} K^{-1})
$k_{f,r}$	: Constant of forward reaction rate

$k_{b,r}$: Constant of backward reaction rate

l_t : Turbulent length scale (m)

M_w : Molecular weight (g mol^{-1})

N : Number of total species in the combustion

n : Number of gaseous combustion species

ne : Number of elements

ng : Number of gaseous species

n_j : Rate exponent for species

O_S : Standard oxygen concentration

O_M : Measured oxygen concentration.

P : Pressure (kPa)

P_i : Partial pressure (kPa)

$\overline{\overline{p}}$: Pressure tensor (kPa)

P_ϕ : Probability density function

$\bar{q}$: Mean of the properties

q_r : Radiation source

R_i : Net rate of products

$\hat{R}_i$: Total reaction source

R_u : Universal gas constant, 8.3146 (kJ $kmol^{-1}K^{-1}$)

S : Total entropy (kJ K^{-1})

S_c : Reaction progress source (s^{-1})

$S_{c,t}$: Turbulent Schmidt number

S_i : External source

T : Temperature (K)

$T_{in/inlet}$: Inlet temperature (K)

T_{ad} : Adiabatic flame temperature (K)

u : One dimensional velocity component (m s^{-1})

V : Total volume (m^3)

y : Species mole fraction

$\tilde{Y}_k$: Density-weighted average mass fraction of the species

Y_i : Local mass fraction of the species

α : Unburnt thermal diffusivity ($m^2\ s^{-1}$)

β_r : Temperature exponent

γ_f : Fine scale fraction of the flow

Γ : Net contribution of third bodies on the reaction rate

ε : Dissipation rate of turbulence ($J\ kg^{-1}\ s^{-1}$)

ε_p : Proportionality constant

ε_t : Convergence tolerance

ξ : Mixture fraction

λ : Lagrangian multiplier

ν : Kinematic viscosity ($m^2\ s^{-1}$)

ν_A : Stoichiometric parameter

μ : Dynamic viscosity ($kg\ m^{-1}\ s^{-1}$)

μ_i : Chemical potential ($kJ\ kmol^{-1}$)

μ_t : Turbulent dynamic viscosity of the species ($kg\ m^{-1}\ s^{-1}$)

ρ : Density of the species ($kg\ m^{-3}$)

τ : Time scale

τ_{char} : Characteristic time scale

τ_{turb} : Turbulent time scale

τ_{chem} : Chemical time scale

υ : Flow velocity ($m\ s^{-1}$)

υ_l : Laminar flame velocity ($m\ s^{-1}$)

$\vec{j}_i$: Diffusion flux

ω : Molar rate of formation

$\tilde{\phi}$: Density weighted average of a scalar quantity

ϕ : Equivalence ratio (fuel/air)

ABBREVIATIONS

EEA	: European Environmental Agency
EU	: European Union
CEN	: European Committee for Standardization
GMS	: Gas Mixing System
FPV	: Flamelet Progress Variable
CFD	: Computational Fluid Dynamics
DNS	: Direct Numerical Simulation
LPG	: Liquid Petroleum Gas
G20	: Pure Methane Gas
G25	: Test Gas
NG	: Natural Gas
EST	: Energy Saving Trust
TDR	: Turn-down Ratio
EC	: European Commission
HVAC	: Heating, Ventilation and Air Conditioning
CE	: European Conformity
ERP	: Energy Related Products
NASA	: National Aeronautics and Space Administration of USA
JANAF	: Joint Army, Navy, Air Force Publication of USA
DO	: Discrete Ordinates
PDF	: Probability Density Function
ED	: Eddy Dissipation
EDC	: Eddy Dissipation Concept
ISAT	: In Situ Adaptive Tabulation
RMS	: Root Mean Square
ST	: Species Transport

CHAPTER ONE
INTRODUCTION

Combustion and its environmental effects are existed consistently in our lives. Combustion of fuels containing hydrocarbons creates dangerous gaseous emissions. This condition brings public health and environmental concerns. Carbon dioxide (CO_2) and water (H_2O) emissions cause greenhouse effects and local smoke. Apart from these, particulate matter (PM), carbon monoxide (CO), nitric oxides (NO_x), hydrocarbons of the combustion in unburned state (HC), oxides of sulfur (SO_x) and formations are also observed. These environmental pollutants directly affect the health of humans and other living things. Therewithal, SO_x and NO_x emissions also cause acid rain (McAllister, 2011).

Combustion is an ultimate energy conversion source for power production, industrial production, heating, ventilation, air conditioning (HVAC), transportation, etc. Besides that, it also causes explosions, building and wildland fires. Besides that, it damages human health through contamination of water and air. Massive use of fossil fuels with combustion alters global ecological balance by way of global warming and contamination (McAllister, 2011).

Chemistry, thermodynamics, heat transfer and also fluid mechanics are all involved in the combustion study, which is a multidisciplinary field. Thus, explanation of the combustion is crucial with the usage of well-balanced interaction between various basic sciences (McAllister, 2011). One of the most crucial problems in engineering applications is combustion processes that involves in turbulent flow, heat transfer, chemical reactions, and complex chemical and physical reactions. Basic engineering implementations on combustion include engines, combustion in production of power with gas turbine, condensers, heating devices, etc. Therefore, it is extremely crucial to estimate the flow, temperature, emissions, and other generated combustion products for various combustion systems. To determine these parameters, numerical modelling approach with finite elements are needed. Modeling combustion is becoming an increasingly prevalent application of computational fluid dynamics (CFD). Additional models for radiative heat transfer, which is another crucial sub-process, as well as

fundamental transport equations for fluid flow and heat transfer, drive the combustion chemistry in combustion processes. Combustion should be treated as a complex subject because of all these basic equations and operations. Therefore, combustion modeling requires a great deal of knowledge and experience that requires years of effort. In combustion modeling, flow, heat transfer including radiation, chemical reaction mechanisms are discussed. Simultaneous modeling of all these components emerges as a significant challenge. The management of all these components depends on the preparation of information, infrastructure, and time planning. In addition to know-how, there is a need to establish a good computer infrastructure and manage it according to time. (Glassmann & Yetter, 2008; Malalasekera & Versteeg, 2007; Warnatz et al., 2006).

Today, the specified combustion systems are utilized in many different industrial and domestic processes. Thus, residential boilers are involved in providing domestic heating and hot water. These boilers generally burn fossil fuels such as natural gas. Therefore, they emit flue gases containing NO_x, CO and CO_2 that are created by natural gas combustion and contribute to global warming and acid rains (Hinrichs et al., 2018). The European Environmental Agency (EEA) report declares that domestic boilers working with natural gas in European countries contribute high amounts of NO_x and CO emissions. Therefore, in order to reduce these effects, European Union (EU) standards such as gas-fired heating boilers standard (EN 15502-1+A1:2015) and Test gases, test pressures and categories of appliances standard (EN 437:2018) have been put into effect by European Committee for Standardization (CEN) (European Committee for Standardization, 2018). Besides, increasing the combustion efficiency in boilers and burners in combustion systems is directly related to the boiler structure, burner geometry and homogeneity of the gaseous fuel-air mixture. Therefore, it is crucial to investigate the combustion parameters and effects that emerges these emissions (Yılmaz et al., 2021).

In the studies carried out in recent years; theoretical calculations, numerical analysis such as CFD and experimental studies used to verify these studies are frequently preferred. These methods, which are mentioned especially in the simulation of chemical reactions taking place in the combustion chamber, are used by researchers.

In the following parts of this chapter, developments on the literature, aim and motivation are discussed.

1.1 Literature Review

1.1.1 Literature Search on Condensing Boilers, Burners, Combustion and Emission Characteristics

Various studies were accomplished concerning condensing boilers, boiler design parameters, gaseous combustion, flow and emission characteristics.

In the thesis study, Naslund (1997) modelled a residential boiler and design parameter research were conducted. Heat load and heating system effects on the performance were evaluated including combustion and emission characteristics. Flue gases were investigated containing burner parameters, steady-state performance, effects of changes in fuel input, boiler performance with a flat burner (Naslund, 1997).

For a condensing gas boiler, Lee et al. (2011) experimentally examined a cylindrical multi-hole premixed burner, which emits fewer NO_x emissions and give better performance. Diameter and arrangement of the holes in a multi-hole, flat and cylindrical shape burner were investigated. Equivalence ratio (ER) and turn-down ratio were calculated for the cylindrical burner. CO emissions were found to be less than 30 ppm and NO_x emissions were obtained less than 40 ppm (Lee et al., 2011).

In order to present the recoverable heat and the efficiency improvement potential of various heat recovery schemes at various outlet flue gas temperatures, Che et al. (2004) used combustion and heat transfer calculations to convert a conventional natural gas fired boiler into a condensing boiler (Che et al., 2004).

Baldi et al. (2017) proposed dynamic energy efficiency monitoring of a condensing boiler. Condensing and non-condensing modes were investigated for mass flow rate estimation. Boiler efficiency are studied with respect to return water temperature (Baldi et al., 2017).

Satyavada and Baldi (2018) obtained efficiency curves are in nominal operating conditions on condensing boiler. Same researchers are also proposed a novel

observation method in their study. In order to change condensing and non-condensing ratios dynamically, their approach is based on a hybrid model. They measured boiler effectiveness and compared with their proposed model under various excess air conditions including inlet water temperature (Satyavada & Baldi, 2018).

Bălănescu and Homutescu were investigated a premixed type condensing boiler system that contains fan to blow air, valve, gas-air mixer, and perforated premixed cylindrical burner. Experimental boiler has 36 kW nominal heat output. Boiler heat output with respect to air blower speed were investigated for various speed ranges. NO_x emissions were examined in response to nominal heat outputs of the boiler (Bălănescu & Homutescu, 2018).

Mohr et al. (2018) were presented ignition phenomena of the premixed combustion inside the combustion region of the condensing boiler. A transient analysis was accomplished with a burning velocity model to understand ignition process and flame stability. Experimental results are utilized for the validation of numerical results. Methane was chosen as fuel and air was selected as an oxidizer. It was found that alterations in the boundary conditions have an impact on the first ignition with regard to the power, combustion chamber pressure, and equivalence ratio relationships. The impact of ignition timing was observed on stability of the flame (Mohr et al., 2018).

De Vries and Levinsky (2020) introduced a novel concept in the formulations of appliance standards in the scope of gas ignition velocity. Domestic appliances need to be designed considering the risk of flashback. The safety margin burning velocity is determined for flashback limit gases. According to standards and approvals, gas quality is assessed in this investigation. Instead of Wobbe index, laminar burning velocity is suggested for the effect of fuel/air ratio on burning velocities for rich and lean fuel situations are examined for group H natural gases. (de Vries & Levinsky, 2020).

Simic et al. (2021) is proposed a novel concept of modelling to predict stability of the performance parameters for domestic heating device such as condensing boilers. Numerical simulations are implemented on a condensing boiler device with a coherent thermodynamic approach. Outwardly accessible data and standard measurement sites

are employed for the results' validation. Calibration is applied with these public data. The experimental reports of the investigation include information on condensate flow rate and exhaust gas temperature. Various parameters of the heating boiler device are investigated from the available data that are found on eco-design requirements, EN15502-1+A1:2015 standard (European Committee for Standardization, 2015) and some manufacturers (Simic et al., 2021).

Li et al. (2006) investigated thermal effectiveness and CO emissions of cooking device with the burners with this study. Raising the thermal performance and reducing pollution of the closed areas are important factors for industry and environmental requirements. Authors had been applied advanced statistical experimental designs to calculate effects of the main cooker-top subjects of the design. The experimental analyses was implemented a design method for premixed gas-fired impinging-flame. Major design subjects of the burner are Reynolds number of the flow, fuel/air mixture ratio, gap of the plate and nozzle and jet flame gap. Water loading test was used as heat-absorption system for heat transfer calculation. Additionally, CO emissions from household gas appliances were measured in accordance with Chinese National Standard (GB 16410) (Li, Wong, Leung, & Probert, 2006).

Hou et al. (2007) investigated a novel type of household burner that works with eddy flames. Five major characteristics, including flow with eddies, flame height, first aeration, gas parameters such as flow rate and pressure, combustion flame, were evaluated by the authors for their effects on the thermal load effectiveness and CO emissions of gaseous burners in the household device (Hou et al., 2007).

Gattei (2008) established an experimental setup for methane-air mixture on domestic cookers for a PhD thesis. Chemical illumination with OH- radical imaging and flame conditions were observed for different gas mixture ratios. Flame stability and properties have been studied. Numerical investigation was implemented on cooktops with two unpredictability parameters of the flame such as back propagation and lift. For gas burner flames of the household device, numerical findings were compared with experimental data. For various equivalence ratios, volume fraction distribution, heat release rate, and the flow field streamlines were computed. (Gattei, 2008).

Stöllinger and Heinz (2008) applied probability density function (PDF) methods and extended for mixing regimes like premixed combustion. Computations presented in the research had been performed by using the CFD code. Besides, a standard scalar mixing frequency model was generalized (Stöllinger & Heinz, 2008).

To examine natural gas combustion, Specchia and Toniato (2009) analyzed the premixed burners that contains metal fiber (Fe–Cr–Al fiber materials) involves in necessary combustion performance. On a commercial residential boiler under real operating conditions, proposed structural catalysts were evaluated. In terms of CO emissions, when compared to commercial burner performance, Pd-based catalytic burners performed better. However, NO emissions increased in the same operating conditions (Specchia & Toniato, 2009).

Akbari et al. (2010) investigated one-dimensional porous burner thermal response under various operating conditions and design parameters. It is emphasized in the paper that inlet gas mixture specifications and structural properties of porous material directly effects thermal conditions and flame stability of the burner. For constant firing ratio, combustion region temperature was found to be proportional with porosity increase and pore density decrease. Burner length was found to have no effect to burner performance (Akbari & Riahi, 2010). Besides that, same researchers were dealt with lean flammability limit and stability of porous burners including with flashback/blow out phenomena (Akbari et al., 2009).

Keramiotis et al. (2012) investigated thermal performance, emissions and working ranges of a porous burner with comprehensive experimental setup. The combustor is consists of two perforated burner with an Al_2O_3 flame capture device and silisium-carbon foam. Operation gases are methane and LPG. Thermal loads and mixture equivalence ratios are surveyed with burner operation range. Thermocouples and IR camera are used for obtaining temperature profiles. From 200 to 1000 kW/m^2 thermal loads are tested in lean combustion regimes (from flashback up to blow off) within range of $0.625 < Ø < 0.83$ equivalence ratios. It is revealed that burner is operated steadily for wide power ranges and various fuels gave low emissions. At 1 atm pressure conditions, average CO and NO_x emissions are obtained as 50 ppm and 25 ppm, respectively (Keramiotis et al., 2012).

Jatoliya et al. (2012) used a perforated matrix burner to carry out an experimental examination of the flame characteristics of premixed liquefied petroleum gas (LPG) and air with various mixture ratios. implemented an experimental investigation of the flame characteristics of premixed liquefied petroleum gas (LPG) - air mixtures with different equivalence ratios on a multi-hole matrix burner. Species concentration measurements (CO, O_2, CO_2 and NO_2) were made by gas analyzer. Besides that, a K-type thermocouple is used to detect temperature throughout the burner surface at various heights. (Jatoliya et al., 2012).

Lee and Hwang (2013) researched flow streamlines, steadiness of the flame, lean premixed flame and its emission characteristics via experiments in a cylindrical perforated burner contains a metal plate. CFD calculations had been applied over flow configuration of cylindrical perforated burner. In the study, advantages of cylindrical burner are given comparing with flat burner. Multi hole metal baffle plate and bronze sintered metal plate are compared according to their combustion characteristics (P. H. Lee & Hwang, 2013).

Aste et al. (2013) conducted an investigation of the impact of household heating on natural gas use and pollution emissions.. NO_x emissions were researched in detail for national perspective of Italy. A new methodological procedure was presented among national domestic boilers with their technologies and heating power. According to their perspective, fuel saving and NO_x emission reduction were evaluated from 1999 to 2011 (Aste et al., 2013).

Yu et al. (2013) performed an experimental study to investigate thermal efficiency and emission characteristics of there different type porous-media burners with ceramic (CM), stainless steel fin (SF) and metal fiber (MF). Experiments were conducted with a commercial condensing boiler burner for different equivalence ratios and loads. According to burner porosity, thermal efficiency, CO and NO_x emissions were obtained. Most appropriate burner was found as burner with metal fiber option (Yu et al., 2013).

Boggavarapu et al. (2014) studied flame structures for methane-air gas mixture with household oven. Flow structure, combustion and heat transfer were calculated by

means of the CFD in the burner. The burner efficiency was calculated experimentally and numerically and comparison had been implemented. A good agreement had been obtained (Boggavarapu et al., 2014).

Zhang et al. (2014) investigated a commercial premixed burner experimentally for optimization of gas mixing system (GMS). Experimental evidence has shown that the homogeneity at the GMS outflow has a significant impact on pollutant emissions. The distribution of orifice plates had a good impact on the single ejector's homogeneity of velocity and fuel-gas mixing. The most appropriate measurements and geometrical parameters offer useful direction for brand-new designs. The effect of the flow distributions on the gas-fired boiler was examined. For gas entry, different orifice plates and ejector types were compared (T. H. Zhang et al., 2014).

Avcı et al. (2015) investigated a thermal system and modelled flue gas domain numerically inside the condensing boiler within the studies of our research team. Since that study, there was no research that have examined the effect of different design parameters of finned tube heat exchanger at combustion region. In this paper, the effects of determined design parameters related to condensing boiler's heat exchanger on the capacity were evaluated numerically by using CFD (Avcı et al., 2015).

Zhao et al. (2015) studied a premixed cylindrical burner with experimental and numerical methods about investigation of low pollutant emission. Nozzle position and diameter dimensions were optimized by employing a validated CFD model. NO_x and CO emissions were analyzed by experiments. Flow and pressure were examined by CFD methods. The methane concentration distribution at the pores in axial direction was given in this study (Zhao et al., 2015).

Petar et al. (2016) investigated design and modeling aspects of a premixed cylindrical multi-hole burner. According to standards and market requirements, CFD analysis were performed for various boundary conditions. Reduced chemical mechanisms were applied and compared in each other in the simulations. Flame structure and emissions had been modelled at first in commercial Chemkin code (ANSYS: San Diego, 2017). A chosen reduced model for simulating combustion for

commercial natural gas was utilized for the simulations. (Petar, Lekic, Vojinovic, & Prochaska, 2016).

Decker (2017) was developed a household biogas fired burner flame port developed and tested for arranging optimal flame port geometry for the doctorate thesis. For a common biogas stove, a variety of circular and rectangular port designs were created. In the thesis study, for household biogas burners, the author created and tested a design tool to acquire the ideal flame port geometry. Thermal efficiency and emission predictions were obtained for the residential biogas burner (Decker, 2017).

Kuntikana and Prabhu (2017) utilized a thermal performance test on multi holed gas burner with cooling technique using air jet instead of water loading test. In the trials with the inline and staggered multi holed plate burner arrangements, impinging flame jets premixed with methane and air were used. While the staggered configuration produced more equal surface heat flux, the inline configuration was more efficient thermally (Kuntikana & Prabhu, 2017).

Lefort et al. (2017) realized an analysis on laminar premixed flames that contain rich mixture of natural gas. The methane-air gas mixture was used and the burner zone temperature values were measured in this study. Numerical commercial codes were used, numerical estimates were made for different laminar blended gases and compared with experiments (Lefort et al., 2017).

Özdemir (2017) investigated flame characteristics of the methane gas mixture in the domestic furnace application. Numerical study was performed with CFD simulations. Calculations were made for temperature, emission, and mixing ratios. Cooking compartment slot effects were examined for temperature uniformity (Özdemir, 2017).

Schiro et al. (2017) researched different fuel compositions and impact on gas using appliances with the help of the standards on reference gas and limit gases in premixed burners. Experimental test stand was installed for measuring emissions for different thermal load conditions and fan speeds (Schiro et al., 2017).

Kuntikana and Prabhu (2018) investigated heat transfer specifications of perforated curved surface burner on impinging flame jets on concave surface. Various burners were used to compare Reynolds numbers and equivalence ratio. Furthermore, wall temperature was analyzed to obtain variations of Nusselt number. Average Nusselt number, thermal efficiency and coefficient of variance change was expressed in this study (Kuntikana & Prabhu, 2018).

Hinrichs et al. (2018) investigated pollutant emissions, temperature profiles of burner and combustion chamber inside cylindrical heating unit. CO and NO emissions were obtained with local measurements at various axial locations. The concentration of CO and CO freezing mechanism were observed in the experimental analysis. Numerical simulations were applied at constant equivalence ratio, pressure, temperatures of unburnt gas and cooling coils. Inlet gas velocities of the burner were determined before the numerical analysis. According to temperature measurements, gas radiation effects were found low because of the closed system design. It was revealed that constant temperatures of the burner surface could be used in the numerical analyses. Besides that, NO pathways were obtained inside the combustion chamber of the condensing boiler. It can be understood from the study that burner flow analysis and ensuring flow uniformity are important for reducing NO emissions of the burner (Hinrichs et al., 2018).

Schiro and Stoppato (2019) studied experimentally premixed burner in a 25-kW commercial premixed condensing boiler. Test rig is established in a laboratory according to condensing boiler standards. Load modulation range is selected as 1:10. Specific thermal load, gaseous emissions, combustion performance, porous metal fiber structure effects on combustion are investigated for various test gases. Furthermore, CO, CO_2, NO_x emissions are calculated for different metal fiber structures and compared with steel only burner. It is clearly stated in the paper that metal fiber layer is crucial decreasing NO_x emissions of premixed burners. Besides, fiber materials increase burner flexible operation range to supply CO emission reduction with equivalence ratio variation (Schiro & Stoppato, 2019).

Jones et al. (2019) gathered experimental data on the emissivity of materials used in high temperature applications from a number of sources. This study provides the

total normal emissivity of a variety of materials as a function of temperature. Emissivity values of condensing boiler heat exchanger and burner metals are supplied with suitable high temperature range which is useful for simulations on real applications (Jones, Mason, & Williams, 2019).

Paterakis et al. (2019) He examined isothermal flow and scalar blending regions in a premixed burner downstream of various axisymmetric diverters. Stratified and fully premixed inlet conditions are compared with axial and radial distance. Blending and cold flow specifications of flame stabilizers were discussed for various fuel-air mixing performance and entrainments levels (Paterakis, Politi, & Koutmos, 2019)

Najarnikoo et al. (2019) used image processing methods to investigate a cylindrical perforated premixed burner in a commercial condensing boiler. Experimental research had been implemented from 11.7 to 17.1 kW thermal load and equivalence ratios from 0.4 to 1.2. Flame images were processed with various color adjustment techniques. Authors developed a method to find a relationship between an image color and flame properties. Flame colors were changed with equivalence ratio variation from green to yellow and then blue. Stable blue flame region was found between 0.7 and 0.73 equivalence ratio values for all thermal load conditions in the research (Najarnikoo et al., 2019).

Ding et al. (2019) performed an investigation on real-time equivalence ratio sensing system for analyzing chemiluminescence data from a perforated premixed burner. It is emphasized in the paper that OH* chemiluminescence intensity indicates equivalence ratio for different fuel components. OH* signals are obtaine with a photo-multiplier tube with a filter that has optical features (Yi Ding et al., 2019).

In the research of Ding et al. (2019) chemiluminescence of methane-air premixed flames are measured in various serial experiments. After their experimental study, a one-dimensional numerical study on flames was conducted for comparing with experimental results. It was found in the paper that OH and CH chemiluminescence have correlation with combustion gases temperature (Y. Ding et al., 2019).

For a cylindrical perforated premix burner utilized in condensing heating devices, Soltanian et al. (2019) applied a chemiluminescence analysis to find optimum equivalence range with flame emission spectroscopy method. Investigation covers between 0.77 - 0.85 equivalence ratio for whole burner power. The burner maximum surface temperature was measured, and the corresponding equivalence ratio was determined. Authors aimed to find the optimum equivalence range for maximum heat release. Burner power show maximum values in the interval of 0.77 - 0.85 equivalence ratio (Soltanian et al., 2019).

Shotet et al. (2020) used fault detection and diagnosis method to predict non-condensing boiler performance. This methodology was applied on the condensing boiler device with calibration, design, and emulator that validates burner. Also it can operate standard and in faulty situations. Theoretical flame temperature, flue gas temperatures with and without vapor conditions are calculated in respect to excess air percentage (Shohet et al., 2020).

Hinrichs et al. (2021) modeled a cylindrical multi-hole burner with porous medium approach, because of the computational difficulties for many burner holes. They applied flamelet progress variable (FPV) approach that employs intricate reaction kinetics with relation to the progress variable and enthalpy. CO and NO emission were obtained for 3D full scale condensing boiler model. Blanquart mechanism was used with 149 species and 1651 reactions. NOMANI model approach was used for NO prediction and Ihme-Pitsch approach for CO, respectively. Burner surface temperatures were obtained over the combustion domain. For radial position of the burner, temperature, CO, and NO emissions were found in the research. Besides, burner surface temperatures were obtained in respect to circumferential position inside the combustion domain (Hinrichs, Schweitzer-De Bortoli, et al., 2021).

Lamioni et al. (2022a) investigated effects of slit patterns on the multi-hole perforated burners for the premixed flames in domestic condensing boilers. 3D numerical simulations with different reaction mechanism were implemented to understand the behavior of premixed fames. Direct integration method is used with temperature patch near the inlet for igniting the flame. Flame shape formation was identified with velocity distribution. Effects of inlet velocity was discussed over slits

and holes of the burner. Temperature, OH mole fractions, velocity fields and NO_x emissions were obtained over the combustion domain with multiple holes and slits (Lamioni et al., 2022a).

Lamioni et al. (2022b) numerically investigated a domestic condensing boiler on the combustion process and pollutant emissions for different types of gases. Effects of burner hole distance and hydrogen addition were reported along the combustion region to temperature, velocity, CO and NO emissions. NO formation pathways were obtained for the different gases in a fixed hole distance condition (Lamioni et al., 2022b).

1.1.2 Literature Search on Theoretical Combustion

It is important to examine theoretical studies involving reaction mechanisms in modeling combustion with CFD. In the scientific literature, many studies including theoretical combustion and reaction mechanisms have been identified.

Rashidi (1998) calculated equilibrium in combustion products with different mathematical methods (Rashidi, 1998). Rakopoulos et al. (1994) developed a fast model for calculating chemical equilibrium compositions in a diesel combustion. Pressure, temperature and equivalence ratio effects were discussed on composition products (Rakopoulos et al., 1994). Thomsen et al. (1999) examined NO emission production in premixed flames and compared two different chemical kinetic mechanisms. Besides that, experimental measurements of NO were compared with premixed flame code (Thomsen et al., 1999).

Grace et al. (2001) developed equilibrium model with Gibbs free energy minimization method to estimate the performance and gas compositions. Coal combustion was investigated in a pressurized rotating liquid bed gasification test facility. Li et al. (2001) applied modifications on an improved dynamic stability model. A good agreement obtained from the gaseous combustion products on the results (Li et al., 2001).

Nabi (2010) theoretically investigated exhaust emissions and combustion parameters such as theoretical fuel mixture ratio and lower calorific value (LCV) for

different oxygenated fuels over diesel engine. Equilibrium constants method were applied to obtain combustion products of pentadecane fuel on diesel engine (Nabi, 2010).

Neron et al. (2012) were performed Gibbs free energy minimization to calculate complex equilibria on adiabatic and non-adiabatic systems. Different thermodynamic models were presented with kinetic and energy boundary conditions. Equilibrium temperature and compositions were calculated for hydrocarbon mixtures (Néron et al., 2012).

Kayadelen & Ust (2013) predicted equilibrium products and thermodynamic properties with computer code. Water injected $C_{\alpha}H_{\beta}O_{\gamma}N_{\delta}$ type fuel combustion was examined with equilibrium constant method. Composition products are presented for two different equivalence ratios. Results were validated with CHEMKIN and GASEQ softwares (Kayadelen & Ust, 2013).

Zajemska et al. (2014) estimated flue gas composition in a power burner that burns natural gas. Combustion calculations were dealt with commercial CHEMKIN software. Flue gas compositions were obtained (Zajemska et al., 2014).

Sieradzka et al. (2020) predicted gaseous products of fuel pyrolysis using CHEMKIN chemical modeling software. Mole fractions of gaseous products are presented for various temperatures (Sieradzka et al., 2020). Mlonka-Medrala et al. performed numerical modeling of pyrolytic gas with CHEMKIN-Pro software. Measured gas compositions showed good agreement for major gaseous products (Mlonka-Mędrala et al., 2021).

Kökkülünk et al. (2013) applied a new steam injection method to control NOx emissions over direct injection diesel engine. Extended Zeldovich mechanism was utilized for calculating combustion products via equilibrium constant method. Engine power, fuel consumption, efficiency and also NO emissions were validated with experimental data (Kökkülünk et al., 2013).

Gonca (2014) utilized the same procedure to determine how steam injection affected NO emissions and performance. Diesel engine used ethanol-diesel mixtures

as fuel. Temperature, pressure, NO emissions, effective power and efficiency were determined and compared with experimental results (Gonca, 2014).

Boukhalfa (2016) modelled methane combustion with chemical kinetic method. Emissions and combustion efficiency were calculated via computer code (Boukhalfa, 2016). Fournel et al. (2015) developed a model for predicting gaseous emissions of biomass fuels. Based on minimizing Gibbs energy, a thermodynamic equilibrium model was developed. Predicted emissions were checked with obtained results. Therefore, a good agreement had been reached (Fournel et al., 2015). Koukkari and Pajarre (2011) applied a Gibbs free energy minimization calculation with an additional Lagrange multiplier. Minimization process could be extended to multiphase system with this approach. Proposed new method had found applications in solving energies of mixtures, and reactive systems (Koukkari & Pajarre, 2011).

Sreejith et al. (2013) presented a thermodynamic approach in biomass containing fuels. In this study, based on minimizing Gibbs energy, depending on temperature and pressure, gas components, lower heat value, energy efficiency of gasification process were investigated parametrically to obtain optimum values (Sreejith et al., 2013).

Hu et al. (2015) compared laminar flame speeds with USC Mech II, GRI Mech 3.0, and also Aramco Mech 1.3 chemical reaction mechanisms according to steady volumetric and opponent flame. These mechanisms were validated up to 6.0 MPa. Methane-air mixture laminar burning velocities and ignition delay times were studied and provided through correlations. Flame speeds in laminar flows were obtained at various temperatures with experiments and calculations with various reaction mechanisms (Hu et al., 2015).

For lean premixed flames, Trisjono and Pitsch (2017) conducted a direct numerical simulation on NO emission production. NO kinetics was applied in a 3-D, premixed turbulent burner via detailed chemical mechanism. Turbulence and NO chemical mechanism in lean premixed flames were investigated with results found in this work. It was found that, production by the NNH route is critical for flame-generated NO. Thus, turbulence substantially effects NO formation (Trisjono & Pitsch, 2017).

In two new closed form equations, Jia et al. (2019) reported the molar entropy and Gibbs free energy of pure gas species. In the temperature interval between 100 and 6000 K, and Gibbs free energies and nitrogen (N_2) molar entropies predicted and compared with experimental data. Among the results of molar entropy and Gibbs free energy of N_2 species, a perfect agreement has been reached by researchers (Jia et al., 2019).

Öztürk and Eyriboyun (2010) calculated the NO_x emission amount for natural gas fuel obtained from four different sources by using chemical kinetic mechanisms. The combustion products were obtained with the help of computer programs in terms of mole and mass ratios for laminar and stoichiometric premix flames. The effect of the number of fuel components, fuel inlet temperature and humidity on the NOx emission resulting from combustion were examined (Öztürk & Eyriboyun, 2010).

Mittal and Pitsch (2013) presented a model for examining premixed combustion under different pressure conditions. Proposed model was based on the flamelet progress variable (FPV) approach that has been utilized to investigate isobaric premixed combustion. A polynomial spreading method is improved to get temperature from the enthalpy of the system. A validation has been done against Direct Numerical Simulation (DNS) studies with different turbulence intensities and length scales (Mittal & Pitsch, 2013).

Kayadelen et al. (2017) investigated the effects of diluent components in different amounts of natural gas on methane combustion. Various pressures, unburned gas temperatures and equivalence ratios were examined. The effects of the main components in the gases on the flame temperature, CO and NO_x emissions were investigated. Optimum equivalence ratio range was obtained. One can understand from the results that combustion of gases which have low H/C ratio directly affect combustion system performance and emissions (Kayadelen, 2017).

Glarborg et al. (2018) reviewed nitrogen chemistry mechanisms that create pollutants resulted from combustion and potential of primary measures on NO_x control. With utilization of active thermochemical table approach, thermochemistry of nitrogen compounds is updated. The nitric oxide mechanisms which are thermal NO,

prompt NO, fuel bond NO and NNH pathway were detailly discussed in the paper (Glarborg et al., 2018).

Schiro et al. (2020) investigated potential of hydrogen enrichment in natural gas using in domestic gas boiler burners. Authors aim to create knowledge about effects of hydrogen-methane fuel blends respect to pollutant emissions, boiler efficiency, flame stabilization, flame control systems and suitable material selection processes. A novel theoretical model was presented for hydrogen enriched natural gas including standardized methane-hydrogen mixtures such as G110, G112, G20 and G222 (Schiro et al., 2020).

Dreizler et al. (2021) highlighted the function of combustion science and technology in systems for low- or no-impact energy transition. Climate neutral systems should be supplied by efficient energy conversion systems. As proposal measures, increased building service efficiency and the annual turnover rate of outdated systems are discussed. The importance and competence of numerical simulations on combustion systems have been proposed with accelerated simulation tools using higher performance computers (Dreizler et al., 2021).

Hinrisch et al. (2021) investigated simplified perforated plate burner that used inside the condensing gas boiler. G20, G21 and G222 fuel gases were used in the investigation. Experimental and numerical in-house code were compared for NO sub mechanisms. Prompt NO mechanism was found to be major NO_x contributor for the flame front of the burner. Laminar burning velocity changes, stand-off distance and flame heat losses were detailly researched in this study. For pure methane, temperature and NO_x mole fractions were obtained in the centerline profiles for four NO sub mechanisms (Hinrichs, Hellmuth, et al., 2021).

In reviewed studies, boiler and combustion performance, flame stability, chemical reaction mechanisms, and emission reduction methodologies were investigated using theoretical, numerical and experimental methods. Many of these studies give knowledge on boilers and combustion, however, there has been no detailed investigation with a comprehensive theoretical and numerical approach including test gases of residential heating devices in the research area. A systematic understanding

of how combustion characteristics inside the combustion region of the condensing boiler contributes to pollutant emissions and thermal performance is still lacking. Thus, studies on the effects of combustion gases and emissions, including combustion and flow characteristics, on thermal performance were implemented within the scope of the thesis.

1.2 Aim and Motivation

Today, condensing boilers play an important role in heating the buildings in constantly developing and growing cities and meeting the hot water needs. Pollutant gases formed due to combustion in condensing boilers have negative effects on nature. In order to reduce these environmental effects, condensing boilers should be complied with the standards with constantly increasing constraints by improving their combustion parameters (European Committee for Standardization, 2015; Yılmaz et al., 2021).

Combustion in condensing boilers is basically solved by gas chemistry, thermodynamics, fluid mechanics and heat transfer calculations. Numerical analysis of combustion systems depends on modeling and analyzing all these components in a coherent way. In analyzes that carried out, it is important to estimate the flow, temperature, flue gas emissions. Considering all these situations, it is seen that the modeling of the combustion system is quite difficult. First, in order to model the combustion system realistically, the most suitable combustion model should be selected for the real operating conditions. If the model selection is made correctly, emissions resulting from combustion and flue gas temperatures can be predicted more accurately. When the literature is examined, it has been observed that there are deficiencies in terms of studies examining premixed inlet conditions on condensing boilers comparatively.

From all these perspectives, it is aimed to examine the effects of combustion gases and emission characteristics on a condensing boiler under various premixed gas inlet conditions. As will be specifically addressed in the thesis' chapters, theoretical, numerical and experimental investigations have been carried out for the combustion region. In addition, within the scope of the thesis, it is intended to examine the

premixed inlet conditions comparatively and observe the compatibility of the results of the relevant models with the experimental data of literature and project studies.

Furthermore, the thesis consists of the studies accomplished on the TÜBİTAK (The Scientific and Technological Research Council of Turkey) 1505 project that is encoded with grant no. 5180092.

Within the scope of the thesis, the parameters of the boiler combustion were investigated with two different theoretical combustion methods. Theoretical combustion methods were compared with a software accepted in the literature and their reliability was tested. Then, the combustion region design was carried out numerically. Necessary reaction mechanisms were defined on this design and CFD analyzes were performed with different numerical model approaches. The numerical results obtained were compared and verified with the literature and the results of the TÜBİTAK 1505 project. After validation, the effects of premixed inlet conditions on temperature, velocity and emission characteristics were parametrically investigated.

In the following chapter of the thesis, development of residential boilers, boiler and burner characteristics, standards and regulations, combustion in condensing boilers are discussed.

CHAPTER TWO
COMBUSTION IN CYLINDRICAL COMBUSTION REGION ON BOILERS

2.1 Development of Residential Boilers

2.1.1 Brief History

Boilers are basically defined devices that produce steam from water. From the scientific point of view, a boiler converts the chemical energy of fuel into heat energy which raises the temperature in water to form hot water or steam (Rayaprolu, 2009). Boilers powered by fossil fuels employ the chemical energy of the fuels to produce steam or hot water. Nuclear fission provides the energy for nuclear fuel boilers. A solar boiler harnesses energy from the sun to create steam, whereas a waste heat recovery boiler utilizes the sensible heat of hot gases from a process. Although the word "boiler" or "steam generator" refers to a device that turns water into steam, not all boilers used for space heating do so. These types of boilers only heat water to required temperatures (Basu et al., 2012).

More than two decades, gas industry has been involved with combustion process on boilers and burners. First decade was passed with basic understanding of combustion phenomena. After the discovery of premixed flame by Bunsen, combustion mechanism chemistry and burning velocity of gases are revealed by Hinshelwood and Semenov in the period of 1920s and 1930s that give opportunity to comprehend fundamentals of boiler combustion. The textbook, *Flame and Combustion in Gases* by Bone and Towned in 1927, is precursor text on flame and combustion characteristics and aroused interest on combustion research (Bone & Townend, 1927).

Hinshelwood and Semenov won Nobel prize in 1956 for their study on chemical reaction mechanisms (Semenov, 1956). In the closing speech, these remarkable statements are given: “When it was found that a great number of reactions were chain reactions, many people in the first enthusiasm thought that almost all reactions were chain reactions and that the simpler mechanisms previously thought of were exceptions. But Hinshelwood put the matter in order. He found substances which could

simultaneously react in two ways, one part reacting by a chain mechanism and at the same time the rest reacting in the old-fashioned way" (Marcus, 2002). Nevertheless, complex mechanism of combustion with chemistry and fluid dynamics, still has missing aspects nowadays (Jones, 1989).

More than 30% of energy of fuel in conventional boilers is lost as waste heat inside the flue gas. Condensing boilers can take out sensible heat of the combustion products and latent heat of evaporation by secondary heat exchange mechanism. Along with this mechanism condensation occurs in the heat exchanger, thus, boiler efficiency rises. Conventional boilers generally have less than 80% efficiency. The technology of residential boilers that have condensing flue gases on their heat exchanger is not new. The first designs are created in 1930's. The "town gas" that derived from coal combustion has substantially corrosive effects on heat exchangers due to condensation (Banks, 2000).

First condensing heating device was introduced by a Canadian boiler company which uses outdoor air for combustion with pulse combustor in the late 1950s. More than 700 boilers were produced until 1966 (Naslund, 1997).

In the beginning of 1970s, combustion research had grown rapidly due to environmental issues and energy necessity by the aid of improvements on computations, higher quality experiments with lasers and accurate measuring devices. Besides that, simultaneous experiments and computational simulation era had started. New discoveries had emerged in the aspects of combustion study area such as laminar-turbulent flames, chemical kinetics, explosions and multiphase combustion (Law, 2007).

Until 1974, more than 90% efficient boilers based on higher heating value have had no wide range of uses with condensing heat exchanger. After this period, American Gas Association put forward boilers with stainless steel heat exchangers that have flue gas temperature of 49 °C (Kirk, 1974). In these type of boilers, latent heat was regained by water bath where exhaust gases pass through. In 1976, Ruhrgas company in Germany was developed a 1 MW boiler with condensing heat exchanger that utilized in space heating (Rado, 1976).

Gasunie Research (Netherlands) and British Gas (United Kingdom) were among the leading research institutes in the early 1980s. In 1979, Gasunie Research introduced a condensing boiler prototype with two heat exchangers for Dutch boiler producers. In 1981, with aid of previous know-how, ten companies had started to build boilers with various designs. Gastec, a Dutch organization founded by natural gas manufacturers and distributors (now merged into KIWA in 2005), made research about boiler materials and corrosion. In a subsequent design, hot tap water producing add-on was applied on condensing boilers with a modulating burner by Gasunie Research (Bootsma & Meijnen, 1992). British Gas studies had been reported in International Gas Conference which was held in 1986 and 1989. Evaluation of burners, controls, flue gases, materials and "wall-hung boiler" concept were introduced in these conferences (Hargreaves & Patterson, 1986; Naslund, 1997).

Wall-hung boilers have popularity recently with less space occupying dimensions and can be fitted to narrow places. Room-sealed and open-flue versions are mostly preferred in residential use (Steele, 1985). The main developments have emerged in the hot water and space heating aspects. Combination boilers heat water directly and there is no necessity to store the water in a separate tank. Early models were unreliable and used only with hot water, but modern systems have a good performance on the applications. Combi central heating systems are preferred by the end-users in recent years (Mitchell, 2008).

In EU countries, natural gas is spread through cities with low cost and east distribution. Eventually, condensing boilers were becoming feasible for residential use and serving prototypes have been developed in the late 1970s in Europe (Banks, 2000). From 1990 to 2005, it is predicted that if condensing boiler usage instead of conventional ones were realized, 20 million tonnes of CO_2 emission would have been prevented from the environment in EU countries (Haug et al., 1998). In the next section, boiler types, design and performance issues are discussed.

2.2 Boiler Characteristics

Boilers are classified according to their types, design parameters and performance. Besides, working pressure and temperature, fuel type, dimensions, shape, heating

purpose, etc. These boilers can utilize with fuels as fuel oil, biomass, liquid petroleum gas (LPG) or natural gas (NG) (Spach & Stanford, 2019).

First residential condensing boilers had been manufactured with two divided heat exchangers. In the second heat exchanger condensation occurs. These types of boilers can be defined as non-condensing boiler that has a condensing heat exchanger (Naslund, 1997). Non-condensing conventional boilers work without condensing mode and flue gas leaves the boiler losing its latent heat to the environment. In this type of boilers, internal condensation must be prevented to avoid corrosion of the metals used in the boiler structure. This is achieved by the boilers having lower inlet water temperatures (Spach & Stanford, 2019).

Nowadays, new designed boilers contain only one heat exchanger. Domestic space heating in Europe mostly is supplied by condensing boilers with single heat exchanger or second heat exchanger attached subsequently (Naslund, 1997). Early fundamental designs are identified by Jannemann as first and second condensing boiler series (Jannemann, 1996). Fundamental condensing boiler designs are demonstrated in Figure 2.1.

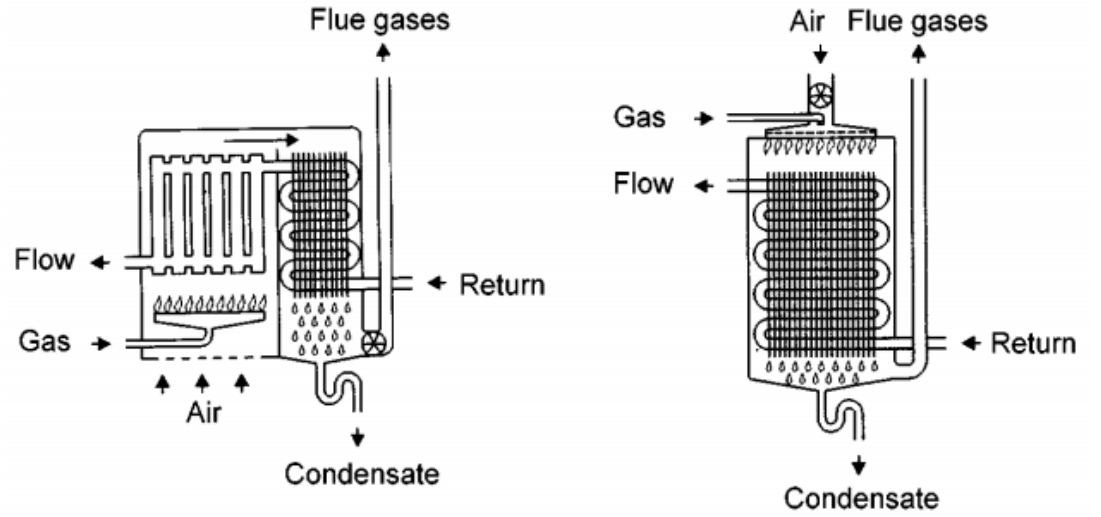


Figure 2.1 Fundamental condensing boiler designs (Jannemann, 1996)

According to British energy saving organization Energy Saving Trust (EST), condensing boilers provide best practice requirements and in United Kingdom whole gas-fired boilers should have condensation with an efficiency higher than 86%. Condensation period should be limited with desired time intervals to provide improved efficiency. Boiler system installation has two different options: hanged on the wall or standing at the floor. Types of gas-fired boilers are expressed as condensing regular (a) and combination boilers (b) that their schematics are shown in Figure 2.2 (EST Report CE30, 2008).

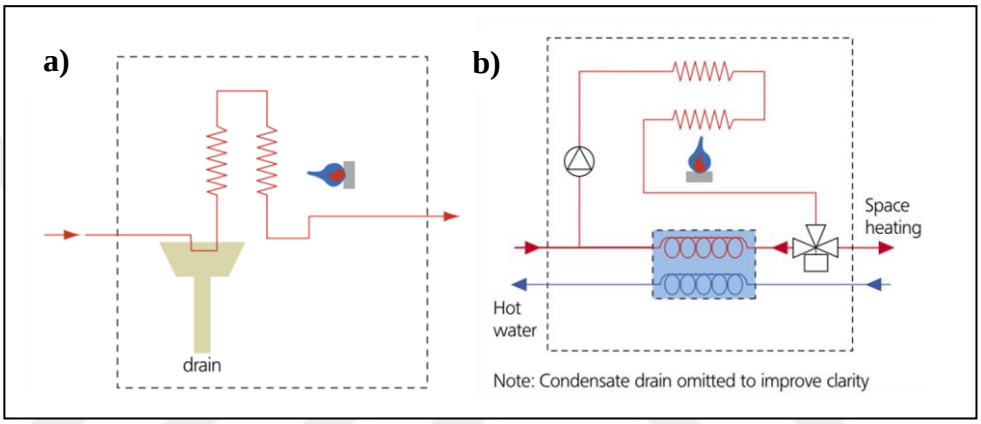


Figure 2.2 Schematics of a) condensing regular and b) combination boilers (EST Report CE30, 2008)

Condensing boilers improve their efficiency by condensed phase of water inside the flue gases. When combustion takes place in boilers, approximately 90% of the energy contained in the fuel turns into sensible heat, causing the temperature to rise. The remaining approximately 10% of energy is transformed into latent heat, which causes the phase change. This latent heat is contained within the water vapor (Spach & Stanford, 2019).

In conventional boiler technology, latent heat is dispersed along with gases of combustion. Condensing boilers recover this latent heat in the water vapor by means of condensation. The process of condensing water vapor will improve the efficiency of a boiler from 78% to 98% according to type of boiler operation (Spach & Stanford, 2019).

2.3 Burner Characteristics

In this part of the thesis, the burners in the boiler combustion chambers will be mentioned. The burners in the boilers can operate in premix or non-premix modes. Boiler performance and emission amounts vary according to the operating mode.

Premixed flames of the burners are shorter, cleaner and burn without much soot than non-premixed flames. Flame temperature is controlled by the system for various reactant mixtures. Reactant and air flow speed can create instabilities such as flash back and lift-off. Flashback creates instabilities and safety hazards. Thus, premixed flame burner operation range is limited by these aspects (Glassmann & Yetter, 2008; McAllister, 2011).

Furthermore, the flames tend to be turbulent, and the flames are hard to be controlled due to their unexpected and complex behavior under realistic working conditions. Besides that, flames of jet diffusion are seen to be more stable. For this reason, their operation range is wider and can be controlled with less effort. Nevertheless, diffusion flames are long and soot formation occurs more than premixed flames. Moreover, turbulent diffusion flames depending on various fuels have higher noise than other type of flames. Hereby, benefits of both type of flames should be taken into account during the design of industrial and domestic burners (Raghavan, 2016).

2.3.1 Burner Types

Gaseous fueled burner classifications have been made with open flame and closed flame burners. Heat transfer is accomplished by the flue gases passing through heat exchangers in the combustion region. On the other hand, indirect burners have different configuration that heat exchange does not occur between flue gases and flame. As further, direct fired burners are classified as non-premixed, partially-premixed and premix burners. Further classifications depending on aeration method, flow regime and operating gas pressure are performed. Gaseous burners with direct fire and their classifications are demonstrated with a flow-chart in Figure 2.3.

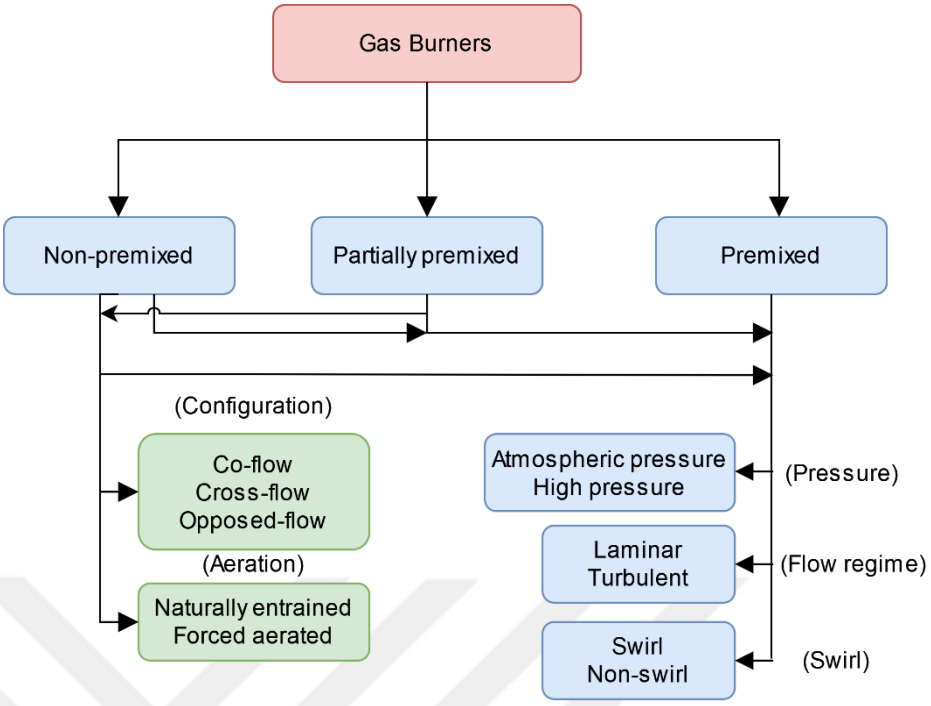


Figure 2.3 Types of gas burners (Raghavan, 2016)

Fuel and air enter the combustion chamber independently in non-premixed burners. These burners can be classified as cross-flow burners, where fuel flows contrary to the air flow, or coherent flow burners, where fuel and air flow parallel to one another. In partially premixed burners, primary air is fed through combustion chamber. Primary air have less air than the stoichiometric condition. This fuel-air mixture is not sufficient for reaction. Thus, secondary air is feed from different ports. Partially premixed burners have several advantages: cleaner and wide range operation can be controlled easier than non-premixed burners. Consequently, domestic appliance and industrial furnace manufacturers prefer partially premixed burners on their burner designs. Premixed burners are supplied by flammable gas mixtures for necessary equivalence ratio. These types of burners are utilized in special applications on which narrow operating conditions (Raghavan, 2016).

Gas-fired burners basically have four overall design classifications as; atmospheric, power, forced and induced draft, premix and pressure power. Atmospheric gas burners utilize at atmospheric pressure, combustible gas and air mix homogenously and entrain the system as a premixed gas mixture. In power burner, which is dominantly used in industry, air flows with the aid of a blower for essential

primary air in combustion. Premixed gas is controlled for optimal ratio of gas and air mixture before the combustion domain. Generally power burners cover a wide range of domestic applications (Jackson, 2012). A premixed gas burner is shown in Figure 2.4 (Soltanian et al., 2019).

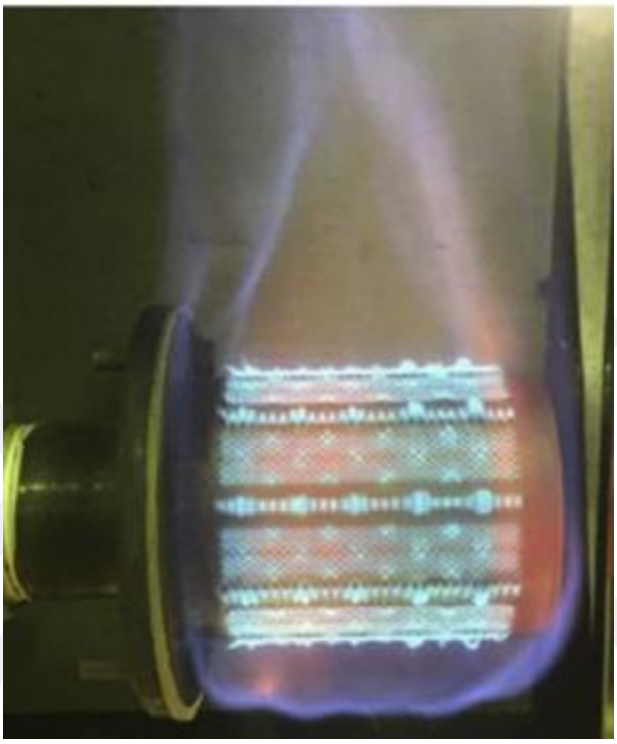


Figure 2.4 A premixed gas burner (Soltanian et al., 2019)

In co-flow burners, the streams of fuel and oxidizer are able to be operated in non-premixed, partially-premixed, or fully-premixed configurations and are parallel to one another. This type of burner features a co-flow port around the core port, which is where the oxidizer is fed, and a core port, often a duct through which the fuel stream happens. A basic co-flow flame configuration of the burner is shown in Figure 2.5.

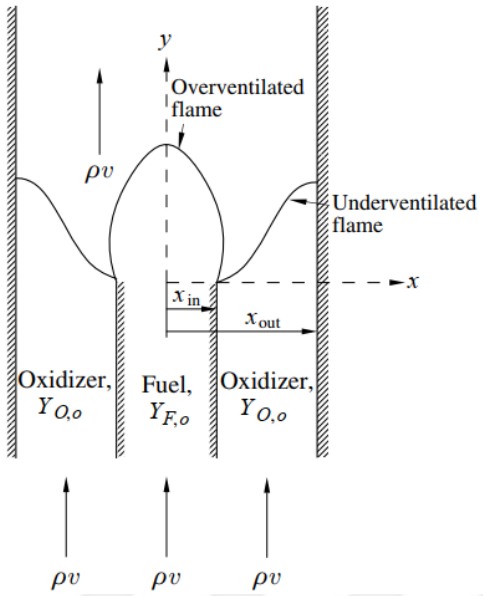


Figure 2.5 A basic co-flow burner flame configuration (Law, 2006)

The degree of mixing between the fuel and the oxidizer and the length of time the reactant spends inside the combustion zone play critical roles in determining flame stability. In turbulent burners flame stabilization is created by bluff body locations in the flow regime, pilot flames and forming swirl. Reaction region stabilization with using rotation is implemented in commercial burners and combustors in the gas turbines (Raghavan, 2016). A can type swirl combustor flow field is shown in Figure 2.6.

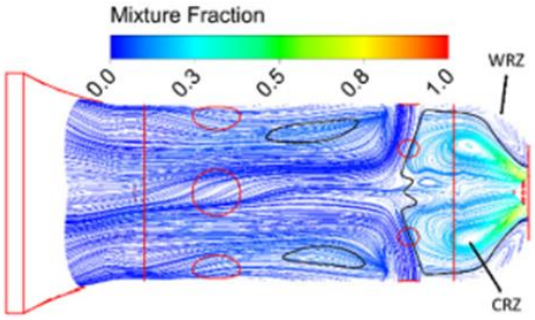


Figure 2.6 Flow field of a can type swirl combustor (K. Zhang et al., 2017)

The well-known Bunsen burner principle is used by atmospheric entrained air burners to operate at atmospheric pressure. Gaseous fuel and air are supplied through a nozzle into a mixing chamber. It can clearly be seen in Figure 2.7. Air from the

atmosphere enters through the holes because of the fuel jet's velocity. Fuel and air merges inside the partially premixed burner.

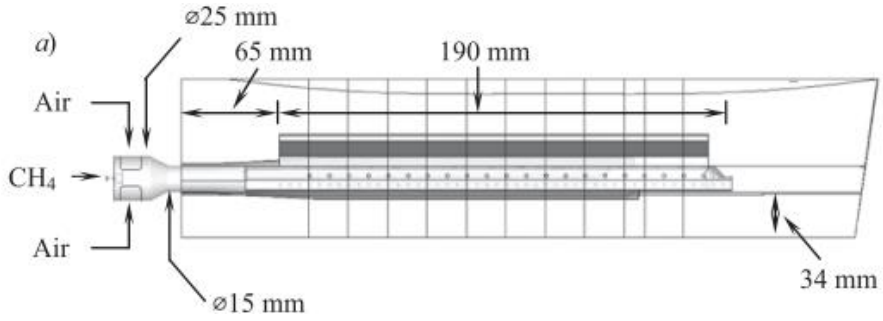


Figure 2.7 A domestic burner in partially premixed mode (Özdemir, 2017)

A forced-aerated, non-swirl, laminar flow cylindrical premixed burner is shown in Figure 2.8.

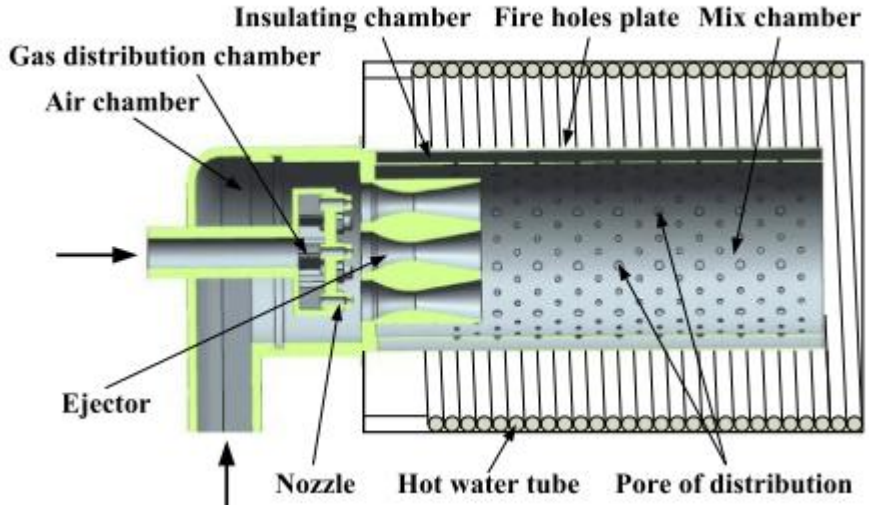


Figure 2.8 A cylindrical premixed burner with holes (Zhao et al., 2015)

Another crucial aspect of the burners is turn-down ratio (TDR). This ratio is found by dividing maximum to minimum flow rates of the fuel. The maximum fuel flow stream is restricted by realization level of the combustion process namely blow-off and by the quantity of supplied first aeration. The flashback limit of the burner restricts the minimum fuel flow rate (Raghavan, 2016). It can be revealed from the Figure 2.9 that alterations of turndown ratio (TDR), the blowoff and flashback are an important parameter for design of the burner (S. Lee et al., 2011b).

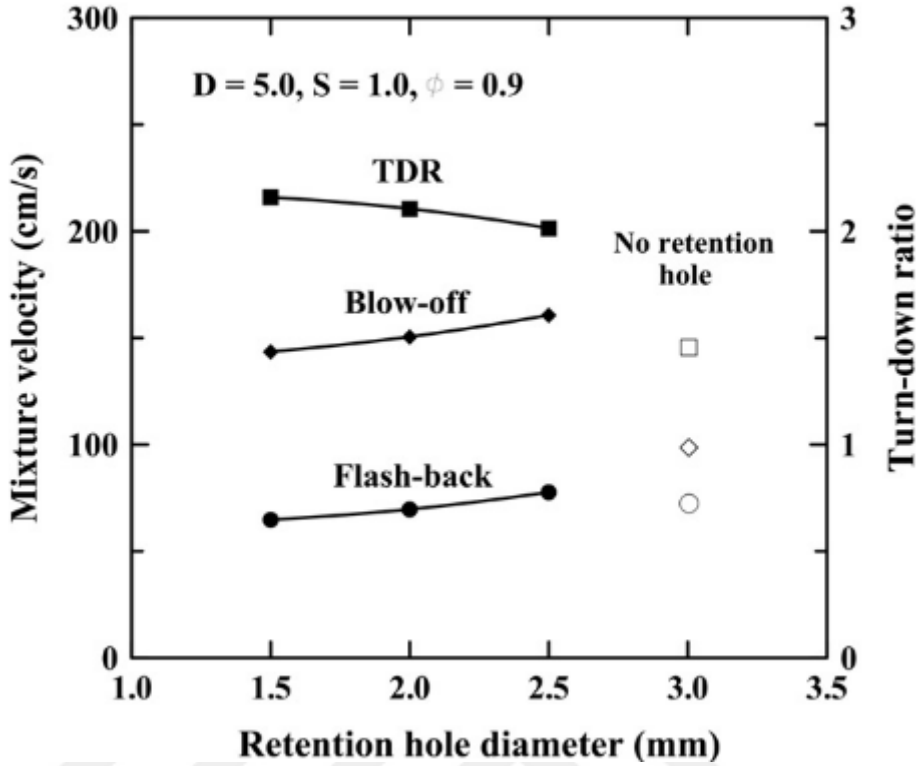


Figure 2.9 Alterations of turndown ratio (TDR), the blowoff and flashback with respect to retention hole diameter (S. Lee et al., 2011b)

Also, combustion stability is directly related with equivalence ratio and heat loads. In Figure 2.10, one can clearly understand that equivalence ratio (ϕ) and heat load alteration in suitable combustion range (S. Lee et al., 2011a).

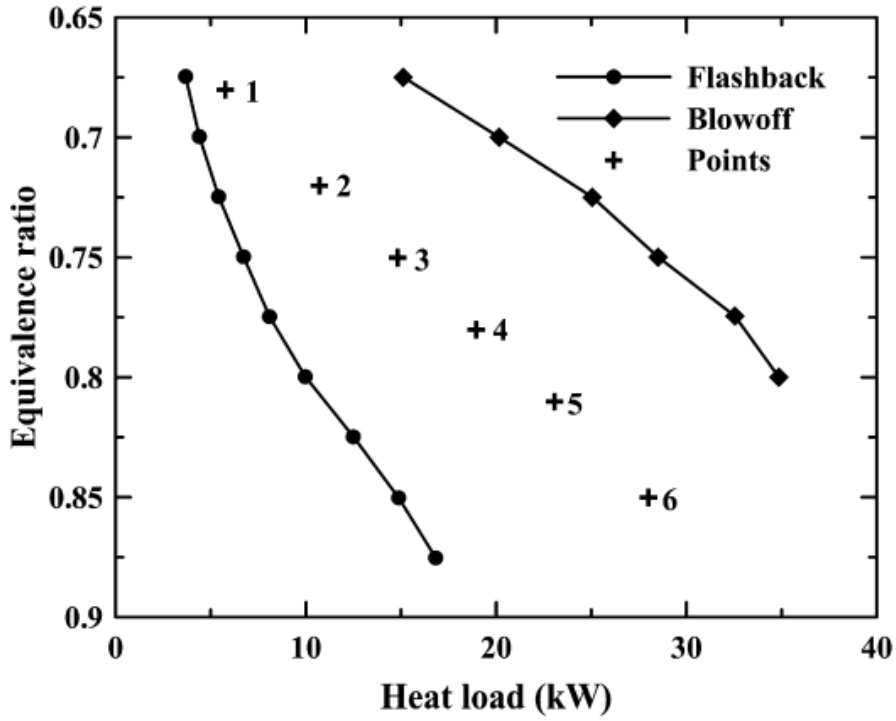


Figure 2.10 Alteration of heat load and equivalence ratio (ϕ) with suitable combustion range (S. Lee et al., 2011a)

2.3.2 Characteristics of Stability, Emission and Performance

Emission control of premixed combustion have concerns about; primarily turndown ratio, flame stability, CO and NO_x emissions (Turns, 2000). Premixed burners have instability difficulties such as lifting off the flame, blow-off and flashback. These instabilities have a negative impact on the burner's performance since they lead to inadequate combustion and a smaller operating interval. Any change in the gas supply pressure while the burner is operating alters the flow rate of the reactant mixture, which may result in an unstable operation. Under poor combustion performance with high pollutant formation, die down of the flame, lifting off or blowing off usually emerge. Besides that, in forced aerated burners, it is possible to reach better control over the pollutant formation and performance due to metering fuel and air supply (Raghavan, 2016). Burner stable operation working ranges depending on power input rate and first aeration is shown in Figure 2.11 (M. L. Smith & Stinson, 1952).

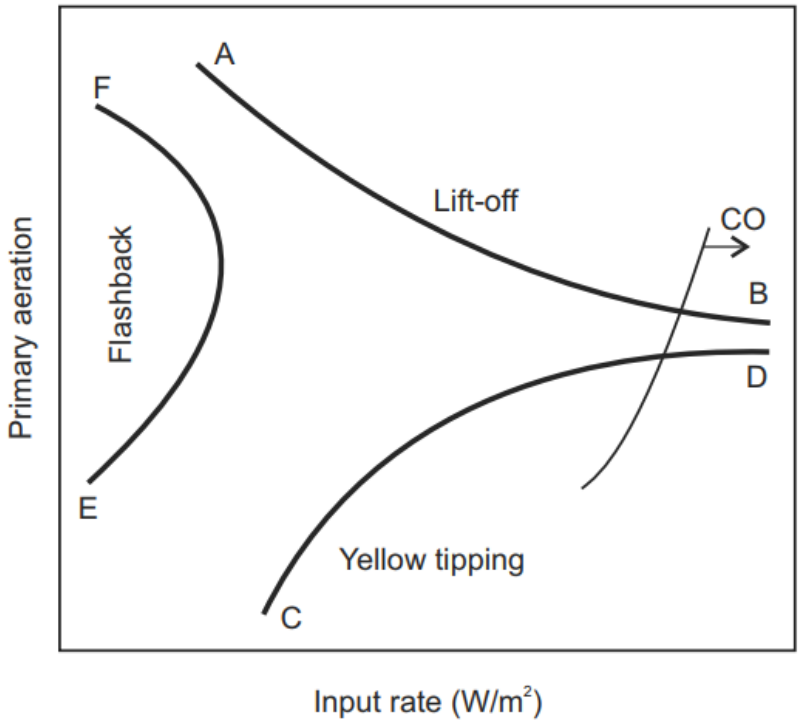


Figure 2.11 Burner stable operation ranges depending on power input rate and first aeration (M. L. Smith & Stinson, 1952)

For domestic, commercial and industrial appliances, various types of burners and systems for combustion have been researched and developed. Nowadays, Bunsen burner is the most used type in conventional residential boilers. However, this type of burner brings two types of problems. These problems are it is necessary that the size of the combustion chamber should be large due to the high flammability and high flame height resulting from the condensing water reaching the heat exchanger surface in high efficiency working conditions. In addition, Bunsen burners have higher NO_x emissions because they have a partial premixed flow and can no longer meet their energy and environmental requirements. A new type of burner using a premixed flame has been developed to overcome these disadvantages (S. Lee et al., 2011b).

Condensing boilers use premixed burner, and the condensing heat exchanger has a complicated structure that reduces NO_x emissions. The boiler industry is also interested in developing condensing boilers to maintain energy saving and environmental policies (S. Lee et al., 2011b).

2.3.3 Operating Parameters of the Burner

In forced aerated burners, the fuel and air stream that go into mixing or combustion chamber is tried to be kept nearly same amounts. The fuel flow rate is determined with flow molar rate and density of the fuel. Following that, the fuel flow rate and its heating value are used to calculate the input heat rate that gets into the burner. The fuel's lower heating value (LHV) is typically used. (Raghavan, 2016).

Obtaining required gas/air mixture, fans are used to supply forced air entrainment as a satisfactory method. However, fans have been used in industrial aerated burners for many years, integration into domestic gas appliances is quite recent. Fan generally provides air supply and removal of the combustion products from combustion zone. Fans can be located either upstream of the burner (forced draught), that kept positive pressure in the appliance or downstream of the burner and heat exchanger (induced draught), consequently placing the appliance under negative pressure. One can understand the mechanically aerated fan driven combustion system diagram in Figure 2.12 (Jones, 1989).

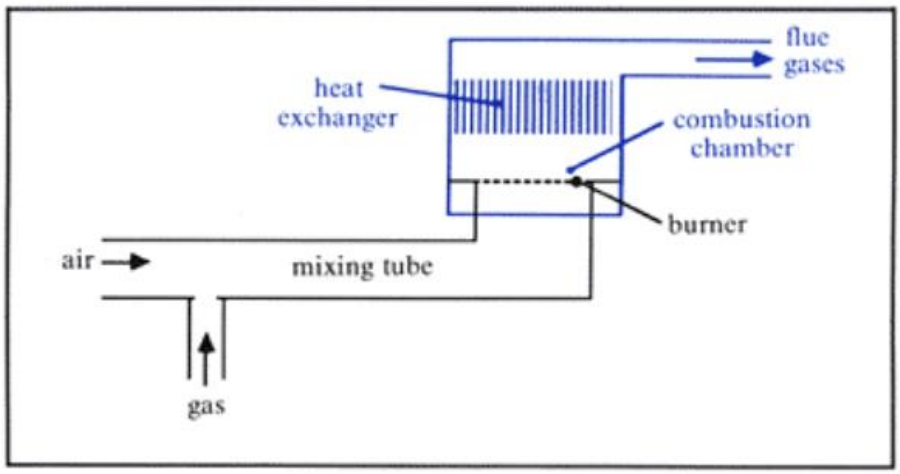


Figure 2.12 Diagram of a fan driven combustion system (Jones, 1989)

In fan driven burners, depending on the desired mode of combustion, the required mass flow rate of air may be delivered through another port either into a mixing chamber or straight into the burning region. Depending on the design, the entire air supply is split into primary air and secondary air. To be sure to maintain complete combustion, a little excess air is fed through the system in practical applications. While

measuring the air and fuel flow, required flame stability and region are supplied inside the combustion domain with suitable insulation and flame holders (Raghavan, 2016).

The design of a suitable fully aerated burner head emerges number of problems to the designer:

1. Fully aerated burners have bigger dimensions than partially aerated burners because of much higher volume flow rates needed.
2. Burner ports should be designed according to preventing flame lift, blow-off and burner overheat.
3. Incomplete combustion ought not to be a problem that there is no flame quenching and suitable gas mixing supplied.
4. Noise can create problems due to high primary aeration inside the burner and the combustion chamber.

One main advantage of the fully aerated burner is that burner has small length flames and momentum effects are more dominant than buoyancy effects. Thus, one designer can install the burner upwards, sideways, or downwards. Therefore, it supplies greater flexibility for placing the burner inside the appliance, especially solving condensing problem inside condensing boilers (Jones, 1989).

2.4 Standards and Regulations

In this part of the thesis, the standards and regulations covering the boilers and the components in the boilers are mentioned.

Directive of the European Commission (EC) with the number of 2002/91/EC is published in 2003. In compliance with this directive, encourage enhancement of building energy performance considering indoor and outdoor air conditions by supplying climate requirements and relevant costs. EC is issued a mandate to CEN in 2004. This mandate question CEN to organize standards for building energy performance, measuring environmental impact in compliance with the published directive. The standards must contain energy usage and loss calculation for residential heated water and heating, ventilation and air conditioning (HVAC) indoor systems

considering essential auxiliary components for supplying comfortable indoor environment (Olesen & de Carli, 2011).

European Union (EU) directive 92/75/EC is created for energy labelling of electrical devices which is upgraded by Directive 2010/30/EU. This directive has been implemented successfully for energy efficient devices about 20 years. Labelling endeavors are resulted as strict energy efficiency requirements on central heating boilers. Gas-fired boilers efficiency requirements with CE labelling are defined in the directive 92/42/EC which was afterwards altered by the directive 2004/8/EC. The framework to determine eco-design requirements for energy-related products established by Directive 2009/125/EEC splits central heating boilers into eight performance levels by product labeling, ranging from A (best) to H (worst). (European Committee for Standardization, 2003). Power of this EU policy gives acceleration to change lower efficiency devices with the higher efficiency ones. In near future, boilers with lower efficiency cannot be sold in the EU countries (De Paepe et al., 2013).

European conformity (CE) label of the boilers are given by *Notified Bodies* that are known by the European Union. A *Notified Body* controls test laboratory of boiler manufacturers according to standards for gas-fired heating boilers (De Paepe et al., 2013).

According to standard of gas-fired heating boilers (EN 15502-1:2012+A1:2015) which is published by European Committee for Standardization (CEN), “A gas-fired heating boiler is an appliance using gas as fuel designed to heat water with the purpose of providing heat to a building (or portion of a building) from one point to multiple rooms using heat emitters such as radiators and convectors to transmit the heat from the water to the room. The boiler may also be used to provide domestic hot water via an indirect hot water storage tank” (European Committee for Standardization, 2015).

In European Union countries, as of September 2015, standards have been set according to the Energy Related Products (ERP) regulations, and the boilers have been labeled according to their energy class. For this reason, the development of energy efficient heating devices has become important. Boiler producers need to do a lot of

engineering work to make their existing and design new products compatible with these legal regulations (Avci et al., 2015).

The gas-fired central heating boilers standard (EN 15502-1:2012+A1:2015) defines common necessities and test methods of heating devices that utilize via atmospheric or fan-driven burners including suitability for purpose, safety, construction, classification, energy usage levels and labelling. Gas-fired heating boilers standard covers type B and C boilers that;

a. utilize with combustion gases according to EN 437 test gases standard,
b. have less than temperature of 105 °C heat transfer fluid while in normal operation,
c. have maximum operating pressure of 6 bars on water lines,
d. can contain condensation under specific conditions,
e. installed inside or protected region of a building,
f. are declared in installation guides as condensing, low temperature or standard boiler,
g. produce hot water,
h. marketed as a solely unit (European Committee for Standardization, 2015).

In the domestic boiler manufacturing sector, boilers utilize commonly with gaseous fuels (Schiro et al., 2017). Premixed burners have lower pollutant emissions in comparison with non-premixed boilers. This situation makes them mandatory in near future inside EU countries (European Committee for Standardization, 2018).

EN 437 Test gases, test pressures and categories of appliances standard gives specific information on the utilization of combustion fuels of first, second and third families. This document needs to be referenced by boiler designers and manufacturers within the scope of appliances and EU countries. The standard offers recommendations about utilizing the gases and pressures for the experiments and appliance tests. This standard incorporates reference requirements from other publications that are out-of-date or not current. (European Committee for Standardization, 2018).

The devices fed by various gas types need to be tested with a reference gas and other limit gases such as flame lift, overheating, flashback, soot, and incomplete combustion. The condensing boilers containing premixed burner have leading technology, but burner designs are still implemented with using a trial-and-error approach. (Schiro et al., 2017). Thus, condensing boiler and its premix burner design need to be carefully evaluated and improved under recommendations of the standards and regulations.

Gas-fired heating devices are tested in structural, combustion performance, electrical safety, and thermal efficiency to ensure safe operation. In order to reach the requirements of all tests and applications, the standards of the relevant device should be evaluated in detail by the designers (Gattei, 2008).

2.5 Combustion in Condensing Boilers

The general definition of combustion is "rapid oxidation producing heat, or both heat and light; also, slow oxidation associated with relatively small amount of heat and no light." The rapid oxidation definition is all that is often used by practical combustion devices. Significance of combustion is coming from energy transformation of stored energy in chemical bonds to heat in different ways (Turns, 2000).

Most of the energy we tend to use these days is predicated on a chemical process known as combustion. The combustion method needs a fuel, essentially an organic compound and oxidizer. Fuel and oxidants along are known as reactants. Atoms and electrons arrange to generate products once a chemical reaction occurs, breaking the bonds between the molecules of the reactants at regular intervals. In combustion reactions, fast oxidization of flammable parts of the reactants leads to energy unharness as products of combustion are shaped. When all other combustible components have entirely oxidized and all carbon, hydrogen, and sulfur atoms have been transformed to carbon dioxide, water, and sulfur dioxide, respectively, combustion is considered to be complete. When this condition did not meet combustion is incomplete. Combustion reaction can be summarized as reactants transforming into products. (Çoban, 2015).

At ambient pressure and room temperature, the fuel air mixture is primarily non-reactive. In addition, if an ignition takes place, the temperature rises quickly or highly concentrated radicals develop, and an area of explosive reaction spreads across the mixture within specific flammability limits (McAllister, 2011).

Both flame-like and non-flame types of combustion are possible. Premixed flames and non-premixed (diffusion) flames are two different types of combustion flames. According to their names, the two kinds of flames premixed and non-premixed (or diffusion) are connected to the reactant mixing process. The types of flame are shown in Figure 4.1 from diffusion to premixed flame. In a premixed flame, the fuel and the oxidizer are combined molecularly before any crucial chemical reactions take place. A cylindrical condensing boiler burner can be an example to premixed flame. On the other hand, a non-premixed flame, the reactants flow separately, and reaction occur when the fuel and oxidizer meet at the combustion region where mixing and reaction both come into existence. Simple candle is a good example of non-premixed flame (Turns, 2000). Flame types from diffusion to premixed flame are shown in Figure 2.13.

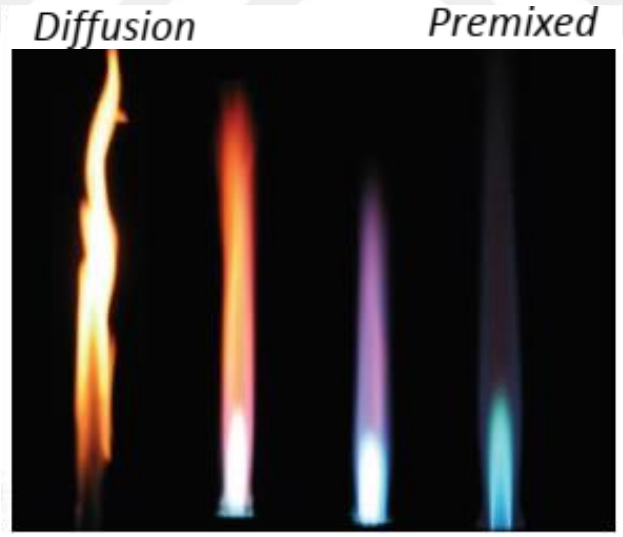


Figure 2.13 Flame types from diffusion to premixed flame (Raghavan, 2016)

General terminology and different classifications of fundamental combustion phenomena are given as below.

Premixed and Non-premixed Combustion: In classification of combustion phenomena, this is most significant case. A combustion system generally includes at

least an oxidizer and a fuel. These components should be merged at the molecular dimension before chemical combustion reaction. Thus, mixing mechanisms influence combustion significantly. Mixing means that one of the reactants molecules should be spilt into other reactant molecules (Law, 2006).

No matter if the reactants are combined or not, the combustion system performs differently. In premixed gaseous mixture, the reactants perfectly merge before the reaction. However, in non-premixed system, the reactants separately goes into the combustor chamber. At the chamber they meet each other the combustion region where stirring and afterwards reaction take place. Besides that, diffusion is dominant factor in non-premixed combustion rather than premixed combustion (Law, 2006).

In Bunsen burner, fuel and oxidizer entrain the combustion region separately and merge through the burner tube. After that, combustion starts with a premixed flame. If air flow rate controlled by a mass flow controller, mixture can fuel rich of fuel lean depending on air content in the combustion region. The excess oxygen in this mixture will remain unreacted and be discharged into the atmosphere if the fuel is lean. However, if it is contains fuel rich mixture, excess fuel may react with oxygen in the surrounding air after going through the premixed flame.. Thus, whole Bunsen flame consists of a premixed flame and non-premixed flame together. The fundamental example of flame is shown as “Bunsen Flame” in Figure 2.14 (Law, 2006).

Laminar and Turbulent Combustion: Here, the flame is defined with flow structure as laminar or turbulent. Streamlines occur in a laminar flow, however, in a turbulent flow quantity have fluctuations in respect to time incidentally. Turbulence mostly creates low mixing and therefore non-premixed combustion systems are strongly influenced (Law, 2006).

Subsonic and Supersonic Combustion: Another way to define the flow is to investigate velocity components. In a subsonic flow, reactions have more time in diffusion which has molecular collisions. These flames come across in real life as candle or pilot flames. In supersonic flow, reaction have less time to proceed and therefore high flow rates causes domination of diffusive transport by convective

transport components. Supersonic combustion is generally seen in fast flights and detonations (Law, 2006).

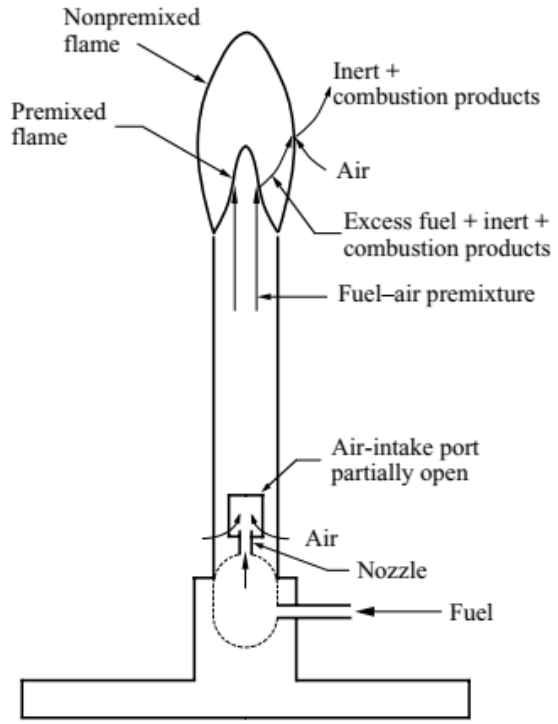


Figure 2.14 Schematic of the Bunsen flame (Law, 2006)

Heterogeneous and Homogeneous Combustion: he most difficult definition of terms in combustion literature is this one. Combustion is typically referred to as homogeneous if both reactants are originally present in the same fluid phase, either liquid or gas. Bunsen flame can be counted as an example of homogeneous combustion. On the contrary, heterogeneous combustion occurs with reactants which exist in different phase in the combustion region. Thus, coal combustion with air is one of the heterogeneous reactions (Law, 2006).

2.5.1 Non-premixed (Diffusion) Flames

The fuel and oxidizer entrain the combustion chamber separately in various combustion processes. As a result of diffusion, which brings fuel and oxidizer to the combustion zone, reactions of combustion are referred to as "non-premixed flames" or "diffusion flames." A candle flame is a good example as a non-premixed (diffusion) flame (McAllister, 2011). Diffusion flame mechanism is demonstrated in Figure 2.15.



Figure 2.15 Diffusion flame mechanism

Various combustion systems are utilized by non-premixed burners in case of safety. Non-premixed burners have less risk of explosion due to the unmixed condition of fuel and oxidizer. In non-premixed combustion systems, fuel and oxidizer entrain the combustion region from different ways. The transport process handled primarily by diffusion effects. In general, chemical reactions happen quickly; however, burning speed is governed more by the speed of the transport and mixing processes than by chemical kinetics. Flames ultimately attain greater stability than other types of combustion. The stable state of diffusion flames provides convenient use in most practical applications, notably gas-turbine engines, and low NO_x combustors. Typical example of non-premixed combustion is demonstrated in Figure 2.16 with a candle flame.

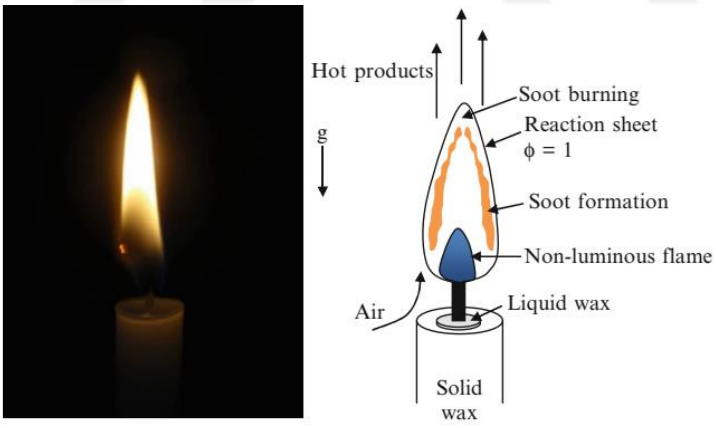


Figure 2.16 A typical candle flame and associated physical processes (McAllister, 2011)

Diffusion flames have a wider combustion region than premixed flames. In this region, chemical reactions occur and the composition changes because of the interaction between reactants and products. A non-premixed flame with a particular elevation is given in Figure 2.17 with respect to concentration of species (Glassmann & Yetter, 2008).

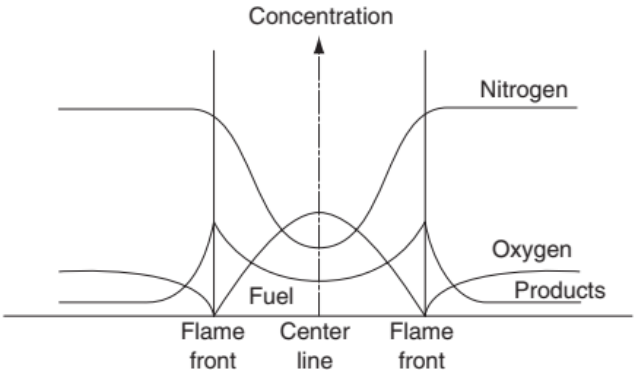


Figure 2.17 A non-premixed flame with a particular elevation with species alterations in jet fuel tube (Glassmann & Yetter, 2008)

Diffusion flames of the jets are defined by typical non-premixed flame properties, such as structure, position, temperature, and height. Computed temperature distribution (a) and experimentally visualization (b),(c),(d) of non-premixed flames are shown in Figure 2.18 (McAllister, 2011).

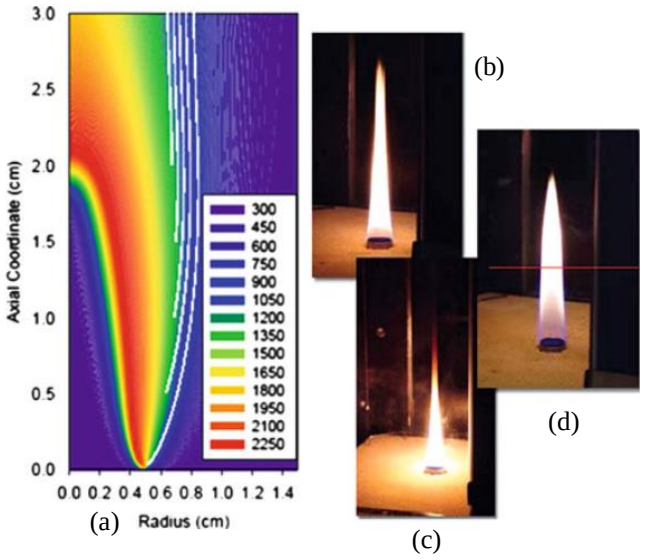


Figure 2.18 The distribution of temperature a) non-premixed numerically calculated flame and laminar flames of b) ethylene, c) P-8 fuel, d) CH_4 (methane) in the air (McAllister, 2011)

2.5.2 Premixed Flames

When combustion occurs with fuel and oxidizer that have been mixed before combustion region, emerging flame is called by “premixed flame”. Premixed flames exist in many practical combustion applications. Three different applications are

shown in Figure 2.19 as a) residential house furnace, b) industrial combustor with premixed conditions and c) residential lean premixed condensing boiler.



Figure 2.19 Premixed flame applications: a) Residential boiler, b) industrial low NOx combustor, c) residential lean premixed condensing boiler (McAllister, 2011)

In premixed flame combustors, fuel and oxidizer have already been combined at the molecular level before the combustion region. Either a spark or a pilot flame can ignite combustion, creating a flame that spreads into the unburned mixture. Knowing this flame's characteristics is essential for creating a functional burner. Diffusion flame mechanism is demonstrated in Figure 2.20.



Figure 2.20 Premixed flame mechanism

Maintaining a suitable design of the burner brings some relevant engineering questions:

1. How fast unburned mixture will be consumed?
2. How will operational conditions affect the speed of the flame? (temperature, pressure, equivalence ratio, etc.)
3. How long will be the flame length and height?
4. How flame characteristics effect the heat transfer mechanism?

These questions need to be evaluated and answered to reach a proper design for the burner of condensing boiler.

2.5.3 Physical Processes of Premixed Flames

A premixed mixture flowing in a duct, after ignition a flame propagates into the unburned gaseous mixture as demonstrated in Figure 2.21. The figure's lower portion depicts the premixed combustion's structural elements (McAllister, 2011).

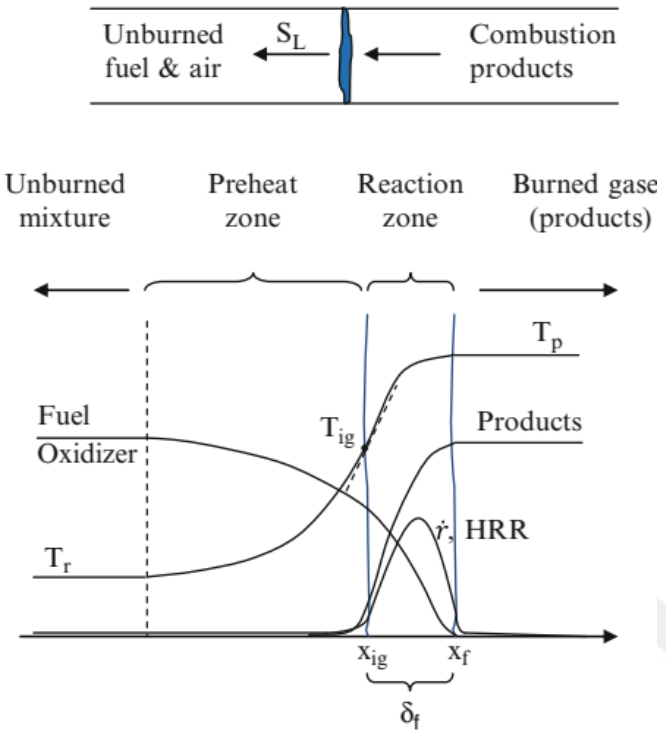


Figure 2.21 Schematic of a premixed flame flows through in a duct (McAllister, 2011)

Flame is quite thin in the burning zone, typically a few millimeters for hydrocarbon fuels under environmental circumstances. Near reaction zone, reactant temperatures raise to an elevated temperature due to burned species of the combustion. As fuel and oxidizer are utilized and products are generated, the reaction rate climbs quickly and then starts to decline. The temperature of the products approaches that of an adiabatic flame. In the combustion region, species emit radiation in different wavelengths that creates various colors on flames. Lean combinations of air and hydrocarbon fuels exhibit the blue color from radiation from excited CH radicals, whereas the reddish-orange color results from radiation from CO_2, water vapor, and ash particles. According to richer gaseous mixtures, C_2 molecules are excited and green color is observed in the flame (McAllister, 2011).

A typical laboratory flame, the Bunsen burner (Figure 2.22a) is an example of laminar premixed flames. Inner core of this flame shows premixed flame characteristics. Air and fuel flow together inside the tube and they mixed each other within this region. After that, combustion begins with a rich premixed inside flame which is covered with a non-premixed diffusion flame. The flame's shape is formed by the velocity profile and heat losses to the tube walls. For maintaining flame stability inside the inner cone, speed of unburnt gas normal component should be same with the flame speed, as demonstrated in Figure 2.22b with vector diagram (Turns, 2000).

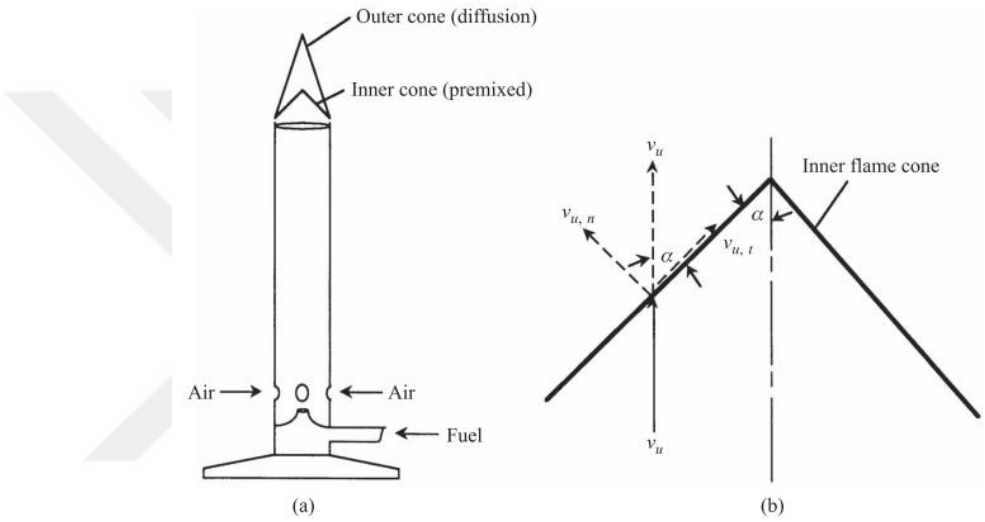


Figure 2.22 a) Bunsen burner, b) normal and tangential component of unburned gas velocity (Turns, 2000)

Common hydrocarbon fuels mixed with oxidizer have a combustion wave velocity of about 400 mm/s. Speed of this propagation wave based on transport variables, concurrent heat diffusion and conduction (Glassmann & Yetter, 2008).

2.5.4 Laminar Premixed Flames

Laminar premixed flames, which are related with diffusion flames, have application in various residential, commercial, and industrial devices and processes. Ovens, furnaces, heating appliances and Bunsen burners can be counted as examples of laminar premixed flame. Advanced residential and domestic cooktop burner is shown in Figure 2.23 and 2.24, respectively (Özdemir, 2017; Turns, 2000). Furthermore,

cylindrical lean premixed burner assembly is illustrated in Figure 2.25 below (P. H. Lee & Hwang, 2013).

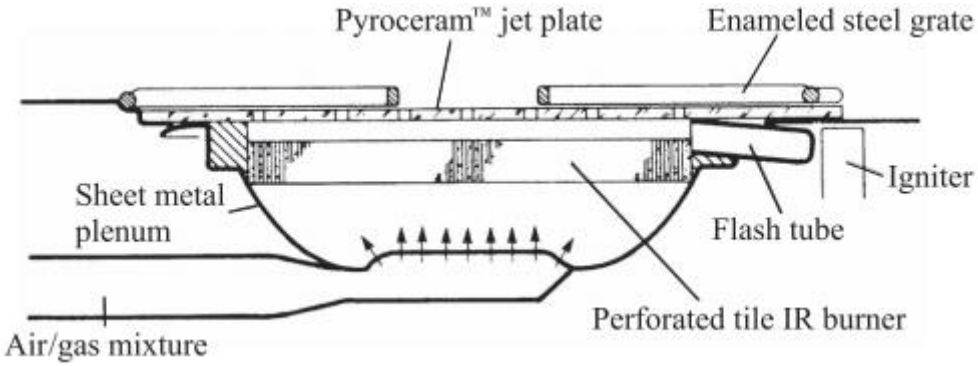


Figure 2.23 Schematic of an advanced residential cooktop burner (Turns, 2000)

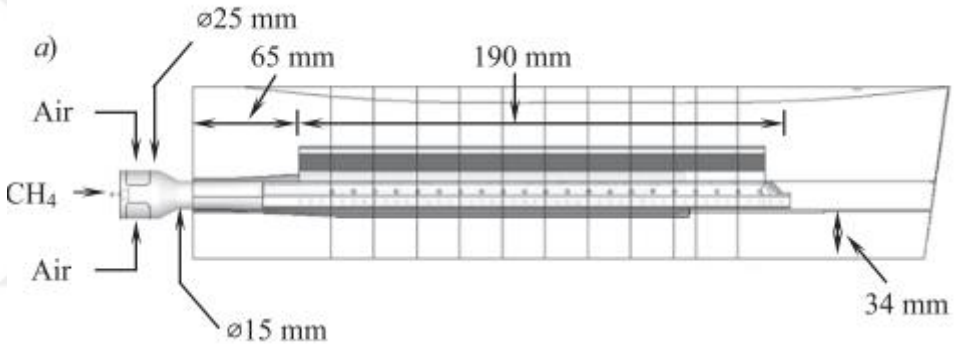


Figure 2.24 Schematic of a domestic cooktop burner (Özdemir, 2017)

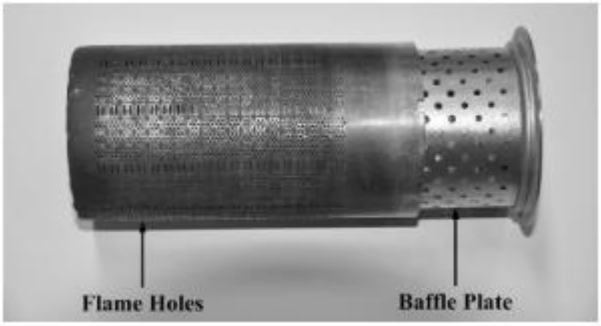


Figure 2.25 Cylindrical lean premixed burner with baffle plates (P. H. Lee & Hwang, 2013)

Premixed flames have small thickness in orders of millimeters at 1 atm. Thus, correct measurement of species concentration is tough. Investigating the characteristics of a common premixed flame, computations with detailed chemistry

and transport are crucial. A typical methane-oxidizer premixed flame structure using a detailed methane mechanism is shown in Figure 2.26. Computations have been realized with GRI 3.0 detailed methane mechanism (McAllister, 2011).

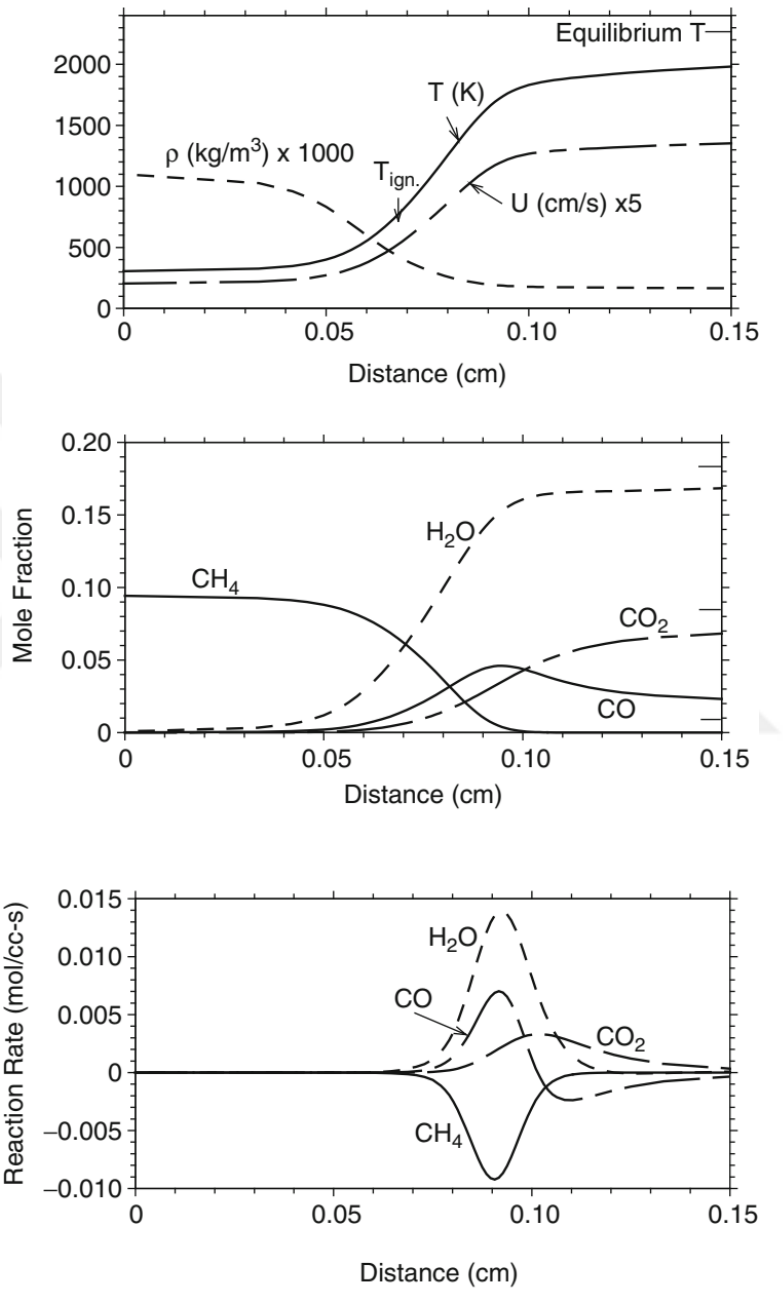


Figure 2.26 Stoichiometric methane-air flame mechanism at standard conditions (McAllister, 2011)

2.5.5 Combustion with Premixed Flames in Condensing Boiler

In the early periods, non-premix flames with Bunsen burners were preferred in condensing boilers. This was causing two separate problems with the burners. The first problem was that when the thermal efficiency increased, the heat transfer increased, but incomplete combustion and soot formation took place. In addition, due to the high flue gas outlet temperatures, nearly 25% of the energy was lost. The second problem was that because the Bunsen flames were large in size, the gases remained in the combustion chamber for longer and NO_x emissions were generated as a result of increased temperature. This situation revealed that devices with Bunsen burner could not meet the energy and environmental requirements specified in the standards (S. Lee et al., 2011b).

Today, instead of Bunsen burners, burners with premix flames are preferred in various practical applications such as ovens, gas turbines and boilers. Because devices with premix flames can meet the high efficiency and low pollutant gas emissions demanded by the standards. In general, premix flames are shorter than non-premix flames in length. Thus, NO_x, CO and soot emissions can be reduced by making precise adjustments to their equivalence ratios (S. Lee et al., 2010). In addition, premix flames reduce the possibility of thermal NO and prompt NO formation. Thus, premix burners provide great convenience in condensing boiler design (Liu et al., 2020).

According to European Environmental Agency (EEA) report for European countries, these residential boilers that commonly burn natural gas have emission factors of 46 g/GJ for CO and 57 g/GJ for NO_x and, respectively. Thus, various standards have been introduced to prevent these pollutant gases' environmental effects on the boilers. Condensing boilers were first introduced in Europe and Asia to meet the requirements in the standards .One of these standards' purposes is to reduce the CO and NO_x emission levels of gas-fired heating boilers following the European Union regulations such as EN 15502-1:2012+A1:2015 (European Committee for Standardization, 2015). Therefore, it is crucial to examine the combustion parameters and effects that create these emissions (S. Lee et al., 2011b; Yılmaz et al., 2021).

The heating unit of the condensing boiler contains a cylindrical combustion region between cooling coils and a perforated, multi-hole, cylindrical premix burner. Cross sectional view of a cylindrical heating unit is shown in Figure 2.27 (Hinrichs et al., 2018).

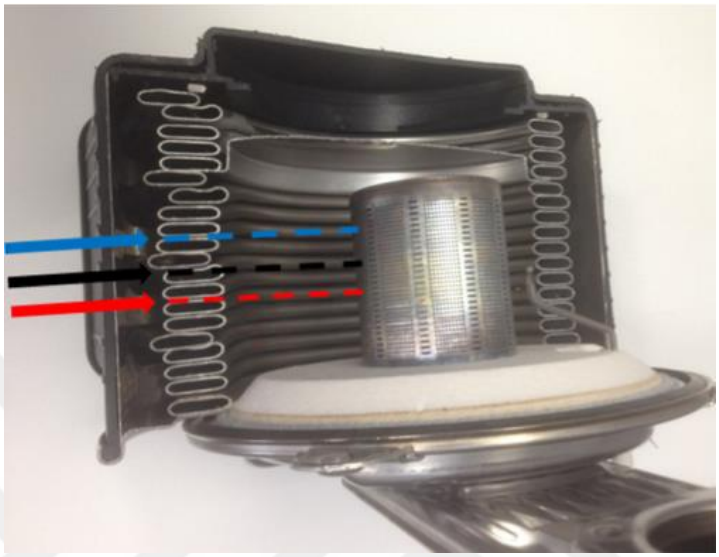


Figure 2.27 Cross sectional view of a cylindrical heating unit (Hinrichs et al., 2018)

A cylindrical, multi-hole, premixed burner (a) and flame image (b) are demonstrated in Figure 1.28.

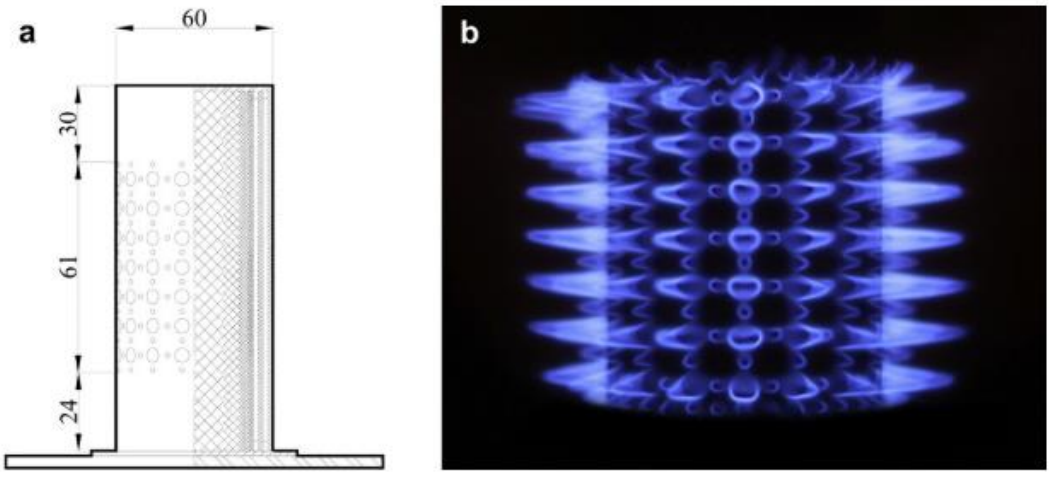


Figure 2.28 a) Cylindrical perforated premixed burner and b) visual of the flame (S. Lee et al., 2011b)

These burners, which have a cylindrical structure, are first produced by punching thin metal plates with many holes and then bending the plate to form a can-like shape. Under the necessary conditions, uniform flow and protection from the flashback are ensured by having guiding channels in its inner structure and a porous cover with a mesh in its outer region.

CHAPTER THREE
THEORETICAL INVESTIGATION OF COMBUSTION IN CYLINDRICAL COMBUSTION REGION

"The human relationship to combustion is as mysterious as it is fraught with madness. From the candle flame to the nuclear blast, it has lit up the human imagination with fear and fascination." Michael Leunig

Michael Leunig's statement explains why we explore combustion processes involving physical and chemical perspectives. In this research process, he states that the flames formed as a result of combustion are also a source of light that illuminates our path.

Equilibrium product temperature and composition are key factors in evaluating combustion systems. The adiabatic flame temperature is the temperature reached when the entire heat produced throughout the reaction is utilized to raise the temperature of the final product. The topics in chemical thermodynamics need to be well understood and reviewed because temperature and gas composition are crucial factors in the combustion process (Glassmann & Yetter, 2008).

In this chapter, theoretical aspects of combustion and investigation in the combustion domain on condensing boiler are explained in detail.

3.1. Methodology

It is necessary to describe in detail intricate chemical kinetic systems composed of hundreds or even thousands of species to analyze the chemical equilibrium. As the carbon ratio in the fuels used in combustion increases, the number of species and reaction steps expand. This condition prevents researchers from physically coping with these major mechanisms. Today's computers can reduce chemical kinetic mechanisms, but even with these reduced mechanisms, solutions to multidimensional problems turn out to be impractical for engineers and researchers. CFD applications for large-scale geometries can process reduced mechanisms, but the processor and memory needs are insufficient for these mechanisms with hundreds of types. In addition, in combustion applications performed with CFD, all parameters must be followed throughout the

domain. For all these reasons, researchers have turned to theoretical methods that can estimate combustion products and adiabatic flame temperatures without the need for chemical kinetic mechanisms (McAllister, 2011).

Thus, engineers and researchers developed practical techniques for applying combustion sciences to engineering issues. Among these methods, Gibbs energy minimization and equilibrium constants methods were accepted by the literature and came to the fore in applications (Gonca, 2014; Kayadelen & Ust, 2013; Nabi, 2010; Néron et al., 2012; Sreejith et al., 2013). Gibbs energy minimization can provide results with the desired precision by using only mathematical methods, without the need for chemical kinetic mechanisms. Equilibrium constant methods, on the other hand, can reach results numerically quickly without the need for complex programs if the equilibrium constants are known. Both methods can be easily adapted to various combustion applications involving different fuel or fuel mixtures. The output data obtained from the specified methods can be used as input data for CFD applications and experimental studies, as well as provide convenience for practical applications.

Equilibrium on chemical processes is commonly dealt with chemical equilibrium and chemical kinetics approaches. Formulations of equilibrium constants and minimization of free energy define the chemical equilibrium with equivalent approaches. In the scope of the thesis, computational codes were created within these two approaches, and a theoretical study was implemented for standard gases as methane (G20), test gas (G25), and natural gas (NG) with various equivalence ratios. The fuel/air ratio is used here to define equivalence ratio (Yılmaz et al., 2021).

For calculating chemical equilibrium, combustion stoichiometry, reactant/product gas properties with various components are crucial aspects. The equations of thermodynamic properties are needed to be developed for combustible gas mixtures. The thermodynamic properties are functions of temperature, pressure and molar fractions of the species participating in combustion. Oxidizer properties are important for combustion (Ferguson & Kirkpatrick, 2016). In this thesis, the main oxidizer is chosen as air. The air is assumed as an ideal gas with 21% oxygen and 79% nitrogen by volume.

After these brief explanations, theoretical investigation methods are explained in the following section of this chapter. Detailed descriptions of the two methods used in the proposed models are presented in Sections 3.1.1 and 3.1.2. The data obtained from these two methods were compared with the commercial software (CHEMKIN) using element potential method. The element potential method is briefly explained in the Section 3.1.3.

3.1.1 Gibbs Energy Minimization Method

The equilibrium state can be expressed as in Equation 3.1 by combining the equations of laws of the thermodynamics.

$$dE = TdS - PdV \tag{3.1}$$

where E is energy, S is entropy, T is temperature, P is pressure and V is volume. This condition shows that the change from any effects of a constant-mass system when the effects of gravitational, electric, and surface forces are neglected. However, the system's energy level alters when mass is introduced. If a molecule (i) added on the system, total system energy rises as μ_i, which is called as chemical potential. A small amount of same material (dn_i) increases the system's overall energy ($\mu_i\, dn_i$). All realizable reversible process improves the system energy according to each type of molecule (i) is defined as in Equation 3.2.

$$dE = TdS - PdV + \sum_i \mu_i dn_i \tag{3.2}$$

Taking into consideration the definition of enthalpy and the fundamentals of Gibbs free energy, Gibbs energy (G) can be expressed with thermodynamic specifications of total enthalpy (H), entropy (S), and temperature (T) in Equation 3.3.

$$G \equiv H - TS \tag{3.3}$$

From the property relations of thermodynamics, dH and dG can be defined as in Equation 3.4 and 3.5.

$$dH = TdS - VdP + \sum_i \mu_i dn_i \tag{3.4}$$

$$dG = -SdT + VdP + \sum_i \mu_i dn_i \tag{3.5}$$

Pressure and temperature are intensive specifications affected by how much matter is present in a system. However, energy, enthalpy, Gibbs energy, volume, number of moles and entropy are extensive specifications that change proportionally with mass. According to the inherent relationship between the total derivative of G and the variables, chemical potential can be expressed as in Equation 3.6.

$$\mu_i = \left(\frac{\partial G}{\partial n_i} \right)_{T,P,n_j} \tag{3.6}$$

Entropy can be used to maintain a system's equilibrium if it reaches its maximum value for all potential possibilities that involve constant volume and energy. While in maximum entropy conditions, any change from its equilibrium condition differential entropy change is zero. In this situation, the last term in Equation 3.2 equals to zero and can be given as in Equation 3.7.

$$\sum_i \mu_i dn_i = 0 \tag{3.7}$$

The property of chemical potential is crucial in reacting systems. In this aspect, while chemical potential decreases in the reaction, equilibrium can only be reached when the expected amount of the reactants and products is equal. Therefore, at constant temperature and pressure, equilibrium can be reached with minimum Gibbs energy condition as in Equation 3.8.

$$\left(dG\right)_{T,P} = 0 \tag{3.8}$$

In the thesis, minimization of Gibbs energy process is based on the NASA's reference report for the computation of complex chemical equilibrium compositions in the combustion. Equilibrium condition for various thermodynamic functions could be maintained by the maximization of entropy or the minimization of the Gibbs free energy. According to thermodynamic state characterization with temperature and pressure, Gibbs energy minimization is an easy and useful process. NASA developed

a multi-functional and multi-purpose computer algorithm and code for obtaining chemical equilibrium compositions and temperature as mainly used in combustion calculations in NASA Lewis Research Center (Gordon & McBride, 1994). This computer code utilizes Gibbs energy minimization method for solving Newton Raphson equations iteratively (Glassmann & Yetter, 2008).

A combustion problem generally is considered a process that contains many product species. Prior to combustion, the fuel and air intervene with an specific equivalence ratio (ϕ). Right after the combustion, the reaction's byproducts are thought to be in equilibrium at a given temperature and pressure. The thermodynamic properties and composition of the reaction product are to be emerged on the reaction. For one mole of fuel, the total combustion reaction can be defined as in Equation 3.9 (Ferguson & Kirkpatrick, 2016).

$$C_a H_b O_c N_d + \left(\left(a + \frac{b}{4} - \frac{c}{2}\right)/\phi\right)(O_2 + 3.76N_2) \rightarrow$$

$$n_1 CO_2 + n_2 H_2 O + n_3 N_2 + n_4 O_2 + n_5 CO + n_6 H_2 + n_7 H + \tag{3.9}$$

$$n_8 O + n_9 OH + n_{10} NO + n_{11} N + n_{12} C(s) + n_{13} NO_2 + n_{14} CH_4$$

Chemical systems that are in chemical equilibrium allow for the calculation of the system's thermodynamic specifications. These specifications can be utilized various problems in chemistry, chemical engineering, and combustion (Gordon & McBride, 1994).

Chemical equilibrium equations are defined in each time interval could solve combustion problems, but it takes so much time. Instead of this, Gibbs free minimization could be used to find an equilibrium state. For a mixture Gibbs free energy of the reaction is demonstrated by Equation 3.10 (Çoban, 2015; Gordon & McBride, 1994).

$$G = \sum_{j=1}^{ns} \mu_j n_j \tag{3.10}$$

Here ns is number of species, μ chemical potential and G is Gibbs free energy. Chemical potential is defined as per kmol by Equation 3.11.

$$\mu_j = \left(\frac{\partial G}{\partial n_j} \right)_{T,P,n_{i \neq j}} \tag{3.11}$$

The mass balance constraints of the minimization are given with Equation 3.12 or 3.13.

$$\sum_{j=1}^{ng} A_{ij} n_j - b_i^0 = 0, \ (i = 1 \ldots ne) \tag{3.12}$$

$$b_i - b_i^0 = 0, \ (i = 1 \ldots ne) \tag{3.13}$$

Here i number of chemical elements (ne), A_{ij} is number of kilogram atoms per kmole of species j and b_i^0 is the assigned number of kg atoms element i for one kmole of reactants in total. Chemical potential can be written with ideal gas assumption in Equation 3.14.

$$\mu_j = \mu_j^0 + RT \ln\left(\frac{n}{n_j} \right) + RT \ln(P), \ (j = 1 \ldots ns) \tag{3.14}$$

where μ_j^0 is chemical potential for gases and G' term can be defined with Equation 3.15.

$$\boldsymbol{G'} = \boldsymbol{G} + \sum_{\boldsymbol{i}=1}^{\boldsymbol{ne}} \lambda_{\boldsymbol{i}} (\boldsymbol{b_i} - \boldsymbol{b_i^0}) \tag{3.15}$$

Here λ_i is Lagrangian multiplier, where equilibrium equation becomes in Equation 3.16.

$$\delta \boldsymbol{G'} = \sum_{\boldsymbol{j}=1}^{\boldsymbol{ng}} \left(\mu_{\boldsymbol{j}} + \sum_{\boldsymbol{i}=1}^{\boldsymbol{ne}} \lambda_{\boldsymbol{i}} \boldsymbol{A_{ij}} \right) \delta \boldsymbol{n_j} + \sum_{\boldsymbol{i}=1}^{\boldsymbol{ne}} (\boldsymbol{b_i} - \boldsymbol{b_i^0}) \delta \lambda_{\boldsymbol{i}} = 0 \tag{3.16}$$

Along with independent variables of δn_j and $\delta\lambda_i$, equation occurs as in Equations 3.17 and 3.18.

$$\mu_j + \sum_{i=1}^{ne} \lambda_i A_{ij} = 0 \tag{3.17}$$

$$b_i - b_i^0 = 0 \tag{3.18}$$

These equations above are not linear with composition variables for obtaining gaseous combustion products. Thus, the Newton Raphson method is used iteratively for predicting moles of compositions (n_j), gaseous species (n), Lagrangian multipliers (λ_j), and if essential also the temperature (T).

By opening these equations to Taylor series and simplification the following set of equations, Equations 3.19 and 3.20 are obtained.

$$\begin{aligned} &\sum_{i=1}^{ne}\sum_{j=1}^{ng} \boldsymbol{A_{kj}A_{ij}n_j}\pi_i + \left(\sum_{j=1}^{ng} \boldsymbol{A_{kj}n_j}\right)\Delta\ln \boldsymbol{n} + \left(\sum_{j=1}^{ng} \frac{\boldsymbol{A_{kj}n_jH_j^0}}{\boldsymbol{RT}}\right)\Delta\ln \boldsymbol{T} \\ &= \boldsymbol{b_k^0} - \boldsymbol{b_k} + \sum_{j=1}^{ng} \frac{\boldsymbol{A_{kj}n_j}\mu_j}{\boldsymbol{RT}} \end{aligned} \tag{3.19}$$

$$\begin{aligned} &\sum_{i=1}^{ne}\sum_{j=1}^{ng} \boldsymbol{A_{kj}A_{ij}n_j}\pi_i + \left(\sum_{j=1}^{ng} \boldsymbol{A_{kj}n_j}\right)\Delta\ln \boldsymbol{n} + \left(\sum_{j=1}^{ng} \frac{\boldsymbol{A_{kj}n_jH_j^0}}{\boldsymbol{RT}}\right)\Delta\ln \boldsymbol{T} \\ &= \boldsymbol{b_k^0} - \boldsymbol{b_k} + \sum_{j=1}^{ng} \frac{\boldsymbol{A_{kj}n_j}\mu_j}{\boldsymbol{RT}} \end{aligned} \tag{3.20}$$

Here H_j^0 is the standard molar enthalpy for a specific temperature (T) for each species and π_i is defined as $\pi_i = -\lambda_i / RT$ (Çoban, 2015; Gordon & McBride, 1994).

An in-house computer model (Model 1) was developed including these equations within the scope of thesis work. Model 1 was created with Java programming language. The proposed model was developed based on complex chemical equilibrium procedure of NASA (Gordon & McBride, 1994) including the Gibbs energy minimization method (Çoban, 2015). Chemical equilibrium, species compositions,

heating values and adiabatic flame temperatures for various equivalence ratios can be predicted with numerical codes of Model 1.

This model has superior features over the commercial software such as CHEMKIN using the element potential method and other methods such as equilibrium constants method. The relevant model can perform calculations without the need for equilibrium constants. By using only mathematical methods, it requires less data and gives very good results with high numerical precision. Furthermore, the proposed model does not need chemical kinetic mechanisms for each fuel type. The algorithm of Model 1 can modified easily to utilize with commercial boilers, gas turbines, engines, and other combustion systems for various fuels or fuel mixtures. Algorithm flowchart of Model 1 is demonstrated in Figure 3.1.

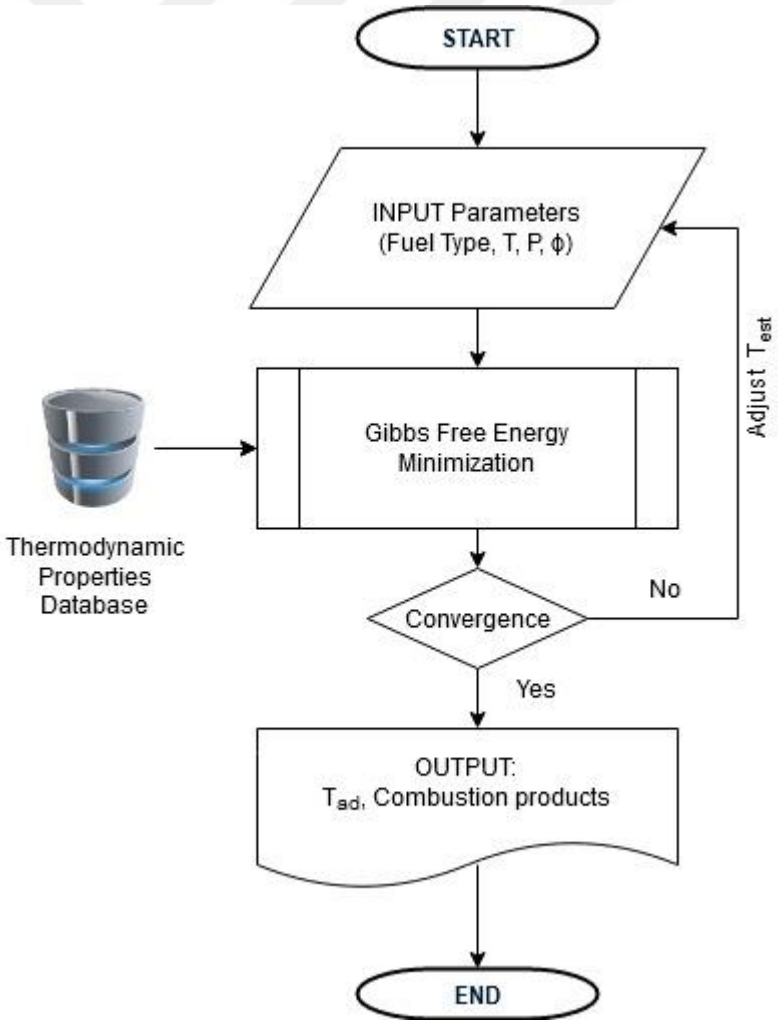


Figure 3.1 Algorithm flowchart of Model 1 (Yılmaz et al., 2021)

As can be seen from the Figure 3.1, fuel type, initial prediction of the temperature, inlet temperature and pressure of the gaseous fuel and air, equivalence ratio are supplied to algorithm as input parameters. Then, the database of thermodynamic properties is used by the main Gibbs energy minimization function for calculating the properties of reactants and products. In this calculation process, it is important to employ suitable curve fitting method. In this process, well-known least-squares curve fitting method is applied to acquire curve fitting coefficients of properties for determined pressure and temperature. These coefficients must be determined correctly, otherwise there will be deviations in the estimated values of the combustion products.

To solve minimization equations, Gibbs energy minimization function processes inputs of the algorithm and thermodynamic properties with Newton Raphson iteration method. The convergence is achieved when the variables reach the absolute criteria ($\varepsilon < 10^{-7}$) in the iterations. One main function and five sub-functions are used in the minimization process. In order to ensure convergence in the Gibbs energy minimization function, the initial estimation values of the Newton Raphson method should be well determined. The logical and appropriately chosen initial prediction values will accelerate the process of convergence in the function. In cases where convergence cannot be achieved, the first estimate values of the adiabatic flame temperature are modified and the process steps are repeated to try to achieve convergence. After the convergence is achieved, the predicted outputs such as adiabatic flame temperature and species compositions are obtained.

3.1.2 Equilibrium Constants Method

In Gibbs energy minimization method, at constant temperature and pressure, equilibrium can be reached with minimum Gibbs energy condition as in the Equation 3.8. For an increasing Gibbs function at a specific temperature and pressure, the progression of the reaction violates the second law of thermodynamics, so this is not possible for chemical reactions. In other words, the reaction must take place with a view to lowering chemical potential. If the pressure and temperature change, the reacting system passes a different equilibrium state. In this case, it is a new temperature and pressure value that minimizes the Gibbs function (Çengel & Boles, 2015; Glassmann & Yetter, 2008).

To write an equation with a basic chemical equilibrium, two reactants (A and B) and two products (C and D) are given at a specific constant temperature and pressure. The number of moles these reactants and products can be determined as n_A, n_B, n_C, and n_D. When the pressure and temperature remain constant, one can consider a general chemical reaction as in Equation 3.21.

$$dn_A A + dn_B B \rightarrow dn_C C + dn_D D \tag{3.21}$$

The equilibrium condition defined in Equation 3.8 brings that the alteration in the Gibbs energy function of the gaseous mixture during the chemical reaction need to be equal to zero. Thus, Equations 3.22 or 3.23 can be defined as below.

$$(dG)_{T,P} = \sum (dG_i)_{T,P} = \sum (\bar{g}_i dn_i)_{T,P} = 0 \tag{3.22}$$

or

$$\bar{g}_C dn_C + \bar{g}_D dn_D + \bar{g}_A dn_A + \bar{g}_B dn_B = 0 \tag{3.23}$$

where $\bar{g}$ is the molar Gibbs energy (or chemical potential) at the known temperature and pressure and n is the differential differences in the number of moles of the reaction species. The relationship between moles of the components, one can write that the theoretical or stoichiometric reaction as in Equation 3.24.

$$\nu_A A + \nu_B B \rightleftharpoons \nu_C C + \nu_D D \tag{3.24}$$

where ν is the stoichiometric coefficient that can be calculated from known reactions. The stoichiometric reaction is important in determining the equilibrium compositions because the mole numbers of the components vary in direct proportion with the stoichiometric coefficients. Therefore, these proportionalities can be given in Equation 3.25.

$$dn_A = -\varepsilon_p \nu_A;\ dn_B = -\varepsilon_p \nu_B;\ dn_C = \varepsilon_p \nu_C;\ dn_D = \varepsilon_p \nu_D \tag{3.25}$$

where ε_p is the proportionality constant and shows the degree of the reaction. In front of the equations of the reactants A and B, a minus sign need to be included that

the number of moles of reactants A and B are running out while the reaction continues. If the expressions in Equation 3.23 and 3.25 are substituted and ε_p is eliminated, Equation 3.26 can be obtained.

$$\nu_C \bar{g}_C + \nu_D \bar{g}_D - \nu_A \bar{g}_A - \nu_B \bar{g}_B = 0 \tag{3.26}$$

Equation 3.26 includes molar Gibbs functions of reactants and products and stoichiometric coefficients. This situation is called as the chemical equilibrium criterion. This condition is valid for every reaction regardless of the phases. Equation 3.26 is defined as a basic equation but can be easily extended to any number of reactants and products if desired.

In this step, the chemical equilibrium criterion must be evaluated for ideal gases. For a condition with known temperature and pressure, a gaseous mixture can be considered inside the chemical equilibrium. The Gibbs function of an ideal gaseous mixture rely on both temperature and pressure. For the reference ambient pressure value (P_0 = 1 atm), Gibbs function values are usually shown in the tables versus temperature. The change of the Gibbs function with pressure at a constant temperature for an ideal gas is described by the Gibbs function and the entropy-exchange relationship for isothermal processes. Therefore, the Gibbs function of one species (*i*) at partial pressure P_i and gaseous mixture *T* can be shown as in Equation 3.27.

$$\bar{g}_i(T, P_i) = \bar{g}_i^*(T) + R_u T \ln P_i \tag{3.27}$$

where $\bar{g}_i^*$ is the Gibbs function of one species (*i*) at reference ambient pressure (1 atm) and temperature T, and P_i is the partial pressure of one component (*i*) in atm. If the Gibbs expression is substituted to Equation 3.26, then Equation 3.28 is obtained.

$$\begin{aligned} &\nu_C[\bar{g}_C^*(T) + R_u T \ln P_C] + \nu_D[\bar{g}_D^*(T) + R_u T \ln P_D] \\ &-\nu_A[\bar{g}_A^*(T) + R_u T \ln P_A] - \nu_B[\bar{g}_B^*(T) + R_u T \ln P_B] = 0 \end{aligned} \tag{3.28}$$

The variation of standard state Gibbs function can be defined as in Equation 3.29.

$$\Delta G^*(T) = \nu_C \bar{g}_C^*(T) + \nu_D \bar{g}_D^*(T) - \nu_A \bar{g}_A^*(T) - \nu_B \bar{g}_B^*(T) \tag{3.29}$$

Equations 3.28 and 3.29 can be merged to obtain Equation 3.30 as shown below.

$$\Delta G^*(T) = -R_u T(\nu_C \ln P_C + \nu_D \ln P_D - \nu_A \ln P_A - \nu_B \ln P_B) = -R_u T \ln \frac{P_C^{\nu_C} P_D^{\nu_D}}{P_A^{\nu_A} P_B^{\nu_B}} \quad (3.30)$$

According to the definitions, the equilibrium constant K_P can be defined for the chemical equilibrium of ideal gas reactions with Equation 3.31 and rearranged to form Equation 3.32.

$$K_P = \frac{P_C^{\nu_C} P_D^{\nu_D}}{P_A^{\nu_A} P_B^{\nu_B}} \quad (3.31)$$

$$K_P = e^{-\Delta G^*(T)/R_u T} \quad (3.32)$$

The equilibrium constant value for an ideal gas mixture at a certain temperature can be found by variation of the standard state Gibbs function for the same temperature value. Tables of equilibrium constants for several reactions could be obtained from various relevant resources (Çengel & Boles, 2015; Ferguson & Kirkpatrick, 2016; Glassmann & Yetter, 2008; McAllister, 2011).

With the knowledge of equilibrium constants, the chemical equilibrium compositions are determined for ideal gas reactions. The partial pressures of combustion mixture components in terms of molar ratios are crucial for determining the compositions. The relation between partial pressures and molar ratios is given as in Equation 3.33 respect to total pressure (P) and total number of moles (N_{total}) in the reaction (McAllister, 2011).

$$P_i = y_i P = \frac{N_i}{N_{total}} P \quad (3.33)$$

Substituting partial pressures in Equation 3.31, Equation 3.34 is obtained for the definition of equilibrium constant for two reactants and products. The number of reactants and products can be easily extended for the requirements of the reacting system.

$$K_P = \frac{N_C^{\nu_C} N_D^{\nu_D}}{N_A^{\nu_A} N_B^{\nu_B}} \left(\frac{P}{N_{total}} \right)^{\nu_C + \nu_D - \nu_A - \nu_B} \tag{3.34}$$

In the equilibrium constants method, which is used in the thesis, chemical equilibrium is supplied by the equilibrium of the reactants and products for the hydrocarbon fuels.

For applications of hydrocarbon combustion, a complete reaction should be defined for important product species in the combustion zone. According to combustion experiments, under ϕ < 3 equivalence ratios, the crucial products emerge from dissolving of O, OH, H, and NO. Thereby, from the Equation 3.9, the number of products can be truncated for only 10 species. Therefore, reaction of the hydrocarbon combustion can be written as in Equation 3.35 (Ferguson & Kirkpatrick, 2016).

$$C_a H_b O_c N_d + \left(\left(a + \frac{b}{4} - \frac{c}{2} \right) / \phi \right) \left(O_2 + 3.76 N_2 \right) \rightarrow$$

$$n_1 CO_2 + n_2 H_2O + n_3 N_2 + n_4 O_2 + n_5 CO + n_6 H_2 + n_7 H + n_8 O + n_9 OH + n_{10} NO \tag{3.35}$$

With knowledge of these basic concepts, a numerical solution algorithm (Model 2) is developed based on Olikara and Borman's method for the estimation of the gaseous components formed at final of the combustion (Olikara & Borman, 1975). The equilibrium constants method is very useful because it can be easily adapted to other fuels and combustion systems. Furthermore, quite satisfactory results can be obtained without the use of commercial and complex software. With this method, the solution is reached based on the Gibbs method, but the calculations are carried out without the need for the coefficient estimates that should be utilized in the Lagrange Multiplier Approach. In addition, the solution is achieved without the complex chemical kinetic mechanisms used by commercial software (CHEMKIN, etc.). If this method need to be used in $\phi \geq 1$ region, water-gas shift reaction equations should be taken into account in the combustion reaction (Ferguson & Kirkpatrick, 2016; Kayadelen & Ust, 2013).

To obtain thermodynamic functions, the report of NASA Glenn Research Center is referenced in the thesis. (McBride et al., 2002). The thermophysical properties are computed with the NASA Glenn coefficients specified for individual species of combustion. According to calculation method of NASA report and other relevant literature, the reactants and products of the combustion are assumed as ideal gas. Thus, temperature is the only parameter for thermophysical properties of the species.

The specific heats of reactants and products are calculated with NASA Glenn coefficients as in Equation 3.36 below (McBride et al., 2002).

$$\frac{C_p^\circ(T)}{R} = a_1T^{-2} + a_2T^{-1} + a_3 + a_4T + a_5T^2 + a_6T^3 + a_7T^4 \tag{3.36}$$

The enthalpy and entropy are computed with the integration of the $C_p^\circ(T)$ and $C_p^\circ(T)/T$ with respect to temperature as demonstrated in Equations 3.37 and 3.38 (McBride et al., 2002).

$$\frac{h^\circ(T)}{RT} = -a_1T^{-2} + a_2\frac{\ln(T)}{T} + a_3 + a_4\frac{T}{2} + a_5\frac{T^2}{3} + a_6\frac{T^3}{4} + a_7\frac{T^4}{5} + \frac{b_1}{T} \tag{3.37}$$

$$\frac{s^\circ(T)}{R} = -\frac{a_1T^{-2}}{2} - a_2T^{-1} + a_3\ln T + a_4T + a_5\frac{T^2}{2} + a_6\frac{T^3}{3} + a_7\frac{T^4}{4} + b_2 \tag{3.38}$$

According to hydrocarbon combustion equation that is defined in Equation 3.35, the atomic balance is calculated with the four main equations as shown in the Equations 3.39, 3.40, 3.41 and 3.42 (Ferguson & Kirkpatrick, 2016).

$$C:\ a = (y_1 + y_5)N \tag{3.39}$$

$$H:\ b = (2y_2 + 2y_6 + y_7 + y_9)N \tag{3.40}$$

$$O:\ c + \frac{2a_s}{\phi} = (2y_1 + y_2 + 2y_4 + y_5 + y_8 + y_9 + y_{10})N \tag{3.41}$$

$$N:\ d + \frac{7.52a_s}{\phi} = (2y_3 + y_{10})N \tag{3.42}$$

Here *N* is determined as the total number of moles in the combustion reaction. The molar fractions are handled from the total number of moles divided by the quantity of each type of mole. In here, the molar fractions are donated as y_i. To supply the general molar equilibrium, the total molar fractions must equal to 1. The Equations 3.43 and 3.44 show general molar equilibrium and definition of molar fraction.

$$\sum_{i=1}^{10} y_i = 1 \tag{3.43}$$

$$y_i = \frac{n_i}{N} \tag{3.44}$$

By merging these equations, three constants can be constituted as in Equation 3.45.

$$\begin{aligned} d_1 &= \frac{b}{a} \\ d_2 &= \frac{c}{a} + 2\frac{a_s}{\phi a} \\ d_3 &= \frac{d}{a} + \frac{7.52 a_s}{\phi a} \end{aligned} \tag{3.45}$$

By substituting and rearranging atomic balance equations and sum of total number of moles, Equations 3.46, 3.47, 3.48, and 3.49 can be rearranged (Ferguson & Kirkpatrick, 2016).

$$2y_2 + 2y_6 + y_7 + y_9 + d_1 y_1 - d_1 y_5 = 0 \tag{3.46}$$

$$2y_1 + y_2 + 2y_4 + y_5 + y_8 + y_9 + y_{10} - d_2 y_1 - d_2 y_5 = 0 \tag{3.47}$$

$$2y_3 + y_{10} - d_3 y_1 - d_3 y_5 = 0 \tag{3.48}$$

$$\sum y_i = 1 \tag{3.49}$$

In the gas phase reactions below, method of the calculation of the K coefficients are given in Equations 3.50 to 3.55 with pressure units of atmospheres (atm). These

coefficients are utilized for the separation of the products and the formation of the NO and OH (Ferguson & Kirkpatrick, 2016).

$$\frac{1}{2}H_2 \rightleftharpoons H \qquad K_1 = \frac{y_7\sqrt{P}}{\sqrt{y_6}} \tag{3.50}$$

$$\frac{1}{2}O_2 \rightleftharpoons O \qquad K_2 = \frac{y_8\sqrt{P}}{\sqrt{y_4}} \tag{3.51}$$

$$\frac{1}{2}H_2 + \frac{1}{2}O_2 \rightleftharpoons OH \qquad K_3 = \frac{y_9}{\sqrt{y_4 y_6}} \tag{3.52}$$

$$\frac{1}{2}O_2 + \frac{1}{2}N_2 \rightleftharpoons NO \qquad K_4 = \frac{y_{10}}{\sqrt{y_4 y_3}} \tag{3.53}$$

$$H_2 + \frac{1}{2}O_2 \rightleftharpoons H_2O \qquad K_5 = \frac{y_2}{y_6\sqrt{y_4}\sqrt{P}} \tag{3.54}$$

$$CO + \frac{1}{2}O_2 \rightleftharpoons CO_2 \qquad K_6 = \frac{y_1}{y_5\sqrt{y_4}\sqrt{P}} \tag{3.55}$$

Equilibrium constant coefficients are taken from the technical report of Olikara and Borman (1975) for calculating properties of equilibrium compositions that curve fitted the JANAF thermodynamic data inside the temperature interval between 600 < T < 4000 K. The curve fitting expression of each constant coefficient is demonstrated in Equation 3.56 (Yılmaz et al., 2021).

$$\log_{10} K_i(T) = A_i \ln(\frac{T}{1000}) + \frac{B_i}{T} + C_i + D_i T + E_i T^2 \tag{3.56}$$

where temperature (T) is given in unit of Kelvin. The curve fitting coefficients of equilibrium constants are given in Table 3.1 (Ferguson & Kirkpatrick, 2016).

Table 3.1 Curve fitting coefficients of equilibrium constants (K_i) (Ferguson & Kirkpatrick, 2016)

K_i	A_i	B_i	C_i	D_i	E_i
K_1	0.432168	-0.112464×10^{5}	0.267269×10^{1}	-0.745744×10^{-4}	0.242484×10^{-8}
K_2	0.310805	-0.129540×10^{5}	0.321779×10^{1}	-0.738336×10^{-4}	0.344645×10^{-8}
K_3	−0.141784	-0.213308×10^{4}	0.853461×10^{0}	0.355015×10^{-4}	-0.310227×10^{-8}
K_4	0.015088	-0.470960×10^{4}	0.646096×10^{0}	0.272805×10^{-5}	-0.154444×10^{-8}
K_5	−0.752364	0.124210×10^{5}	-0.260286×10^{1}	0.259556×10^{-3}	-0.162687×10^{-7}
K_6	−0.004153	0.148627×10^{5}	-0.475746×10^{1}	0.124699×10^{-3}	-0.900227×10^{-8}

When the pressure, temperature and equivalence ratio variables are known, Equations 3.39 to 3.43 and Equations 3.46 to 3.55 forms eleven equations and eleven unknowns. These unknowns are constituted from mole fractions of species (y_i) and total number of moles (N) of the combustion products.

When the Equations from 3.46 to 3.49 and 3.50 to 3.55 are rearranged, four unknown variables (y_3, y_4, y_5, y_6) and four non-linear equations can be obtained. These non-linear equations can be linearized and computed by the Gauss-Seidel and Newton-Raphson iteration methods to determine gaseous products of the combustion. The use of these two methods together accelerates the convergence of the equations and provides the result to be reached more quickly. Initial prediction values can be estimated by low-temperature combustion when starting iterations.

Main thermophysical properties (internal energy, specific volume, entropy and enthalpy) are obtained from the calculation of determined compositions of the gas mixture. These properties are highly depending on pressure and temperature. Calculating the specific heat is extremely important for obtaining all the main thermophysical components such as enthalpy and entropy. To obtain the specific heat (C_p), it is necessary to obtain variations in mole fractions respect to partial derivatives of pressure ($\partial y_i/\partial P$) and temperature ($\partial y_i/\partial T$) (Ferguson & Kirkpatrick, 2016).

Another in-house computer model (Model 2) was developed including these equations and definitions within the scope of thesis work. Model 2 was coded in MATLAB programming environment (Mathworks, 2019). The proposed model was developed based on equilibrium constants method of Olikara and Borman that calculates properties of equilibrium combustion products (Olikara & Borman, 1975)

and Equilibrium Combustion Solver program (Ferguson & Kirkpatrick, 2016). The model consists of four different class functions and a main function that determines the equilibrium combustion products. Chemical equilibrium, species compositions, heating values and adiabatic flame temperatures for various equivalence ratios can be predicted with numerical codes of Model 2.

This model has advantages over the commercial software such as CHEMKIN using the element potential method and other methods such as Gibbs energy minimization. The relevant model can work without Lagrange Multipliers that need to be used in Gibbs energy minimization method. It also does not need the additional chemical kinetic parameters required by the CHEMKIN software. Also, it can be easily utilized to various industrial or domestic combustion applications. Algorithm flowchart of Model 2 is demonstrated in Figure 3.2.

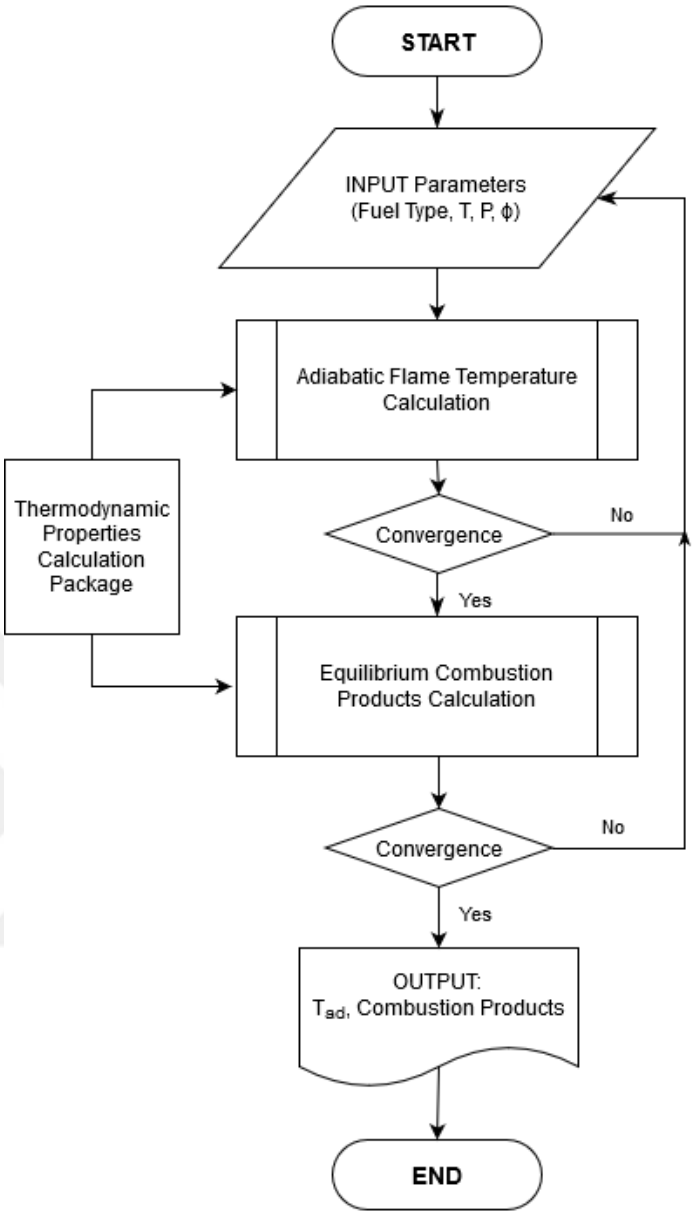


Figure 3.2 Algorithm flowchart of Model 2 (Yılmaz et al., 2021)

In the algorithm flowchart of Model 2, the first step is the definition of input parameters such as temperature, pressure, fuel type, and equivalence ratio. Fuel type need to be as given pure gas or mixture of gases with relevant composition ratios. Adiabatic flame temperature calculation function handles the input parameters and calculates numerically the adiabatic flame temperature by processing data of thermodynamic properties calculation package. It is assumed as zero heat transfer to the environment, adiabatic flame temperature is obtained by equalizing the enthalpies of reactants and the products with the required tolerance ($\varepsilon < 10^{-7}$). If the convergence

is not achieved, the initial approximation of the adiabatic flame temperature should be modified. Before the calculation step of equilibrium combustion products, thermodynamic properties of reactants and products are taken from database of thermodynamic properties by using curve fitting coefficients. Later, equilibrium combustion production calculations are realized with the equations of equilibrium constants that are constituted from atomic level balance and total mole fraction of the species. Non-linear equations of equilibrium constants are linearized iteratively with Newton Raphson method. The initial estimates of the species fractions must be correctly identified, otherwise the obtained numerical solution may diverge. Furthermore, combination of Newton Raphson and Gauss-Seidel methods speeds up the numerical solution. The convergence accuracy of equilibrium constant equations are selected as $\varepsilon_t < 10^{-7}$ in the calculations. After the convergence is achieved, species compositions are determined as outputs in final step of the Model 2.

3.1.3 Element Potential Method

In the thesis, the data obtained from Gibbs energy minimization (Model 1) and equilibrium constants methods (Model 2) were compared with the commercial software (CHEMKIN) that utilizes the method of element potential. For the chemical equilibrium analysis, the element potential method is known as a powerful technique. This method is useful in complicated problems especially working with several phases. It is effective with computer implementation and can be used as a general-purpose program. The method is interchangeable and robust on the calculations of multi or single-phase chemical problems (Reynolds, 1986).

The combustion kinetics code CHEMKIN that created by Sandia National Laboratories now in use is an upgraded version of the commercial software Chemkin II code (ANSYS: San Diego, 2017b). For the gaseous species, thermodynamic properties are stored in the database in terms of polynomial fits to the specific heats. The CHEMKIN software has the same format that utilized in the NASA chemical equilibrium code (R.J. Kee et al., 1980). The CHEMKIN software is used for a variety of tasks, including the formulation, resolution, and assessment of gas-phase chemical problems. It has changeable and useful tool for solving simulations of chemical kinetics. The software contains two libraries of interpretation and gas-phase

subroutine. The Interpreter program reads user defined chemical reaction mechanisms with symbols of each species. The output of Interpreter produces a data file that has link to library of gas-phase subroutine. This library contains approximately 100 flexible Fortran subroutines that can collect information about thermodynamic properties, equation of states, sensitivity parameters, and rates of chemical production (Robert J. Kee et al., 1989).

In addition to reacting flow applications of CHEMKIN, the software contains an equilibrium model. Chemical state of a mixture is determined by this model under equilibrium conditions. Different numbers of gas phase or condensed species can be included in a equilibrium calculations. Among the thermodynamic data for species in the combustion reaction, model can determine phase equilibrium as well as chemical equilibrium. In the software, chemical equilibrium is maintained by the element-potential method that is based on Stanford software named as STANJAN. The CHEMKIN equilibrium model uses the routine library of STANJAN in the solution method of software. The equilibrium specifies species or phase equilibrium. The obtained results from the software are dependent solely on the thermodynamic properties of the species according to user chemistry mechanism, as well as the initial conditions and compositions. The initial composition determines amount of chemical atomics elements in the combustion system. Initial value of equilibrium temperature can be utilized to choose burned or unburned equilibrium state where these states are emerged in the system (ANSYS: San Diego, 2017b).

3.2. Theoretical Investigation Parameters of the Study

In the scope of the thesis, numerical codes were developed including aspects of Gibbs energy minimization and equilibrium constants methods. Theoretical investigations were carried out for standard gases as G20, G25, and NG with different equivalence ratios. Properties of these gases are given in Table 3.2 (Yılmaz et al., 2021) for standard test conditions given in EN 437:2018 Test gases, test pressures and appliance categories standard (European Committee for Standardization, 2018).

Table 3.2 Compositions of the standard gases G20, G25 and NG (Yılmaz et al., 2021)

Gas Type	Composition by mole (%)
Methane (G20)	CH_4 = 100
Test gas (G25)	CH_4 = 86
	N_2 = 14
Natural Gas (NG)	CH_4 = 95.72
	C_2H_6 = 2.45
	C_3H_8 = 0.84
	N_2 = 0.78
	CO_2 = 0.17

Regarding the use of appliance gases from the first, second, and third families, this standard specifies the test gases, test pressures, and classifications of appliances. It is a main reference document that contains the extent of the Council Directive on the harmonization of the Laws of the European Union in relation to the specific standards for gas appliances (European Committee for Standardization, 2018).

In this study, the reactants' temperature and pressure were defined as 300 K and 1 atm. The air composition in the inlet of the combustion chamber was specified as 21% O_2 and 79% N_2. Other minor species in the air were neglected. The walls of the combustion chamber were defined as adiabatic. The fuel/air ratio is used here to define equivalence ratio. The constant pressure- enthalpy approach was applied to the combustion domain (Yılmaz et al., 2021).

3.3. Theoretical Investigation Results

The gas compositions formed due to combustion and adiabatic flame temperatures were investigated depending on the equivalence ratio for the three different gases (G20, G25, and NG). These gases are defined in the relevant domestic boiler standards such as test gases (European Committee for Standardization, 2018) and gas-fired heating boilers standards (European Committee for Standardization, 2015). The range of equivalence ratios (ϕ = 0.6 - 0.9) was determined based on the operating conditions where domestic heating boilers are more efficient and have lower emissions (S. Lee et al., 2010, 2011b, 2011a; Mohr et al., 2018; Soltanian et al., 2019).

According to the selected equivalence ratio range, the Gibbs energy minimization method was applied in Java programming language as Model 1. The Equilibrium constant method was applied in the MATLAB environment as Model 2 for theoretical investigation of the specified gases combustion. The obtained results were compared with CHEMKIN commercial software that uses the element potential method. The reliability of Models 1 and 2 was tested with the CHEMKIN which includes 325 equations for 53 species and offers precise results via GRI-Mechanism (G. P. Smith et al., n.d.).

3.3.1 The Variation of Adiabatic Flame Temperature with respect to Equivalence Ratio for G20, G25, and NG fuels

Figure 3.3 shows the effect of equivalence ratio on the adiabatic flame temperatures for G20, G25, and NG fuels (Yılmaz et al., 2021). When the adiabatic flame temperature results are evaluated, Models 1 and 2 show good agreement with the CHEMKIN results. It is inferred that the adiabatic flame temperatures of G20, G25, and NG tend to increase with the equivalence ratios. Maximum adiabatic flame temperatures were observed at $\phi = 0.9$ because this ratio was the closest value to the stoichiometric ratio, as expected. Model 1 overestimated adiabatic flame temperature around $\phi = 0.9$ while comparing Model 2 and CHEMKIN results.

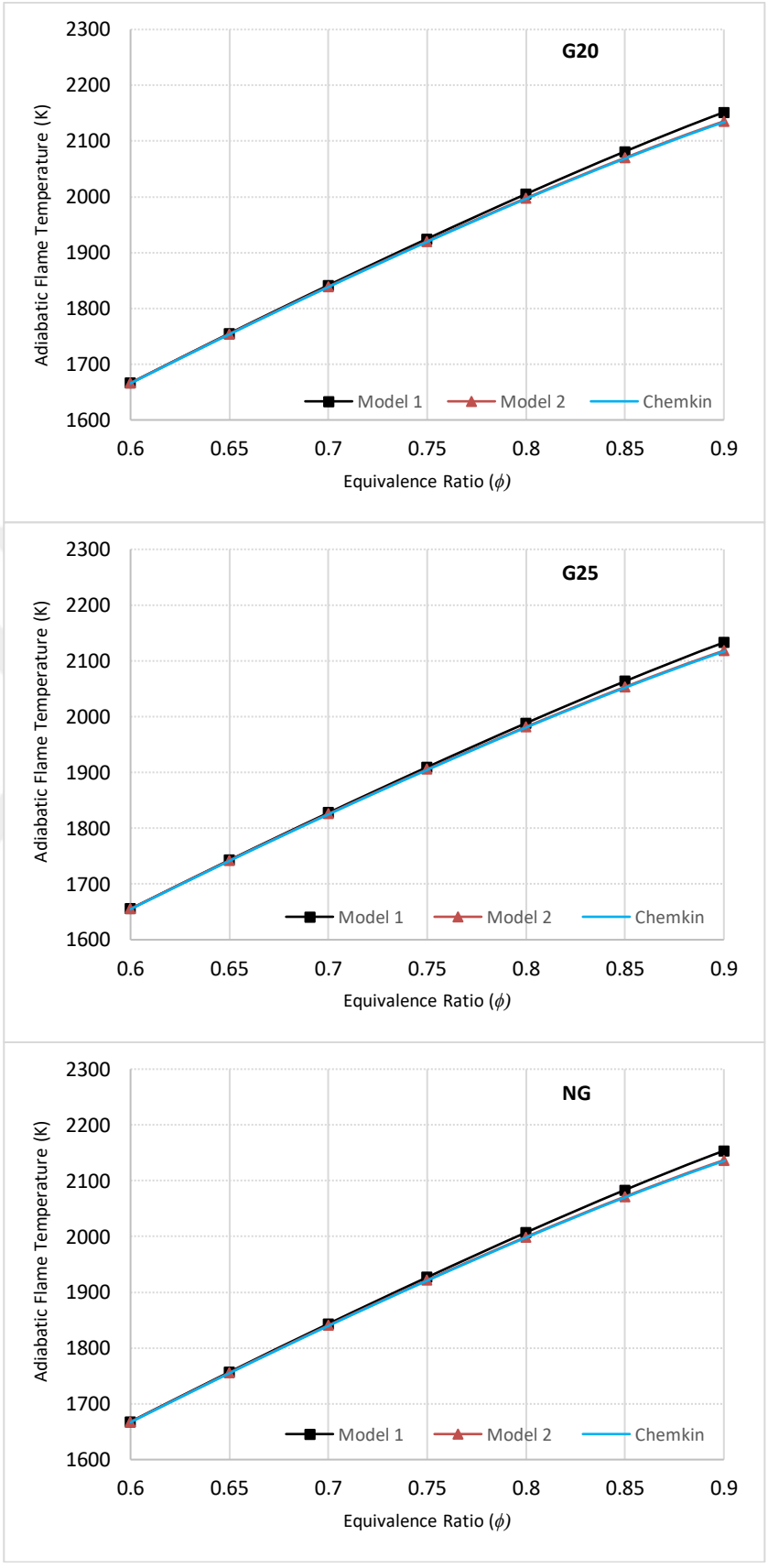


Figure 3.3 Adiabatic flame temperature and equivalence ratio changes for G20, G25, and NG fuels (Yılmaz et al., 2021)

3.3.2 The Variation of Gaseous Emissions with respect to Equivalence Ratio for G20, G25, and NG fuels

Investigation of CO emissions is necessary for flame presence and stability in domestic boilers. Figure 3.4 depicts mole fractions of CO emissions varying with equivalence ratios for G20, G25, and NG fuels (Yılmaz et al., 2021). By evaluation of Figure 3.4, it can be observed that the mole fractions of CO were coherent with CHEMKIN results in investigated equivalence ratio range. CO emissions tend to increase with an equivalence ratio as expected in domestic boilers. The peak values of CO emissions are observed at $\phi = 0.9$ for all models and fuel types. The main reason for this is the CO quenching effect due to higher flame temperatures. G25 fuel gave lower CO emissions in the investigated equivalence ratio range.

NO emissions, which have harmful effects on the environment, are limited by standards. Therefore, it is crucial to determine and reduce the amount of NO emissions (European Committee for Standardization, 2015). Figure 3.5 shows the variation of NO emissions with equivalence ratio for G20, G25, and NG fuels (Yılmaz et al., 2021). It is apparent from Figure 3.5 that NO emissions increased with the equivalence ratio due to the thermal and prompt NO mechanisms (McAllister, 2011) in the premixed combustion of domestic boiler burners. NO emissions reach peak values at $\phi = 0.85$ for all models and fuel types. G25 fuel has lower NO emissions in the investigated equivalence ratio range.

Other major combustion equilibrium products are N_2, O_2, CO_2, and H_2O. Variations of the mole fractions with equivalence ratio for G20, G25, and NG fuels are shown in Figure 3.6, 3.7, 3.8 and 3.9 for these products (Yılmaz et al., 2021). It is clearly seen that Model 1 and Model 2 results have good agreement with CHEMKIN results for all equivalence ratio ranges.

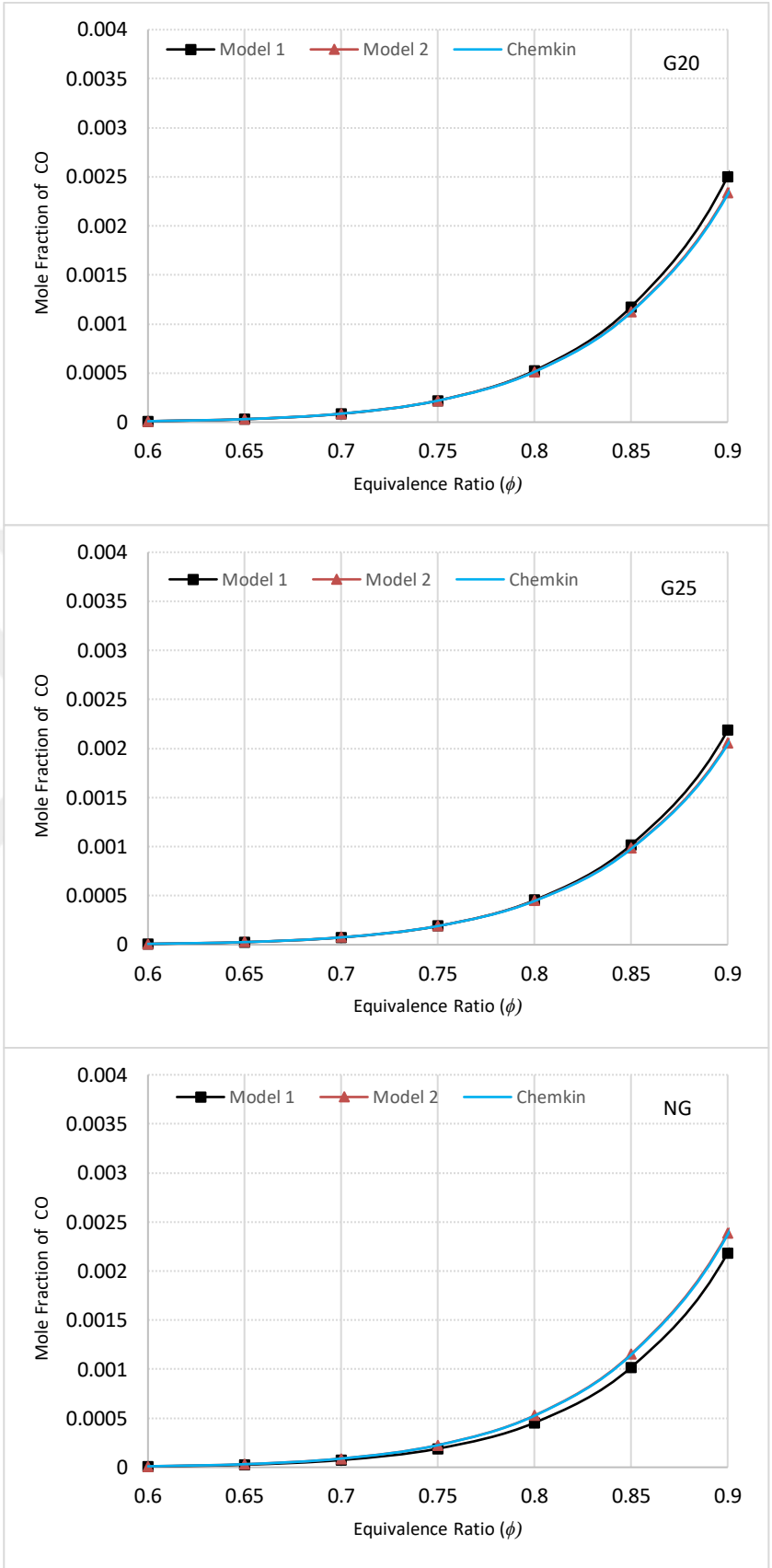


Figure 3.4 Mole fraction of CO with respect to equivalence ratio for G20, G25, and NG fuels (Yılmaz et al., 2021)

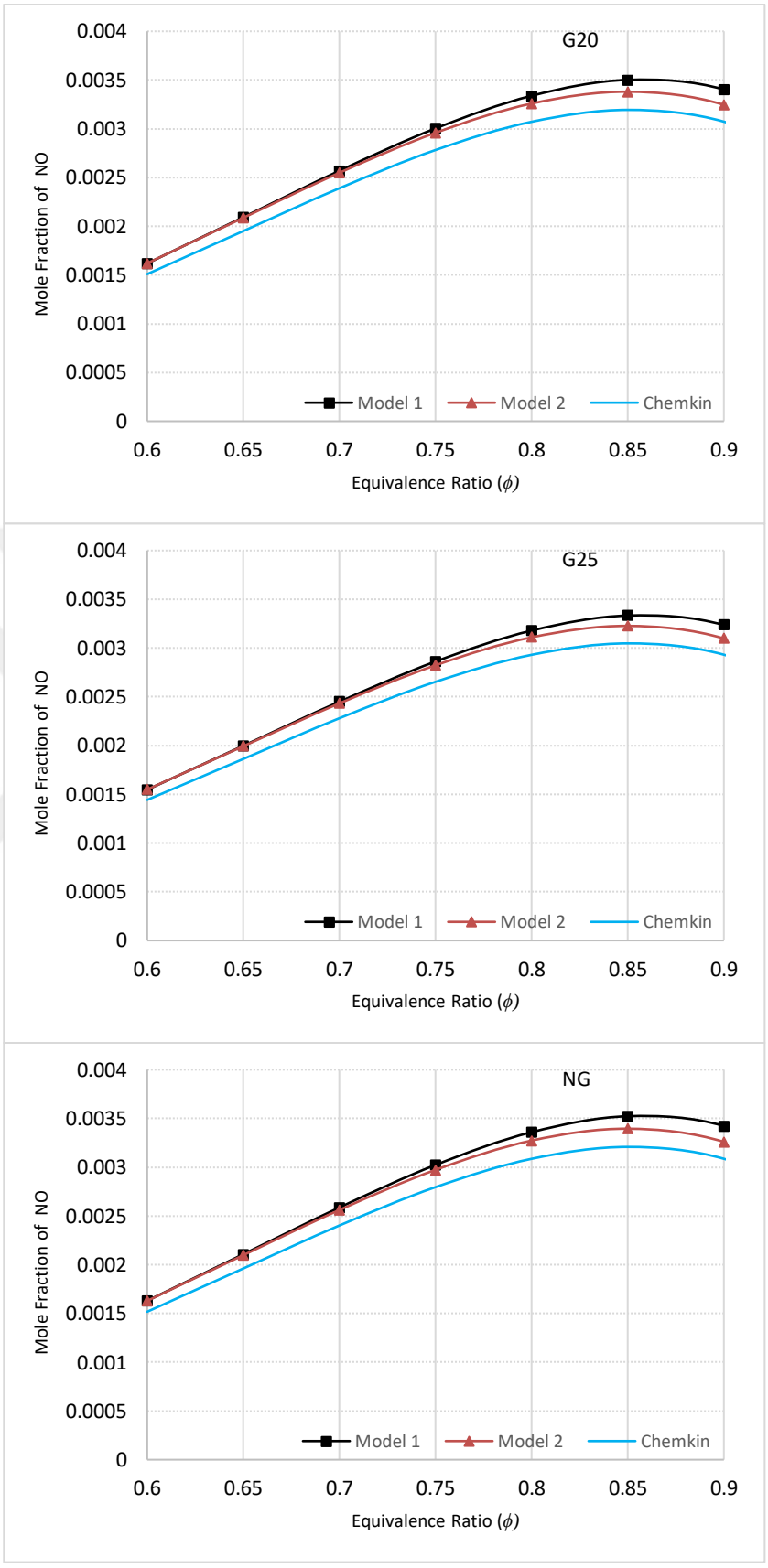


Figure 3.5 Mole fraction of NO with respect to equivalence ratio for G20, G25, and NG fuels (Yılmaz et al., 2021)

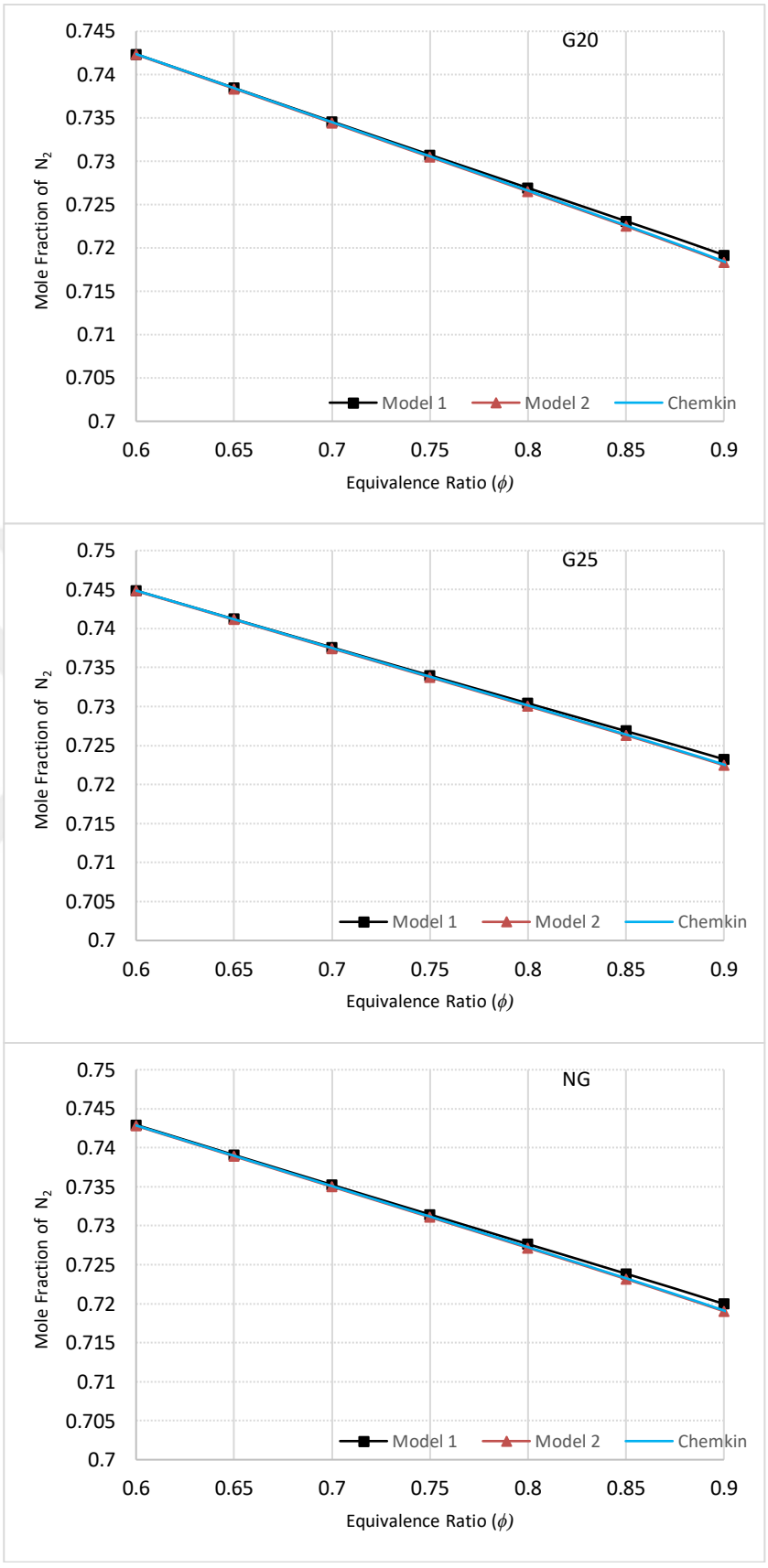


Figure 3.6 Mole fraction of N_2 with respect to equivalence ratio for G20, G25, and NG fuels (Yılmaz et al., 2021)

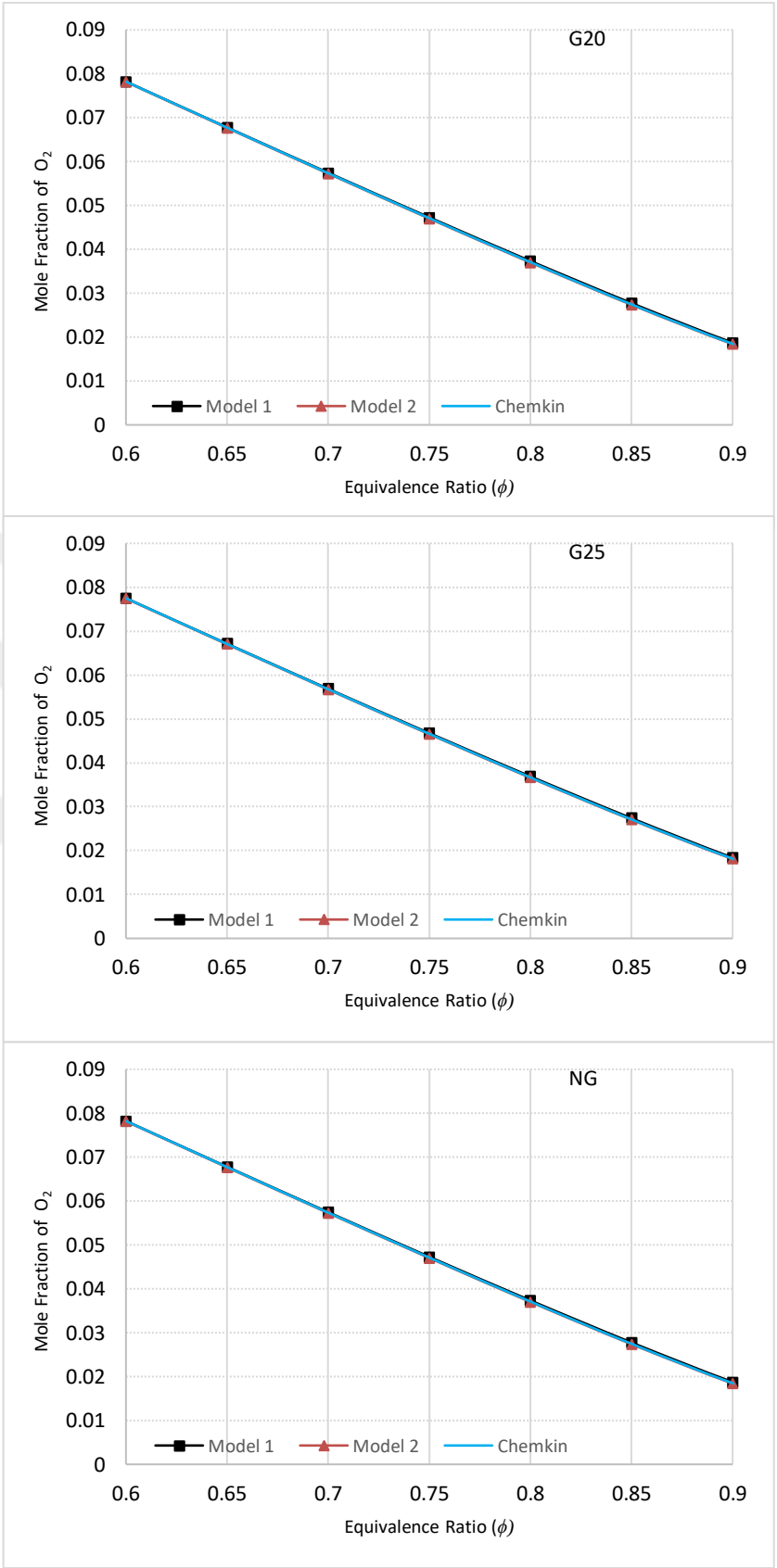


Figure 3.7 Mole fraction of O_2 with respect to equivalence ratio for G20, G25, and NG fuels (Yılmaz et al., 2021)

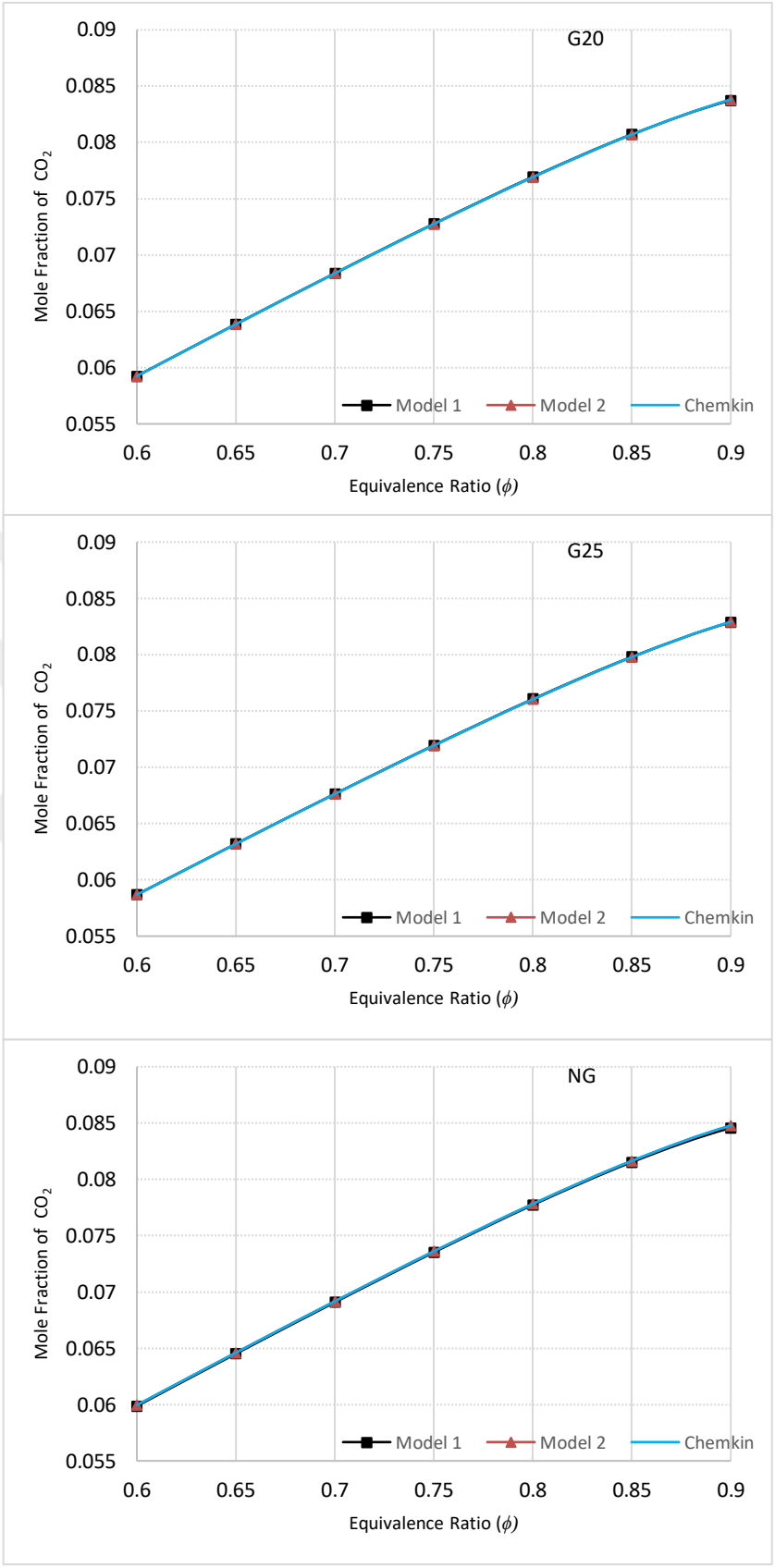


Figure 3.8 Mole fraction of CO_2 with respect to equivalence ratio for G20, G25, and NG fuels (Yılmaz et al., 2021)

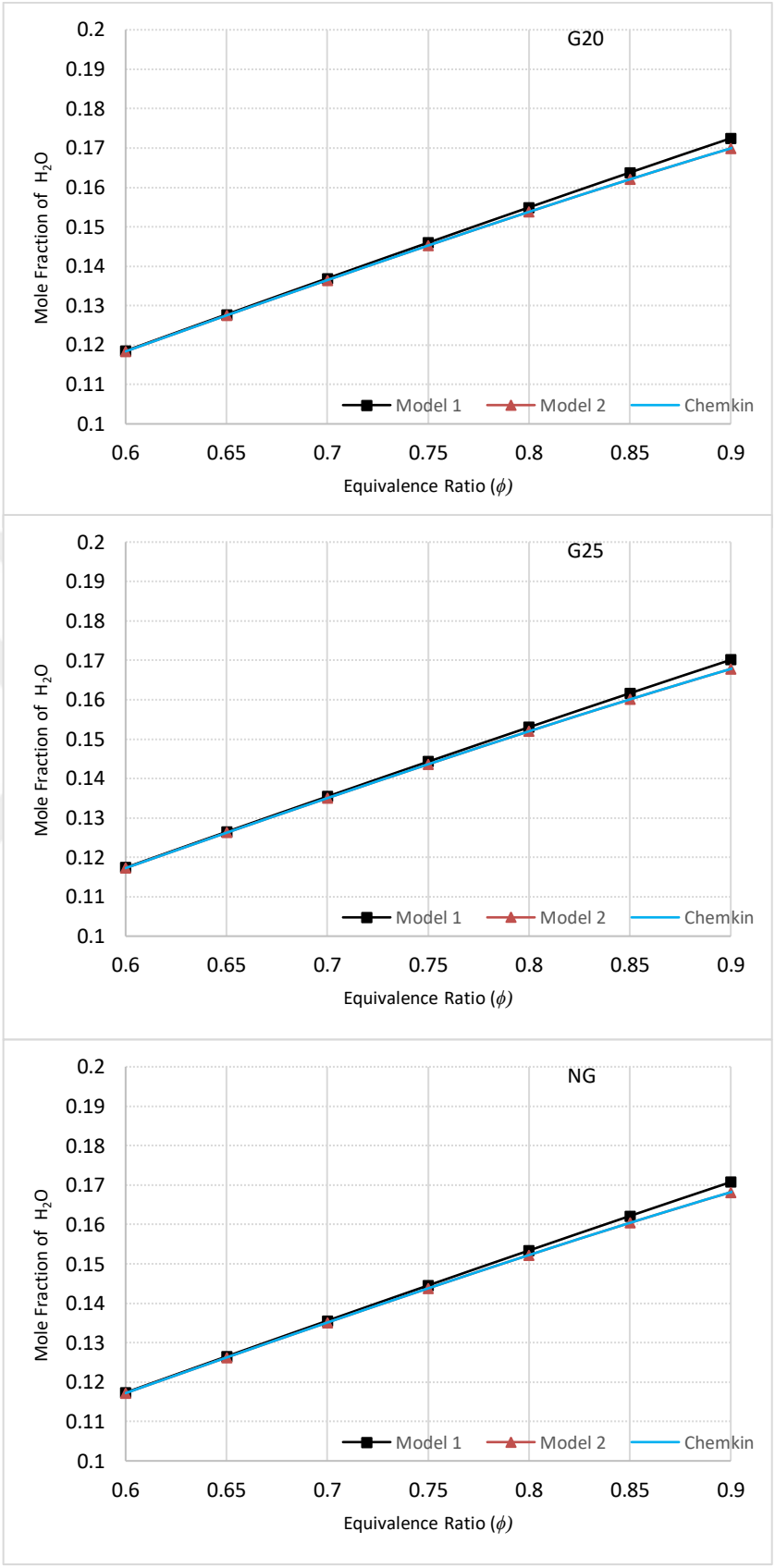


Figure 3.9 Mole fraction of H_2O with respect to equivalence ratio for G20, G25, and NG fuels (Yılmaz et al., 2021)

3.3.3 Comparison and Reliability of Proposed Models

The reliability of the proposed models is demonstrated with provided comparisons in Tables 3.3, 3.4, and 3.5, showing deviations according to reference values taken from CHEMKIN results (Yılmaz et al., 2021). Suitable three different operating conditions (ϕ=0.65, 0.7, and 0.75) (S. Lee et al., 2011b) for the domestic boiler were selected as comparing mole fractions and adiabatic flame temperatures. In Tables 3.3, 3.4, and 3.5, minor deviations were observed in mole fractions of O_2, N_2, CO_2, H_2O, CO, and NO comparing with the CHEMKIN results. When the results were compared, deviations of Model 2 are lower than Model 1. The deviations of evaluated comparatively, one can clearly observe that the results from Model 1 and 2 results comparing with CHEMKIN were obtained considerably below 1%.

Table 3.3 Mole fraction deviations of equilibrium products and adiabatic flame temperatures for G20, G25, and NG fuels (ϕ= 0.65) (Yılmaz et al., 2021)

G20					
ϕ = 0.65	**Model 1 Results**	**Model 2 Results**	**CHEMKIN Results**	**Model 1 Deviations (%)**	**Model 2 Deviations (%)**
T_{in} [K]	300.00	300.00	300.00		
T_{ad} [K]	1755.21	1754.50	1753.50	0.0976	0.0573
O_2	6.78E-02	6.77E-02	6.77E-02	0.0770	-0.0952
N_2	7.38E-01	7.38E-01	7.38E-01	0.0034	-0.0092
CO_2	6.39E-02	6.38E-02	6.38E-02	0.0141	-0.0004
H_2O	1.28E-01	1.28E-01	1.28E-01	0.1990	-0.0002
CO	3.00E-05	3.09E-05	3.08E-05	-2.4895	0.5047
NO	2.09E-03	2.09E-03	1.95E-03	7.2764	6.9667
G25					
ϕ = 0.65	**Model 1 Results**	**Model 2 Results**	**CHEMKIN Results**	**Model 1 Deviations (%)**	**Model 2 Deviations (%)**
T_{in} [K]	300.00	300.00	300.00		
T_{ad} [K]	1742.87	1742.30	1741.34	0.0880	0.0551
O_2	6.71E-02	6.70E-02	6.71E-02	0.0678	-0.0924
N_2	7.41E-01	7.41E-01	7.41E-01	0.0028	-0.0088
CO_2	6.32E-02	6.32E-02	6.32E-02	0.0129	-0.0004
H_2O	1.26E-01	1.26E-01	1.26E-01	0.1838	-0.0002
CO	2.60E-05	2.69E-05	2.68E-05	-2.8815	0.5041
NO	2.00E-03	1.99E-03	1.86E-03	7.2591	7.0177
NG					
ϕ = 0.65	**Model 1 Results**	**Model 2 Results**	**CHEMKIN Results**	**Model 1 Deviations (%)**	**Model 2 Deviations (%)**
T_{in} [K]	300.00	300.00	300.00		

T_{ad} [K]	1757.04	1755.80	1754.86	0.1237	0.0533
O_2	6.78E-02	6.77E-02	6.77E-02	0.0855	-0.0956
N_2	7.39E-01	7.39E-01	7.39E-01	0.0138	-0.0092
CO_2	6.45E-02	6.46E-02	6.46E-02	-0.1399	-0.0004
H_2O	1.26E-01	1.26E-01	1.26E-01	0.2123	-0.0002
CO	3.09E-05	3.18E-05	3.16E-05	-2.2164	0.4879
NO	2.11E-03	2.10E-03	1.96E-03	7.4547	6.9552

Table 3.4 Mole fraction deviations of equilibrium products and adiabatic flame temperatures for G20, G25, and NG fuels (ϕ = 0.7) (Yılmaz et al., 2021)

G20					
ϕ = 0.7	**Model 1 Results**	**Model 2 Results**	**CHEMKIN Results**	**Model 1 Deviations (%)**	**Model 2 Deviations (%)**
T_{in} [K]	300.00	300.00	300.00		
T_{ad} [K]	1841.43	1839.20	1838.16	0.1775	0.0564
O_2	5.74E-02	5.73E-02	5.73E-02	0.1868	-0.1321
N_2	7.35E-01	7.34E-01	7.35E-01	0.0107	-0.0108
CO_2	6.84E-02	6.84E-02	6.84E-02	0.0243	-0.0010
H_2O	1.37E-01	1.36E-01	1.36E-01	0.3233	-0.0007
CO	8.53E-05	8.69E-05	8.64E-05	-1.2923	0.5505
NO	2.57E-03	2.55E-03	2.39E-03	7.5011	6.6329
G25					
ϕ = 0.7	**Model 1 Results**	**Model 2 Results**	**CHEMKIN Results**	**Model 1 Deviations (%)**	**Model 2 Deviations (%)**
T_{in} [K]	300.00	300.00	300.00		
T_{ad} [K]	1827.59	1825.70	1824.65	0.1613	0.0576
O_2	5.68E-02	5.67E-02	5.68E-02	0.1682	-0.1282
N_2	7.38E-01	7.37E-01	7.38E-01	0.0093	-0.0104
CO_2	6.76E-02	6.76E-02	6.76E-02	0.0224	-0.0009
H_2O	1.35E-01	1.35E-01	1.35E-01	0.2980	-0.0005
CO	7.39E-05	7.55E-05	7.51E-05	-1.5438	0.5483
NO	2.45E-03	2.43E-03	2.28E-03	7.4437	6.6846
NG					
ϕ = 0.7	**Model 1 Results**	**Model 2 Results**	**CHEMKIN Results**	**Model 1 Deviations (%)**	**Model 2 Deviations (%)**
T_{in} [K]	300.00	300.00	300.00		
T_{ad} [K]	1843.37	1840.70	1839.60	0.2047	0.0598
O_2	5.74E-02	5.73E-02	5.73E-02	0.1956	-0.1325
N_2	7.35E-01	7.35E-01	7.35E-01	0.0218	-0.0109
CO_2	6.91E-02	6.92E-02	6.92E-02	-0.1293	-0.0009
H_2O	1.36E-01	1.35E-01	1.35E-01	0.3388	-0.0007
CO	8.78E-05	8.92E-05	8.87E-05	-1.0147	0.5330
NO	2.59E-03	2.56E-03	2.40E-03	7.6790	6.6214

Table 3.5 Mole fraction deviations of equilibrium products and adiabatic flame temperatures for G20, G25, and NG fuels (ϕ = 0.75) (Yılmaz et al., 2021)

G20					
ϕ = 0.75	**Model 1 Results**	**Model 2 Results**	**CHEMKIN Results**	**Model 1 Deviations (%)**	**Model 2 Deviations (%)**
T_{in} [K]	300.00	300.00	300.00		
T_{ad} [K]	1924.85	1920.50	1919.30	0.2888	0.0623
O_2	4.73E-02	4.70E-02	4.71E-02	0.3755	-0.1790
N_2	7.31E-01	7.30E-01	7.31E-01	0.0227	-0.0123
CO_2	7.28E-02	7.27E-02	7.27E-02	0.0365	-0.0022
H_2O	1.46E-01	1.45E-01	1.45E-01	0.4986	-0.0018
CO	2.20E-04	2.21E-04	2.19E-04	0.3530	0.6096
NO	3.00E-03	2.96E-03	2.78E-03	7.9616	6.3376
G25					
ϕ = 0.75	**Model 1 Results**	**Model 2 Results**	**CHEMKIN Results**	**Model 1 Deviations (%)**	**Model 2 Deviations (%)**
T_{in} [K]	300.00	300.00	300.00		
T_{ad} [K]	1909.53	1905.70	1904.51	0.2634	0.0625
O_2	4.68E-02	4.65E-02	4.66E-02	0.3421	-0.1740
N_2	7.34E-01	7.34E-01	7.34E-01	0.0201	-0.0117
CO_2	7.19E-02	7.19E-02	7.19E-02	0.0342	-0.0020
H_2O	1.44E-01	1.44E-01	1.44E-01	0.4584	-0.0016
CO	1.90E-04	1.91E-04	1.90E-04	-0.1502	0.6064
NO	2.86E-03	2.82E-03	2.65E-03	7.8490	6.3899
NG					
ϕ = 0.75	**Model 1 Results**	**Model 2 Results**	**CHEMKIN Results**	**Model 1 Deviations (%)**	**Model 2 Deviations (%)**
T_{in} [K]	300.00	300.00	300.00		
T_{ad} [K]	1926.89	1922.00	1920.80	0.3171	0.0627
O_2	4.73E-02	4.70E-02	4.71E-02	0.3850	-0.1795
N_2	7.31E-01	7.31E-01	7.31E-01	0.0345	-0.0123
CO_2	7.35E-02	7.36E-02	7.36E-02	-0.1172	-0.0022
H_2O	1.45E-01	1.44E-01	1.44E-01	0.5169	-0.0018
CO	2.26E-04	2.26E-04	2.25E-04	0.5083	0.5914
NO	3.02E-03	2.97E-03	2.80E-03	8.1391	6.3260

CHAPTER FOUR
NUMERICAL INVESTIGATION OF COMBUSTION IN CYLINDRICAL COMBUSTION REGION

Experimental approach on combustion is an expensive and time-consuming process. That is why; researchers are seeking for numerical approaches. Among the numerical approaches to investigate combustion, computational fluid dynamics (CFD) is preferred as a useful tool (Malalasekera & Versteeg, 2007).

CFD is a promising tool to improve the design and operation of an aerodynamic equipment. Nowadays, CFD is being used in many areas, including the analysis of commercial burners, to study combustion equipment..- The nonlinear relation between turbulent fluid dynamics and complex chemical reactions has prevented widespread usage (Baukal, 2003). The use of CFD approach for all combustion applications is limited due to the following problems:

- Physics of reacting flow domains are too complex. The reacting flow domain contains uncertainty on chemical reaction kinetics of the hydrocarbon fuels, unknown behavior of turbulent flows and stirring, unsteady distributions of the pollutants, radiation characteristics of the surfaces and combustion gases.
- The variations in reacting flow domains' spatial and temporal time scales. Flow characteristics and reaction kinetics need to be resolved to the optimum characteristic size.
- Full scale modeling of the combustion domain brings higher computational cost, difficulties, and solution divergence in CFD codes.
- Common CFD tools of the combustion are not optimized for the combustion equipment such as commercial burners (Baukal, 2003).

Thus, relevant constraints to address design or operational issues leave engineers uncertain about how to effectively use CFD predictions. However, burner design trends and standards are pushing the designers to investigate the operating conditions and process parameters of the commercial burners. Conventional designs and empirical approaches are insufficient for current design requirements. At this stage, studies with CFD gain importance and realistic working parameters are tried to be

achieved without costly experiments. Key parameters need to be investigated related to utilizing CFD in burner and combustion region design, optimization, and evaluation. Besides, while performing CFD studies, it is important to select and use the suitable model in the combustion process. In this thesis section, numerical CFD studies are given with the validation of the results.

In the following sections of the chapter, reacting flow modelling in combustion simulations, reacting flow models in CFD codes, modelling combustion domain, governing equations, numerical investigation parameters of the study, validation of numerical results with experiments, results and parametric studies are discussed.

4.1 Reacting Flow Modelling in Combustion Simulations

Combustion is one of the most crucial phenomena in engineering, which includes heat transfer, radiative heat transfer, turbulent fluid flow, chemical reactions and other different processes. Common engineering applications for combustion are engines, combustors for creating power, boilers, furnaces and other alternative combustion systems. Crucial aspects of the combustion analysis could be defined as predicting temperatures, fluid flow, product concentrations, emissions emerged from combustion systems. Besides that, the design of a combustion system should be accomplished according to standards, technical requirements, emission limits and environmental effects.

Reacting flow modelling via CFD is one of the most important concerns in recent studies. Combustion problems are solved by CFD with the transport equations of fluid mechanics and heat transfer including models on chemical reaction mechanisms, radiation heat transfer and other different sub-models for the combustion (Malalasekera & Versteeg, 2007). As an example, CFD solution of methane and oxidizer flame temperature contours on a plate is demonstrated in Figure 4.1 (Kadam et al., 2019).

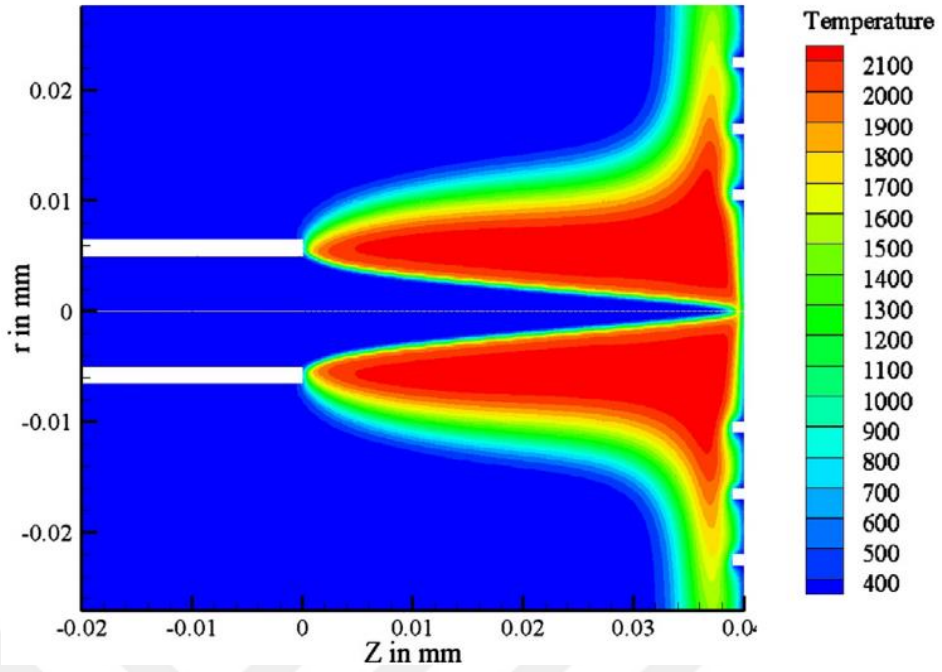


Figure 4.1 Methane-air flame jet temperature contours on square ribbed plate (Kadam et al., 2019)

4.1.1 Generalized Three-Dimensional Navier-Stokes Equations for Reacting Flow Simulations

General conservation equations for three-dimensional Navier-Stokes equations can be derived over combustion domain with the general formula as in Equation 4.1 (Bird et al., 2002; Warnatz et al., 2006).

$$\frac{\partial \rho}{\partial t} + div\vec{\phi}_f = q_f + s_f \tag{4.1}$$

Here ρ is the density in relation to time, $\vec{\phi}_f$ is change of the flux such as heat conduction, momentum transport, etc., q_f is change of the producing components such as chemical reaction, s_f is long range processes such as gravity, radiation, etc. General mass conservation and species mass conservation equations are defined with the formulas in Equations 4.2 and 4.3 (Bird et al., 2002; Warnatz et al., 2006).

$$\frac{\partial \rho}{\partial t} + div(\rho\vec{v}) = 0 \tag{4.2}$$

$$\frac{\partial \rho_i}{\partial t} + div(\rho_i \vec{\upsilon}) \; + \; div \; \vec{j}_i = M_i \omega_i \tag{4.3}$$

Here ρ is the mass density with respect to time, i is the number of species, υ is the flow speed, j_i is the diffusion flux, ω is the formation molar rate and M_i is the molecular mass of the species. Non-reactive flow Navier-Stokes equations are derived by merging the momentum conservation equation and mass conservation equation as in Equation 4.4. Here $\overline{\overline{p}}$ is the pressure tensor and $\vec{g}$ is the gravity (Bird et al., 2002; Warnatz et al., 2006).

$$\frac{\partial(\rho \vec{\upsilon})}{\partial t} + div(\rho \vec{\upsilon} \otimes \vec{\upsilon}) \; + \; div \, \overline{\overline{p}} = \rho \vec{g} \tag{4.4}$$

Besides that, energy equation of the reacting flow can be defined as in Equation 4.5. Here u is the one-dimensional velocity component, j_i denotes diffusion flux, q_r is the radiation source in the combustion domain (Bird et al., 2002; Warnatz et al., 2006).

$$\frac{\partial(\rho u)}{\partial t} + div(\rho u \vec{\upsilon} \; + \; \vec{\mathrm{j}}_i) \; + \; \overline{\overline{p}} : \mathrm{grad} \, \vec{\upsilon} = q_r \tag{4.5}$$

Generally, combustion equipment has turbulent reacting flow rather than laminar flow. In turbulent flow fluids are mixing fast and turbulent flow is complex. Thus, this maintains smaller combustion chamber comparing with laminar flame structures. Still turbulent flow and chemical reaction mechanism are not clearly identified. Because of that, mathematical models of turbulent reacting flow are less than laminar combustion models (Warnatz et al., 2006).

Velocity and its components are well-understood in laminar flow. But in turbulent flow, velocity, temperature, density, and species composition fluctuate continuously. These fluctuations create vortices by shear force. Vortex motions speed up the mixing process enormously. Furthermore, interface of the species is greatly extended due to these vortices and molecular mixing is greatly increased in reacting turbulent flows. Turbulent flame modelling with CFD is shown in Figure 4.2.

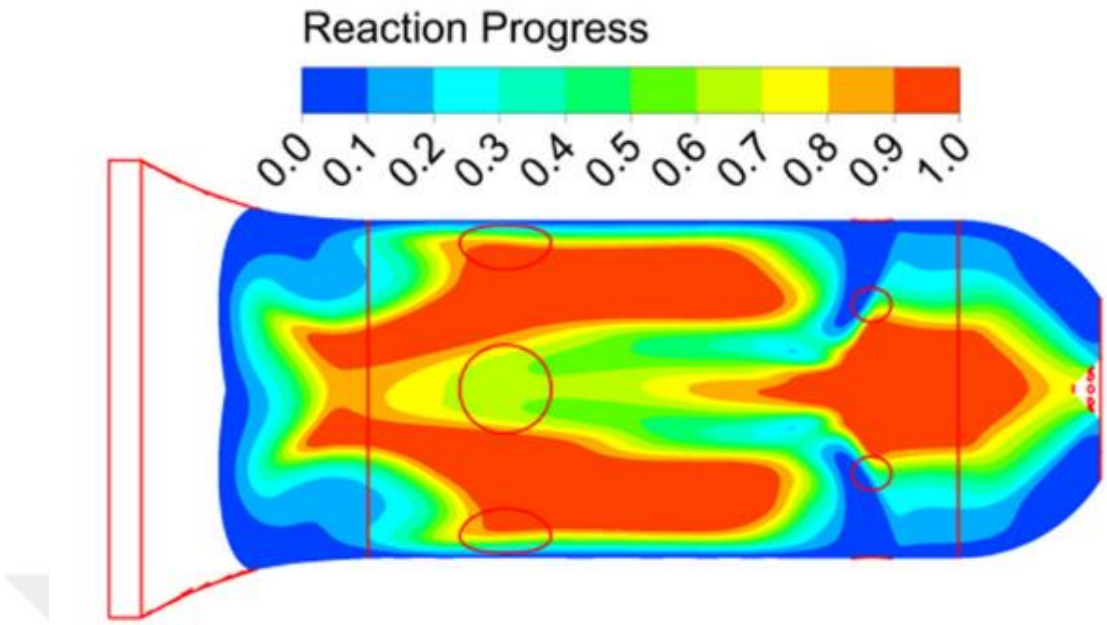


Figure 4.2 Turbulent flame modelling with CFD modelling (K. Zhang et al., 2017)

4.1.2 Reaction Mechanisms

Fuel combustion occurs more than a single reaction with various number of steps. These steps continue till the products reach the equilibrium. Ultimate equilibrium condition can be defined by chemical kinetics. One of the crucial parts of the chemical kinetics is reaction mechanism of the combustion (Malalasekera & Versteeg, 2007). It is now clearly being known that a simple global reaction of hydrogen to produce water has nearly 40 elementary reactions for enough chemical mechanism. A main example of hydrocarbons such as natural gas has 53 species and 325 reactions according to GRI-Mech 3.0 mechanism, University of Berkeley (G. P. Smith et al., n.d.). All interactions of these reactions determine the combustion behavior. Generally main rate-limiting reactions specify overall combustion process rate (Warnatz et al., 2006). Analyses implemented within the scope of the thesis are based on the GRI 3.0 mechanism.

4.1.2.1 Detailed Mechanisms

Various types of reaction occur in combustion mechanisms. These reactions could be given as reactions of different orders, consecutive, competitive, opposing, chain and

chain branching reactions. These reactions can be analyzed with detailed reaction mechanism approaches (Malalasekera & Versteeg, 2007).

Most known detailed mechanisms of methane combustion is GRI 2.11 that contains 49 species and 277 elemental reactions (Bowman et al., 2003), most current version GRI 3.0 mechanism which contains NO formation and San Diego mechanism with 57 species and 268 reactions (Mechanical and Aerospace Engineering (Combustion Research), 2001) Another useful detailed chemical mechanism was proposed by Blanquart et al. (2009) with 149 species and 1651 reactions for high temperature combustion (Blanquart et al., 2009).

4.1.2.2 Reduction Mechanisms

The computational complexity of the detailed mechanisms has led the researchers to find alternative reduced mechanisms for low computational costs. These efforts supply more practical reaction schemes with less equations which contain main reactions to estimate crucial major and minor species. For methane combustion, a five-step reduced mechanism was suggested by researchers that is given in Equation 3.6 (Hewson & Bollig, 1996).

$$\begin{aligned} CH_4 + 2H + H_2O &\longleftrightarrow 4H_2 + CO \\ H_2O + CO &\longleftrightarrow H_2 + CO_2 \\ 2H &\longleftrightarrow H_2 \\ O_2 + 3H_2 &\longleftrightarrow 2H_2O + 2H \\ H_2 + 2CO &\longleftrightarrow C_2H_2 + O_2 \end{aligned} \tag{3.6}$$

Natural gas combustion detailed mechanism contains 325 reactions and 53 species according to GRI 3.0 mechanism. Accuracy of reduced mechanisms are crucial for combustion simulations and comparisons can be found in the literature (Malalasekera & Versteeg, 2007). Reduced mechanism should be carefully investigated, and computational cost and performance ratio must be monitored according to specific requirements within pressure and temperature range of the mechanism.

For the thesis study, different reduced mechanisms are obtained from literature and external resources. Advantages and disadvantages are compared before using in the combustion simulations. These reduced and detailed mechanisms contain pure methane, natural gas and blend gases (ANSYS: San Diego, 2017a; Ansys Inc., 2021; Blanquart et al., 2009; Skjøth-Rasmussen et al., 2004; Trisjono & Pitsch, 2017). Here, some common reduced mechanisms are given with several species and reactions:

- CH_4 combustion five step mechanism (Hewson & Bollig, 1996)
- CH_4 -air reduction mechanism with 17 species and 42 reactions (Bowman et al., n.d.)
- Natural gas combustion with 19 species and 84 reactions (Reduced mechanism of the GRI Mech 1.2, 1994)
- Natural gas combustion with 22 species and 105 reactions (Reduced mechanism of the GRI Mech 1.2, 1994)
- Natural gas combustion with 32 species and 213 reactions (Hinrichs et al., 2018; Trisjono & Pitsch, 2017)

4.1.3 Reacting Flow Models in CFD

4.1.3.1 Reacting Flow Models in Commercial CFD

Reacting flow modelling in commercial code ANSYS Fluent (Ansys Inc., 2021) involves interactions between flow, turbulent mixing, heat transfer and chemical reactions. Because of the complex chemical kinetic mechanism of the combustion, nonlinear turbulence-chemistry relation should be considered carefully. Main physical parameters dealt within combustion are transport equations, turbulence models and chemistry parameters in CFD codes. Main physical parameters in CFD modelling of combustion is demonstrated in Figure 4.3 (Malalasekera & Versteeg, 2007; Warnatz et al., 2006).

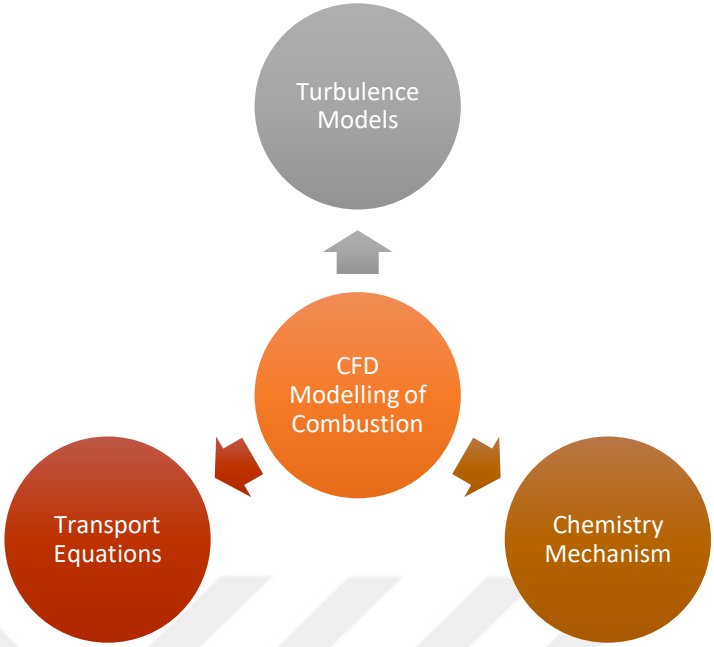


Figure 4.3 Main physical parameters in CFD modelling of combustion (Malalasekera & Versteeg, 2007; Warnatz et al., 2006)

Reacting flow also requires additional physics for solving combustion problems as radiation models (P1, Discrete Ordinates (DO)), real gas effects, pollutant models, etc. Additional physics parameters and models in CFD modelling of combustion are shown in Figure 4.4 (Ansys Inc., 2021).

Radiation Models	Effects of Real Gas	Pollutant Models
• P1 • Gray DO • Non-grat DO	• Lee Kesler • Peng Robinson • Redlich Kwong	• NO_x • Soot • SO_x

Figure 4.4 Additional physics in CFD modelling of combustion (Ansys Inc., 2021)

Reacting flow in CFD is strictly depending on chemistry and flow configuration aspects. Chemistry parameters with respect to flow configuration in CFD modelling is given in Figure 4.5. Flow configuration is divided into three subsections in CFD applications:

- Premixed combustion

- Non-premixed combustion
- Partially premixed combustion

Chemistry configuration is also divided into three subsections:

- Fast chemistry
- Finite chemistry
- Finite-rate chemistry

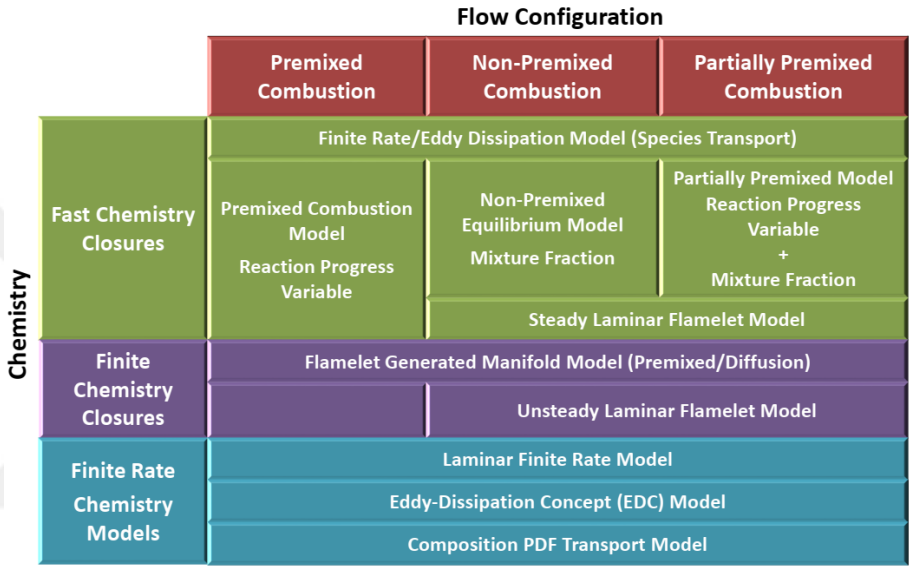


Figure 4.5 Chemistry parameters with respect to flow configuration in CFD modelling (Ansys Inc., 2021)

Species model section contains five different options for combustion modelling: Transport of species, Premixed, Non-premixed, partially premixed combustion and PDF transport of composition.

4.1.3.2 Flamelet Model Approach and Flamelet Generation

In combustion simulations, one or two step mechanisms are basic methodologies to predict chemical interactions. Instead of these mechanisms, a comprehensive method is utilized as known commonly "flamelet model" approach. This method is a compromise approach between basic and complex chemistry. According to the model, a group of stretched laminar flamelets make up the turbulent flame. A basic sketch of the laminar flamelet is shown in Figure 4.6 (Malalasekera & Versteeg, 2007).

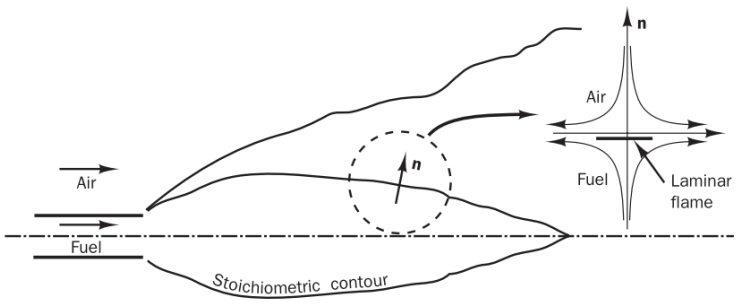


Figure 4.6 Basic schematic of the laminar flamelet (Malalasekera & Versteeg, 2007)

Laminar flamelet profiles are generated with set of solutions on governing partial differential equations in mixture fraction of space. Resulting flamelet profiles are collected to create a flamelet library which contains temperature, species and density profiles for different scalar dissipation rates (Malalasekera & Versteeg, 2007). Flame reaction progress and flame structure are presented in Figure 4.7.

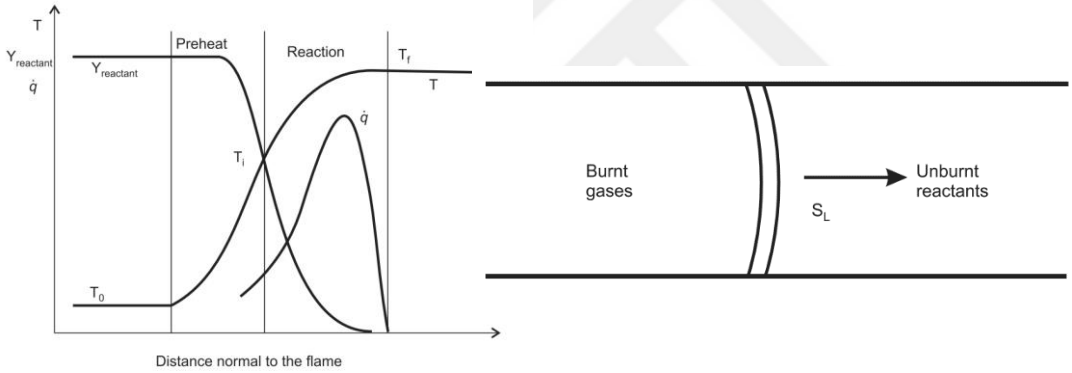


Figure 4.7 Flame reaction progress and flame structure (Raghavan, 2016)

4.1.3.3 Probability Density Function Approach

The probability density function (PDF) for fluctuating scalars is typically used to derive mean quantities using a normal statistical method. In combustion applications these scalars will be mixture fractions. A randomized quantity variable ϕ and the distribution function $F_\phi(\Psi)$ can be written as in Equation 4.7 (Kuo, 2005).

$$F_\phi(\psi) = \text{Prob}\{\phi < \psi\} \tag{4.7}$$

where $Prob\{\phi < \Psi\}$ is given as probability and $\phi < \Psi$ relation should be supplied for a given Ψ value. The probability density function $P_\phi(\Psi)$ is created by derivation of the distribution function as in Equation 4.8. The average of the mean scalars can be determined using the probability density function $q(\Psi)$ as in Equation 4.9 (Kuo, 2005).

$$P_\phi(\psi) = \frac{dF_\phi(\psi)}{d\psi} \tag{4.8}$$

$$\bar{q} = \int_{-\infty}^{\infty} q(\psi) P(\psi) d\psi \tag{4.9}$$

In combustion problems, mixture fraction (ξ) based probability function should be defined. This probability function is called as density-weighted probability function $P_\phi(\xi)$. Average of any scalar quantity weighted by density $\tilde{\phi}$, that shows the function of ξ, can be determined as shown in Equation 4.10.

$$\tilde{\phi} = \int_0^1 \phi(\xi) \tilde{P}(\xi) d\xi \tag{4.10}$$

Density based other scalars (e.g. mass fractions or emissions of species) are calculated for combustion simulation applications. As an example, the density-weighted average mass fraction of *i* is given with Equation 4.11.

$$\tilde{Y}_k = \int_0^1 Y_k(\xi) \tilde{P}(\xi) d\xi \tag{4.11}$$

According to different flow types, probability density function forms differently. Commercial CFD codes are utilizing this approach to find properties of scalars at their mesh locations (Malalasekera & Versteeg, 2007). Probability density function change in a jet flow is given in Figure 4.8.

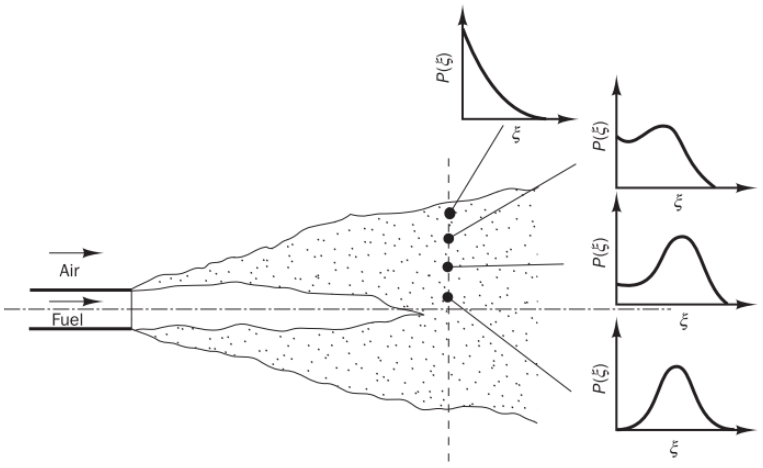


Figure 4.8 Probability density function change in a jet flow (Malalasekera & Versteeg, 2007)

4.2 Modelling of Combustion Domain and Governing Equations of Numerical Study

4.2.1 Modelling with Species Transport (ST) and Finite-Rate Chemistry

Conservation and energy equation for two or three-dimensional reacting flows can be solved by CFD codes to model combustion by merging and chemical transport. For each reactive species, conduction, convection, diffusion, and reaction sources are included in these conservation equations.. Generalized mass and species conservation equations are defined with these formulas (Bird et al., 2002; Warnatz et al., 2006)

Chemical reactions can contain multiple simultaneous reactions in fluid phase (volumetric chemical reactions) or in the porous region. Besides that, wall, particle surface and electrochemical reactions, chemical vapor deposition, reacting channel and reactor network models can be modeled with Species transport (ST) modeling approach. Volumetric reactions are defined in CFD codes by species that given with volumetric molar ratios or mass fractions. Species properties, mixture materials and reactions etc. need to be taken from databases. If a non-existing property or material occur, then these properties must be clearly defined in the required fields. While handling with chemical species conservation equation, Each species' local mass fraction is estimated using the CFD algorithm, Y_i, to solve the convection and diffusion equation of i^{th} species. Equation 4.12 displays the generalized conservation equation used in CFD programs (Agarwal et al., 2018; Poinsot & Veynante, 2005).

$$\frac{\partial(\rho Y_i)}{\partial t}+\nabla(\rho\vec{\upsilon}Y_i)=-\nabla\vec{J}i+R_i+S_i \tag{4.12}$$

where J_i is the diffusion flux of i species, R_i is resultant rate of products through chemical reaction and S_i is the resultant rate of user defined external sources or distributed phase. According to total number of species (N) in fluid form, an equation of this state is calculated for N-1 species. The sum of all mass fractions that defined in the combustion system must give unity. To supply this condition, last species (N^{th}) is selected as nitrogen while the oxidizer is air. For modelling of mass dispersion, the CFD codes handle the problem with a dilute approximation according to Fick's law (Poinsot et al., 2001). For laminar reacting flows, the diffusion flux can be defined as demonstrated in Figure 4.13.

$$\vec{J}_i=-\rho D_{i,m}\nabla Y_i-D_{T,i}\frac{\nabla T}{T} \tag{4.13}$$

where $D_{i,m}$ and $D_{T,i}$ are the mass and thermal (Soret) diffusion coefficients for i in the reactants, respectively. In turbulent reactions, CFD codes calculate the mass diffusion with the Equation 4.14 including the effect of turbulent Schmidt number (Sc_t) (Poinsot & Veynante, 2005).

$$\vec{J}_i=-\left(\rho D_{i,m}+\frac{\mu_t}{Sc_t}\right)\nabla Y_i-D_{T,i}\frac{\nabla T}{T} \tag{4.14}$$

where μ_t and D_t are turbulent viscosity and diffusivity in the mixture, respectively. In multicomponent reacting flows with mixing, species diffusion effects substantially the enthalpy transport. Thus, this effect needs to be defined in CFD codes with the Equation 4.15 (Poinsot & Veynante, 2005).

$$\vec{J}_i=\nabla\left[\sum_{i=1}^{n}h_i\vec{J}_i\right] \tag{4.15}$$

Source terms are provided in Equation 4.12. This equation is solved in CFD codes for turbulent flows with three different approaches and one relaxation model:

- Finite-rate kinetic approach that reaction rates are defined common finite chemistry.

- Eddy dissipation model approach that driven by turbulence with omitting chemistry timescales. This method abstains from computationally expensive Arrhenius chemical kinetics approach.
- Eddy dissipation concept (EDC) model approach contains chemical kinetics in detail with turbulent flames. This model is consisting of timescales of both kinetics and turbulence. Computing detailed chemical kinetics creates higher computational load of CFD solvers.
- Relaxation to Chemical Equilibrium Model supports all three models to obtain equilibrium in the numerical solutions.

The generalized finite-rate formulation can be implemented to nonpremixed, premixed and partially premixed flames in combustion systems.

4.2.1.1 Finite-Rate Kinetics without Turbulence-Chemistry Interaction (no TCI)

In this approach, turbulence fluctuations are omitted, and chemical source terms are computed with general-rate expressions. This approach is suitable for laminar flows with known formulation and for turbulent flows that contain complex chemistry with faster timescales of turbulence than timescales of chemistry. For N_R reactions of species participated in, resultant source of chemical species (i) that emerges from combustion is calculated as total reaction source in Equation 4.16 (Poinsot & Veynante, 2005).

$$\hat{R}_i = M_{w,i} \sum_{r=1}^{N_R} \hat{R}_{i,r} \tag{4.16}$$

where $M_{w,i}$ is the molecular weight and R is the molar rate of emerging or destructing i in the reaction r. General form of r_{th} reaction can be defined as in Equation 4.17 (Poinsot & Veynante, 2005).

$$\sum_{N}^{i=1} \nu'_{i,r} \mathrm{M}_i \underset{kf,r}{\overset{kb,r}{\rightleftharpoons}} \sum_{N}^{i=1} \nu''_{i,r} \mathrm{M}_i \tag{4.17}$$

Here the notations are given as;

N= number of species

$v'_{i,r}$ = stoichiometric coefficient for reactants in the reaction

$v''_{i,r}$ = stoichiometric coefficient for products in the reaction

M_i = each species (i)

$k_{f,r}$ = forward rate constant

$k_{b,r}$ = backward rate constant

The molar rate of emerging or destructing is shown with Equation 4.18 (Poinsot & Veynante, 2005).

$$\hat{R}_{i,r} = \Gamma(v''_{i,r} - v'_{i,r})\left(k_{f,r} \prod_{j=1}^{N} [C_{j,r}]^{n'_{j,r}} - k_{b,r} \prod_{j=1}^{N} [C_{j,r}]^{n''_{j,r}} \right) \tag{4.18}$$

where,

$C_{j,r}$ = molar concentration of species in the reaction [kmol/m^3].

$n'_{j,r}$ = rate exponent for reactants in the reaction

$n''_{j,r}$ = rate exponent for products in the reaction

Γ = net contribution of externals for the reaction ratio

The forward rate constant ($k_{f,r}$) for reactions can be calculated by Arrhenius expression in Equation 4.19 (Turns, 2000).

$$k_{f,r} = A_r T^{\beta} e^{-(E_r/R_u T)} \tag{4.19}$$

where β_r is thetemperature exponent, A_r is the pre-exponential factor, E_r is the reaction activation energy (J/kmol) and R_u is the universal gas constant (J/kmol.K).

4.2.1.2 The Eddy-Dissipation Model

The rate of combustion and eddy dissipation are related in the Eddy-Dissipation Model. This model includes turbulent kinetic energy and the rate at which it dissipates along with the mean concentration of reactive species. In some premixed flames, turbulence merges gently hot products and cold reactant into the combustion region where reaction emerges quite fast. In these cases, one can approximate that combustion is limited by mixing and complex chemical kinetic rates can be neglected. Instead of this, instantaneous burn occurs upon mixing. For this approximation, Eddy-Dissipation (ED) model (Magnussen & Hjertager, 1977) can be integrated within CFD codes. From these model, the net rate of products of species (i), $R_{i,r}$ is defined with the Equations 4.20 and 4.21 (Poinsot & Veynante, 2005).

$$R_{i,r} = \nu'_{i,r} M_{w,i} A \rho \frac{\varepsilon}{k} \min\left(\frac{Y_{\Re}}{\nu'_{\Re,r} M_{w,\Re}} \right) \tag{4.20}$$

$$R_{i,r} = \nu'_{i,r} M_{w,i} A B \frac{\varepsilon}{k} \left(\frac{\sum_P Y_P}{\sum_j \nu''_{j,r} M_{w,j}} \right) \tag{4.21}$$

where Y_P is the mass fraction of products of reaction P, $Y_{\Re}$ is the mass fraction of products of reaction $\Re$, A and B are given as constants (A = 4.0, B = 0.5). In Equations 3.20 and 3.21, The large eddy merging time scale regulates the rate of chemical reaction., k/ε, which is defined in the common Eddy-Breakup Model (Spalding, 1971). According to this model, combustion continues whenever turbulence occurs in the domain ($k/\varepsilon > 0$). Thus, a combustion starting source is not needed to start the combustion. However, in premixed flames, the reactants burn and finish immediately, therefore, the CFD codes solve this problem with interaction of finite-rate and eddy-dissipation model in which both rates of finite rate combustion (Eq. 4.18), eddy-dissipation (Eq. 4.20) and rates (Eq. 4.21) are computed. Between Equation 4.20 and 4.21, minimum value is chosen for the net reaction rate. After the ignition starts, the eddy-dissipation (ED) rate is often lower than Arrhenius rate, and the chemical reactions can be approximated as mixing-limited (Poinsot & Veynante, 2005; Turns, 2000).

4.2.1.3 The Eddy-Dissipation-Concept (EDC) Model

The eddy-dissipation-concept (EDC) model is an modified approach of the eddy-dissipation model that contains chemical mechanisms in detail for turbulent reactions (Ansys Inc., 2021; Magnussen, 1981; Sun et al., 2021). CO and NO, which are among the critical emissions limited by the standards, are gases that have a harmful effect on the environment. During the premixed combustion process, CO emerges from dissociation of CO_2 at high combustion temperatures. Besides, NO is generated throughout the combustion region because of the dissociation of N_2 and O_2 into their lower states. Thus, their following interactions of oxygen and nitrogen in the molecular phase (Ferguson & Kirkpatrick, 2016). NO is formed via four different types of pathways: thermal, prompt, fuel, and N_2O (Hinrichs, Hellmuth, et al., 2021; Trisjono & Pitsch, 2017). Owing to the large time scale of NO generation, the EDC model is used to predict the NO formation. As a detailed chemical mechanism, an improved mechanism called GRI Mech 3.0 is utilized to simulate natural gas combustion, including NO production and reburn chemistry (G. P. Smith et al., n.d.). GRI Mechanism is mostly preferred in the literature as a reference model due to its reliable and robust results (Hinrichs, Hellmuth, et al., 2021; Konnov et al., 2018; G. P. Smith et al., n.d.).

In this model, molecular mixing of the reactants is considered to occur in isolated and concentrated regions which is called as fine scales contains small rate of fluid. The fine scale ratio of the flow is defined with the Equation 4.22 (Gran & Magnussen, 1996).

$$\gamma_f = \left(0.75\frac{C_{D2}}{C_{D1}}\right)^{1/4}\left(\frac{\nu\varepsilon}{k}\right)^{1/4} \tag{4.22}$$

where C_{D1} = 0.134 and C_{D2} = 0.50 are constants of the model, υ is the kinematic viscosity, ε is the ratio of dissipation, k is the turbulent kinetic energy. Time scale between fine structures and the ambient can be predicted with the Equation 4.23 (Gran & Magnussen, 1996).

$$\tau = \left(\frac{C_{D2}}{3}\right)^{1/2} \left(\frac{\nu}{\varepsilon}\right)^{1/2} \tag{4.23}$$

In CFD Codes, combustion emerges with constant pressure reactor approach via initial conditions of reacting species and temperature. According to reaction rates, combustion reactions will continue in given time scale and they are integrated with in situ adaptive tabulation (ISAT) fast chemistry algorithm (Pope, 1997). The EDC may be used with detailed chemical mechanisms, but numerical integrations are complex and require higher computer resources than standard eddy dissipation model.

4.2.1.4 The Relaxation to Chemical Equilibrium Model

While handling finite-rate, eddy dissipation or EDC models in CFD codes, chemical reacting species occur according to given chemical kinetic mechanism. Reacting species are driven to supply equilibrium state in this relaxation to chemical equilibrium model. Thus, the reaction source becomes in the i^{th} mean species on the equation of species conservation as shown in Equation 4.24 (Agarwal et al., 2018).

$$R_i = \rho\left(\frac{Y_i^{eq} - Y_i}{\tau_{char}}\right) \tag{4.24}$$

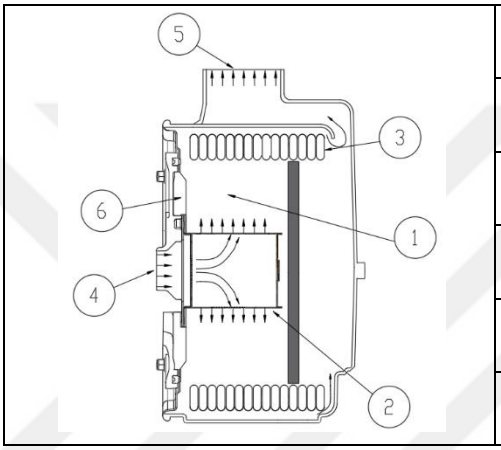
where Y_i is the mean mass fraction for species (i) and ρ is the density and the superscript is given as chemical equilibrium, τ_{char} is a characteristic timescale. For eddy dissipation model, $\tau_{char} = \tau_{turb}$ approximation is accepted. Besides that, $\tau_{char} = \tau_{turb} + \tau_{chem}$ approach is preferred in the simulations. In this model, species are driven to chemical equilibrium instead of detailed whole reaction process. Thus, the model needs to supply more reliable predictions of intermediate fractions such as CO, OH and O which is useful for calculating NO_X emissions.

4.3 Numerical Investigation Parameters of the Study

4.3.1 Combustion System Overview

The combustion system of a commercial condensing boiler unit which has 24 kW nominal power were investigated in this thesis. This condensing boiler was used as a heating device and the burner of the heating device utilizes methane (G20) and natural

gas fuels (NG) with 20 mbar pressure in respect to "Test gases, test pressures and categories of appliances standard" (EN 437:2018) (European Committee for Standardization, 2018). According to "Gas-fired heating boilers standard" (EN15502-1:2012+A1:2015), the NO_x class of the boiler is 6, which means NO_x emissions need to be lower than 56 mg/kWh (European Committee for Standardization, 2015). The combustion system characteristics of the specified device were used to verify the numerical model with the literature data. The schematic of a condensing boiler unit with its components is demonstrated in Figure 4.9.



1	Combustion region
2	Burner
3	Helical coils of heat exchanger
4	Premix gas inlet
5	Flue gas outlet
6	Insulation

Figure 4.9 Schematic of the commercial condensing boiler

When the combustion system of the heating device is examined in detail through main components, pre-mixed gas is supplied to the burner via the connection line and fuel-air mixer after the fan. In the scope of the thesis, the CAD drawing of the combustion domain for the heating device was obtained for the capacity of 24 kW. Air and fuel come into the system at the surrounding environmental temperature. Then, both gases are combined in the gas mixer to obtain the premixed fuel-air mixture at the molecular level. Premixed gas is forced into the combustion region with the help of a fan. While this phenomenon happens, the gas contacts with the walls system, which is hotter due to the conduction; therefore, when the gas leaves the burner, it has an initial temperature higher than the external temperature. This inlet temperature is one of the investigation parameters of this study.

After that, the gas mixture enters the combustion region by passing through the perforated cylindrical holes of the burner. In holes on the burner surface, flames

develop in the combustion region. As a result of the flames formed in the holes, high temperatures occur, and the heat is transmitted radially throughout the combustion region. Flue gases formed from combustion quickly hit the heat exchanger surfaces and pass between the helical coils of the heat exchanger.

Meanwhile, heat transfer takes place on the coils of heat exchanger surfaces. The gases coming to the heat exchanger outlet region are released from the flue gas outlet towards the chimney. CO and NO emissions emerge and alter between the burner holes and the outlet of the helical coil heat exchanger. It is assumed that there will not be much change in emission ratios after this region (Hinrichs et al., 2018).

The heating unit of the boiler contains a cylindrical combustion region between cooling coils and a perforated cylindrical premix burner. Location of the burner inside the heating device is shown in Figure 4.9.

4.3.2 Numerical Modelling of the Combustion Domain with Premixed Burner

Within the scope of studies, CAD model of the perforated cylindrical premixed burner was obtained as a solid body and combustion region is modeled according to actual dimensions. The burner used in the numerical investigation is a cylindrical, multi-hole premixed combustor that is adapted for the combustion domain of the condensing boiler. The burner is made of stainless-steel material. It has a structure resistant to high temperatures and corrosion. Isometric and cross-sectional view of the burner as solid model is presented in Figure 4.10a and 4.10b, respectively.

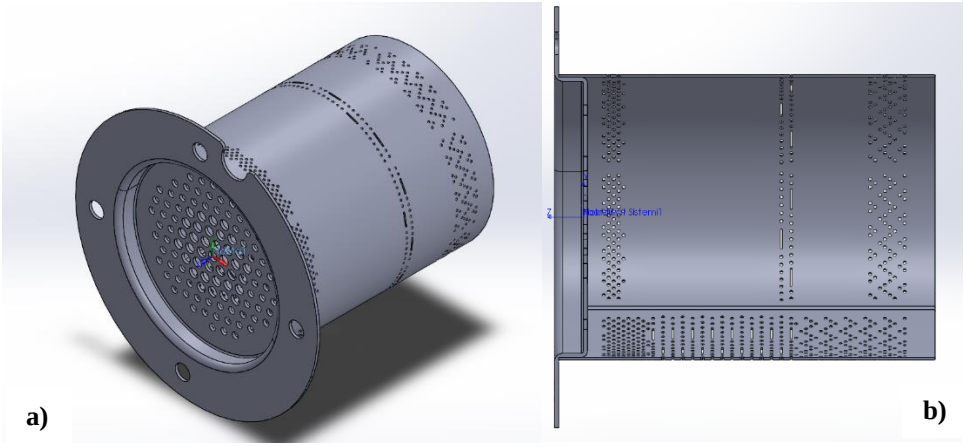


Figure 4.10 View of the burner as solid model: a) isometric and b) cross-sectional

According to condensing boiler configuration, combustion region is designed as a three-dimensional (3D) computational model. Model domain was built according to real operating conditions, boundary limits and physical requirements. The fluid domain of the combustion was designed between the burner and heat exchanger tube surfaces. Thanks to the symmetrical structure of the examined combustion zone, combustion region was sliced as 60- degree sector domain. In order to take advantage of this symmetrical structure, reduce the computer load and increase the calculation speed, a two-dimensional (2D) computational domain was extracted that has a flat surface with zero thickness. The isometric view, sliced 60º sector and two-dimensional (2D) dimensional of the combustion domain are demonstrated in Figure 4.11a and 4.11b, respectively.

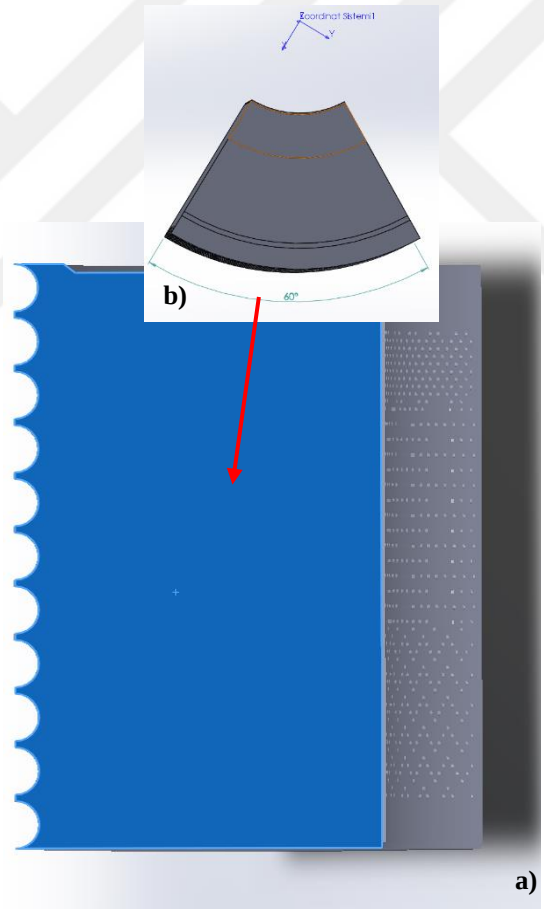


Figure 4.11 a) Isometric view of the 2D combustion domain and b) sliced 60º sector

4.3.3 Boundary Conditions and Simulation Setup

The combustion zone, which is examined as a computational domain, is surrounded by a premixed cylindrical burner, insulated surfaces, and coils of the heat exchanger. Premixed burner, insulation and heat exchanger coils are given in detail with Figure 4.12.

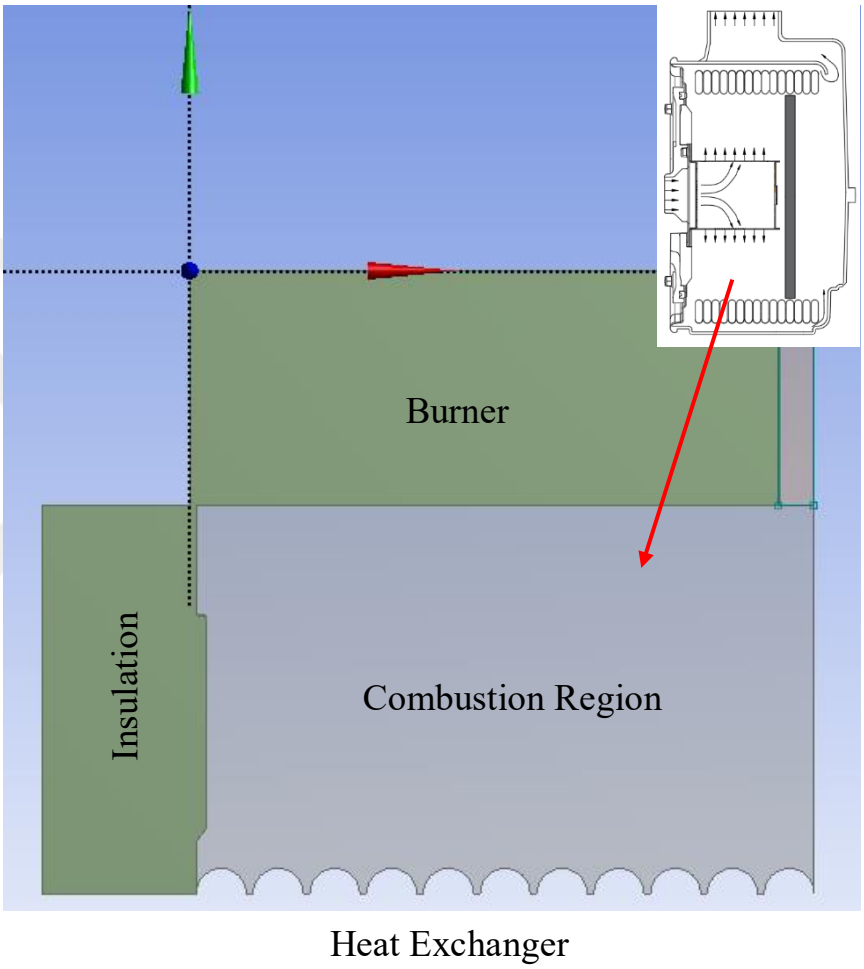


Figure 4.12 Two-dimensional combustion region

According to the studies carried out within the scope of the project studies and the information obtained from the literature (Hinrichs et al., 2018; Hinrichs, Schweitzer-De Bortoli, et al., 2021; Lamioni et al., 2022a; S. Lee et al., 2011b), the premixed gas starts to burn immediately after leaving the burner and a flame develops close to the burner surface in the combustion region side. To precisely model and compare this flame region, the symmetrical calculation area was obtained from this two-

dimensional region, similar to the literature (Figure 4.13). As seen in Figure 4.14, to reduce the computational effort on combustion analysis and simulate the flame accurately over the burner, a novel, double-holed, the 2D symmetrical computational domain is selected from this surface. Based on the project studies, flame distribution is considered symmetric over the combustion region.

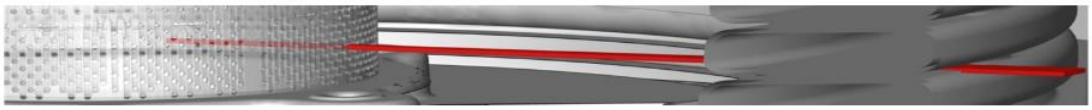


Figure 4.13 Single hole combustion zone calculation area from the literature (Hinrichs et al., 2018)

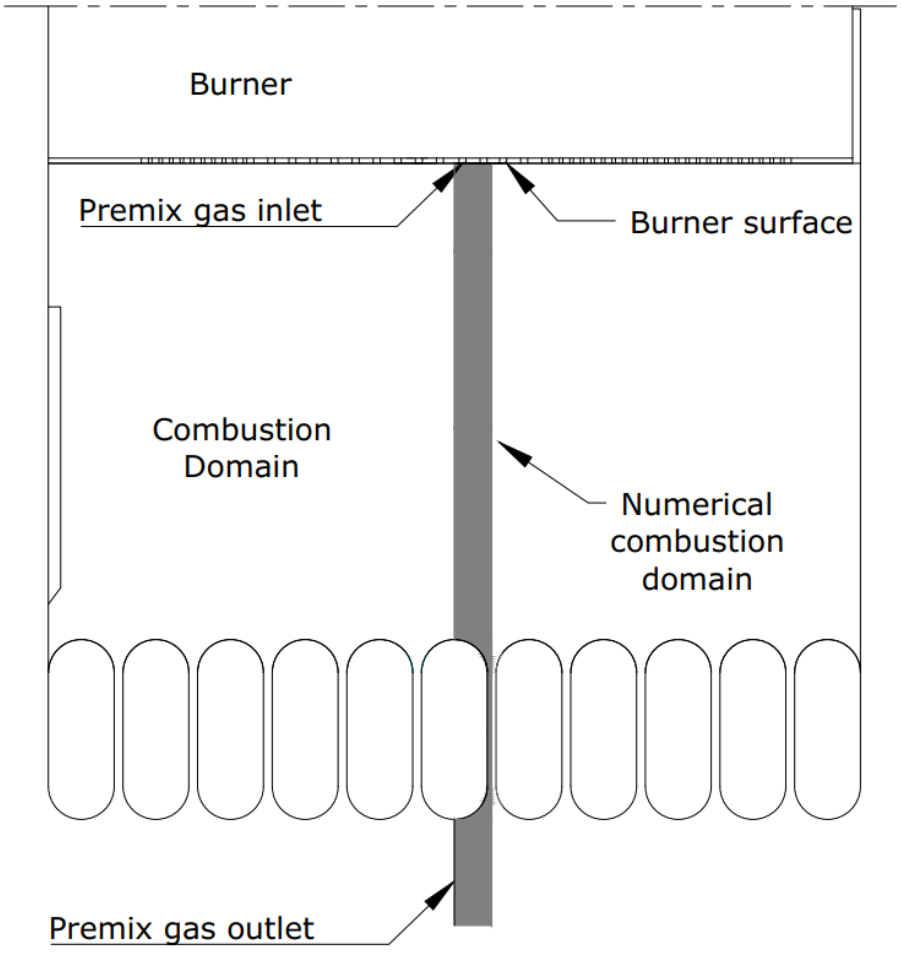


Figure 4.14 Location of the double hole on the burner and 2D symmetrical combustion domain

After specifying the general boundary conditions, parameters of the numerical study should be defined to the numerical setup in a careful manner. In the thesis,

numerical study was applied on a double hole, 2D combustion domain after the cylindrical premixed burner with CFD RANS simulation. Pressure-based solver was utilized on the simulations under steady-state conditions with the coupled algorithm using second-order upwind scheme for convection terms and a central differencing scheme for diffusion terms (Ansys Inc., 2021; Lamioni et al., 2023). Parameters of the numerical simulation setup are demonstrated in Table 4.1 for the combustion domain.

Table 4.1 Numerical setup parameters of the combustion domain

Numerical Setup Parameter	**Value**
Fluid domain	2D Planar
Viscous model	k-ε (2 equation)
Wall functions	Standard
Radiation model	Discrete Ordinates (DO)
Chemistry model	Species Transport (ST)
Reaction Type	Volumetric
Mixture material	Methane-Air
Chemistry mechanism	GRI 3.0
Turbulence-chemistry interaction (TCI)	Eddy Dissipation Concept (EDC)

In here, the pressure-based coupled algorithm calculates a coupled system of equations including the momentum equations and the continuity equation that based on pressure. The stabilized burner flame conditions are represented by Navier-Stokes equations with turbulent flow in low Mach number. Premixed combustion is initialized by relaxation process in the CFD code to supply the chemical equilibrium in the combustion domain. The ISAT rapid chemistry algorithm is then used to implement the chemistry computation. The normalized residuals preserve the numerical convergence.

Before applying ISAT algorithm, the relaxation process is implemented in the CFD code. In relaxation to chemical equilibrium, reacting species are pushed to the supply equilibrium state. In there, species are driven to chemical equilibrium instead of a detailed whole reaction process. CO and NO emission results are converted based on the standard oxygen concentration of 3% according to Directive 2010/75/EU of European Council on industrial emissions (European Council, 2010; Garan et al., 2023). The emission concentration at the standard percentage (%) oxygen

concentration is calculated using the following formula in Equation (4.25) (European Council, 2010).

$$E_S = \frac{21 - O_S}{21 - O_M} \; x \; E_M \tag{4.25}$$

Here, E_S is calculated emission concentration at the standard percentage oxygen concentration. E_M is measured emission concentration at premix gas outlet numerically. O_S is standard and O_M is measured oxygen concentration, respectively.

As stated in Table 4.1, in the thesis studies, ST combustion model approach is applied on the combustion domain. The energy model is opened in the combustion volume region and energy treatment is considered as non-adiabatic. Radiative heat transfer is activated in the combustion domain, which is crucial for CFD modeling of combustion (Malalasekera & Versteeg, 2007). Computations of the radiative heat transfer are carried out with Discrete Ordinates (DO) method which is commonly preferred in combustion simulations (Hinrichs et al., 2018; Warnatz et al., 2006). The entire spectrum of optical thicknesses is included in the DO model. Thus, the model enables to resolve issues with surface-to-surface radiation and combustion-related radiation (Ansys Inc., 2021). The weighted-sum-of-gray-gases model (WSGGM) is used as an adequate compromise between a gray-gas model and a comprehensive model that takes into account certain bands. (Coppalle & Vervisch, 1983). Absorption coefficient is based on WSGGM domain with zero scattering coefficient.

In the combustion model, the turbulence chemistry interaction is provided with the model of Eddy Dissipation Concept (EDC) (Ansys Inc., 2021). GRI 3.0 chemical mechanism is used with 53 species and 325 reactions individually (G. P. Smith et al., n.d.). Here, it is important to consider the transport of enthalpy caused by species diffusion since it can significantly affect the enthalpy field. Lewis number is calculated for each species including thermal conductivity, density, heat capacity and mass diffusion coefficient. Mass diffusivity and thermal diffusion coefficients are applied for 53 species of GRI 3.0 mechanism. Diffusion energy source, full multicomponent diffusion and thermal diffusion is activated in the combustion domain.

Methane-air mixture enters combustion region as lean premix gas with $\phi = 0.8$ equivalence ratio. The chosen equivalence ratio is inside the suitable range ($0.6 < \phi < 0.9$) that is an optimal lean premixed condition range for condensing boilers (S. Lee et al., 2011b, 2011a; Mohr et al., 2018; Soltanian et al., 2019; Yılmaz et al., 2021). In condensing boiler devices, it is assumed that the fuel and air are mixed at the molecular level through the gas mixer located before the premix gas inlet (4) indicated in Figure 4.9 In the numerical study, the equivalence ratio (ϕ=0.8) was kept constant in accordance with this assumption. Under actual conditions, the gas velocity depends on the revolution per minute of the fan which drives the premix gas through the system and the pressure drop encountered by the flow. On the other hand, the temperature depends on the air flow rate and the heat convection coefficient, as well as the heat conduction from the burner and the structure of the duct that connects fan and the premix gas inlet (4). In the present study, since it is modeled after the burner outlet (Figure 4.14), velocities and temperatures are analyzed at different values parametrically.

The fact that the equivalence ratio is constant rightfully suggests that the capacity will change with increasing velocity. However, in the study, a 2D symmetry model was used to analyze combustion characteristics and emissions with different inlet conditions. If the total capacity of the device needed to be correlated with the heat transfer results of this symmetrical model, it is needed to be multiplied with a coefficient that represents the number of the burner holes and heat exchanger surface. Therefore, the same capacity can be assumed if the aforementioned coefficient is variable. A more straightforward explanation is if the number of hole decreased inversely proportionally to the velocity increment, the flue gas flow rate and the capacity of the device can be assumed constant.

According to stated aspects, boundary conditions of the combustion domain are shown in Figure 4.15 for the combustion domain. As can be understood from Figure 4.14, flow domain is determined as 2D planar, double-holed and symmetrical cross-sectional surface body. Premixed gas inlets (A-B), flue gas outlet (E), symmetry (C) and heat exchanger coil surfaces (D) are defined as boundary conditions for CFD analysis for this determined region. Methane-air premixed gas mixture enters the

domain from double holes that are defined as velocity-inlet boundary condition. Inlet flow velocity is given as 0.5 m/s which is approximated from the experimental flow results of literature and conventional experimental data of the project. Inlet temperature is defined as constant temperature with 500 K for each hole. This temperature is obtained from conventional experimental data of the project and literature data (Hinrichs, Schweitzer-De Bortoli, et al., 2021; Soltanian et al., 2019). Boundary condition in the outlet is determined as zero pressure outlet at the end of the pipe walls. Walls of heat exchanger pipes are defined as constant temperature with 350 K considering 1 mm stainless steel pipe wall thickness. This value is determined according to literature studies (Hinrichs et al., 2018; Hinrichs, Schweitzer-De Bortoli, et al., 2021) and experimental studies with thermal camera measurements in the scope of TUBITAK 1505 Project. Symmetry boundary condition is defined in left and right sides of the numerical combustion domain.

According to the working principle of this device, premixed gas enters the combustion zone through the burner holes. Until the premix gas mixture reaches here, it heats up slightly by contacting the conduction-heated system walls. In the combustion process of the gas entering through the holes, the transport of chemical species and heat transfer take place in accordance with the equation specified in Equation 4.3. In the flue gas, convection and radiation effects constitute the main heat transfer mechanism. Afterwards, the resultant flue gas flows through the combustion chamber. When the hot combustion gases meet the heat exchanger, the flue gas accelerates due to the narrowing section. This situation increases the convection effects and heat is transferred from the heat exchanger surfaces to the water.

As seen in Figure 4.15, the region of the combustion gases passing through the heat exchangers was defined more realistically in order to examine the combustion exit region in detail. This region between the heat exchanger coils, the additional volume of combustion chamber was added to the fluid region by evaluating the project studies and current literature data. In the relevant region, there are more fluctuations in the combustion region for the CO and NO emissions, which are given importance in the standards, compared to other regions. The cross-sectional narrowing in the outlet

region of the combustion region increases the velocity of the combustion flue gases at the outlet region.

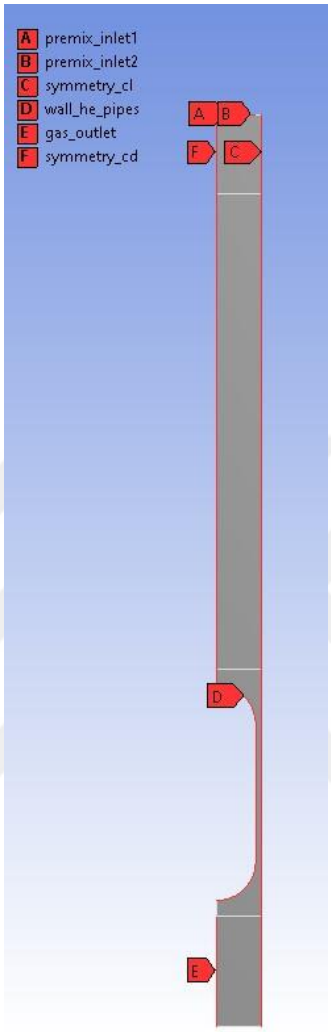


Figure 4.15 Boundary conditions of the combustion domain

The fact that the heat exchanger surface temperatures are quite low compared to the combustion chamber affects the chemical transformations of the accelerated combustion products. Parametrical analyses are defined as shown in Table 4.2.

Table 4.2 Boundary condition parameters of the analyses

Parameter name	Parameter type	Unit	Value
Equivalence ratio (ϕ)	Constant	-	0.8
Surface temperature of coils (T_{wp})	Constant	[K]	350
Premixed gas inlet temperature (T_{in})	Investigation variable	[K]	300 – 400 - 500
Premixed gas inlet velocity (V_{in})	Investigation variable	[m/s]	0.5 - 1.0 - 1.5 - 2.0

For the parametric analyses, average data were taken from the lines determined along the combustion direction. Data acquisition lines were created in a total of 48 lines as seen in Figure 4.16. These lines are created more frequently in flame front and heat exchanger region to obtain data in the numerical study. In here, the ratio y/L represents the dimensionless line position along the combustion domain.

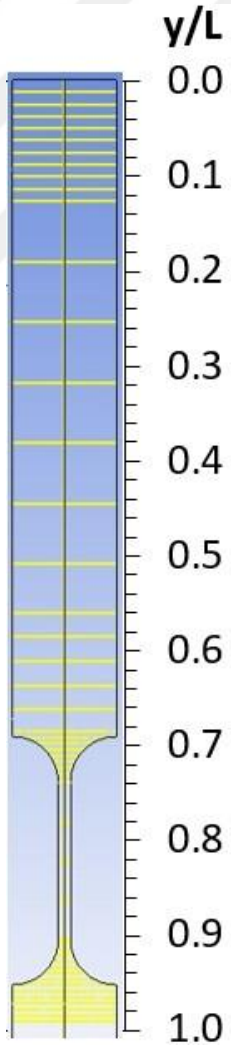


Figure 4.16 Dimensionless locations of data acquisition lines along the combustion domain

4.3.4 Mesh Generation

The mesh structure of numerical simulation model including premixed gas inlet (a), helical coil walls (b) and burnt gas outlet (c) is shown in Figure 4.17. The mesh consisted of approximately 41000 quadratic elements with average mesh quality of 0.96. Global mesh size is taken as 0.1 mm. The mesh size is adapted considering the balance of flame and flow in the premixed gas inlet region (Figure 4.17a). In addition, 10 inflation layers are created to capture the heat transfer effects better on the walls of heat exchanger with 0.25 mm total thickness and 1.2 growth rate (Figure 4.17b).

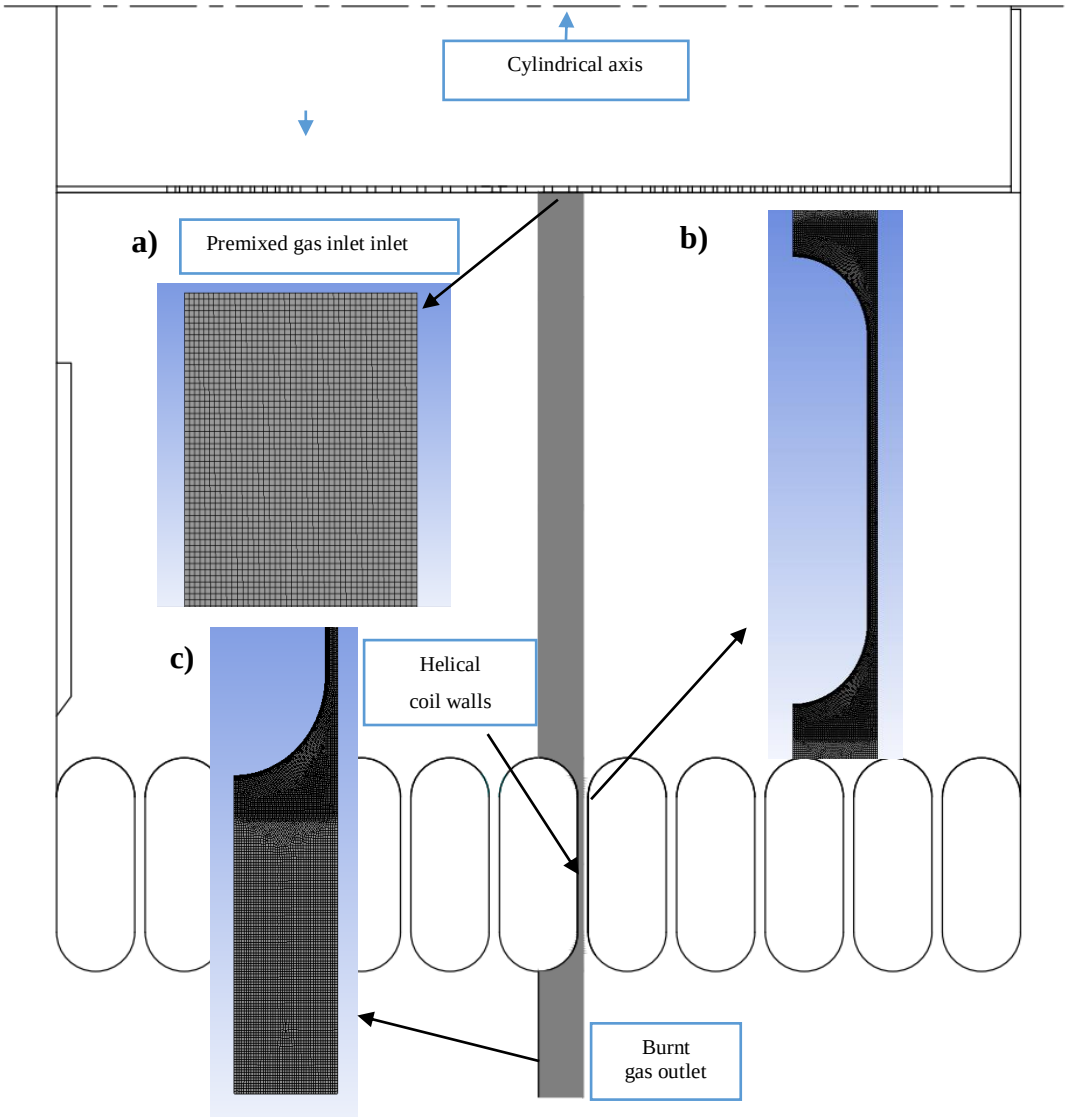


Figure 4.17 The mesh structure: a) premixed gas inlet b) helical coil walls c) burnt gas outlet

4.3.5 Mesh Independency

Before the combustion analysis, flow homogeneity must be ensured for the premix combustion to take place in the combustion chamber and numerical analyses must be performed independent from the grid size (Büyükakın, 2019; Malalasekera & Versteeg, 2007). Therefore, within the scope of the thesis, a mesh independency study was carried out by considering the parameters specified on the numerical simulation model.

The mesh independency analysis was implemented for numerical simulation domain with cold simulation of the premixed mixture. Providing independence from the mesh with cold analysis is important for predicting the flame and flow in a balanced way with combustion models in the mesh. (Malalasekera & Versteeg, 2007; Warnatz et al., 2006).

To examine the mesh accuracy of the CFD model, five different cases are compared as very coarse (7900), coarse (16800 elements), medium (24700 elements) fine (41000 elements) and very fine (68000 elements) on the combustion domain with the dimensionless length specified in Figure 4.17. The fuel-air mixture used in cold flow analyses is defined in numerical domain according to the equivalence ratio of 0.8. The velocity distribution across the domain was chosen as a parameter for comparison.

The very coarse mesh consisted of approximately 7900 quadratic elements with average mesh quality of 0.834. Global mesh size is taken as 0.25 mm with automatic quadratic method as body sizing. Face sizing is adapted as 0.125 mm near the heat exchanger coils. Around walls of the heat exchanger, 10 layers of inflation are applied with 1.2 growth rate and 0.25 mm total thickness.

The coarse mesh consisted of approximately 16800 quadratic elements with average mesh quality of 0.914 Global mesh size is taken as 0.15 mm with automatic quadratic method as body sizing. Face sizing is adapted as 0.1 mm near the heat exchanger coils. Around walls of the heat exchanger, 10 layers of inflation are applied with 1.2 growth rate and 0.25 mm total thickness.

The medium mesh consisted of approximately 24700 quadratic elements with average mesh quality of 0.936. Global mesh size is taken as 0.125 mm with automatic quadratic method as body sizing. Face sizing is adapted as 0.075 mm near the heat exchanger coils. Around walls of the heat exchanger, 10 layers of inflation are applied with 1.2 growth rate and 0.25 mm total thickness.

The fine mesh consisted of approximately 41000 quadratic elements with average mesh quality of 0.961. Global mesh size is taken as 0.1 mm with automatic quadratic method as body sizing. Face sizing is adapted as 0.05 mm near the heat exchanger coils. Around walls of the heat exchanger, 10 layers of inflation are applied with 1.2 growth rate and 0.25 mm total thickness.

The very fine mesh consisted of approximately 68000 quadratic elements with average mesh quality of 0.978. Global mesh size is taken as 0.075 mm with automatic quadratic method as body sizing. Face sizing is adapted as 0.035 mm near the heat exchanger coils. Around walls of the heat exchanger, 10 layers of inflation are applied with 1.2 growth rate and 0.25 mm total thickness.

Mesh independency results for five different mesh cases, depending on the average velocity, are given in Figure 4.18.

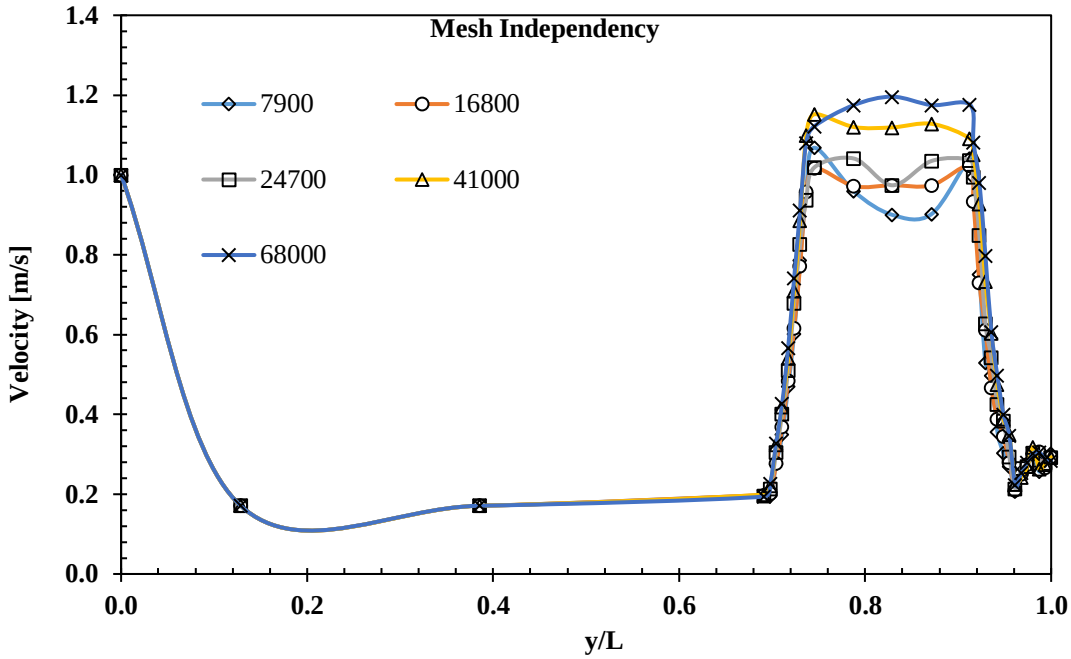


Figure 4.18 Variation of the average velocity along the combustion domain for five different mesh cases

Table 4.3 shows mesh independency deviations with average velocity on data acquisition lines.

Table 4.3 Mesh independency with average velocity on data acquisition lines

Grid	Number of elements	Average velocity on data lines [m/s]	Deviation (%)
Very coarse	7900	0.504	-13.48
Coarse	16800	0.501	-14.09
Medium	24700	0.524	-10.12
Fine	41000	0.565	-3.10
Very fine	68000	0.602	-

When mesh independency results are compared, one can understand that similar results were obtained in terms of velocity distribution for five different cases. Minimum deviation is observed comparing with very fine mesh in fine mesh. Therefore, it has been deemed appropriate to use fine mesh size with 41000 elements in terms of ease of numerical calculation and computational speed.

4.4 Validation of CFD Model with Numerical Results of the Study

In this section, CFD analyses are compared with literature and project data. Validation of CFD model has been realized for premixed inlet velocity of 0.5 m/s and temperature of 500 K. In order to compare results obtained from the ST model to verify the CFD analysis results, the average of the data was obtained from the data acquisition lines in Figure 4.16 and gas outlet region planes in Figure 4.19.

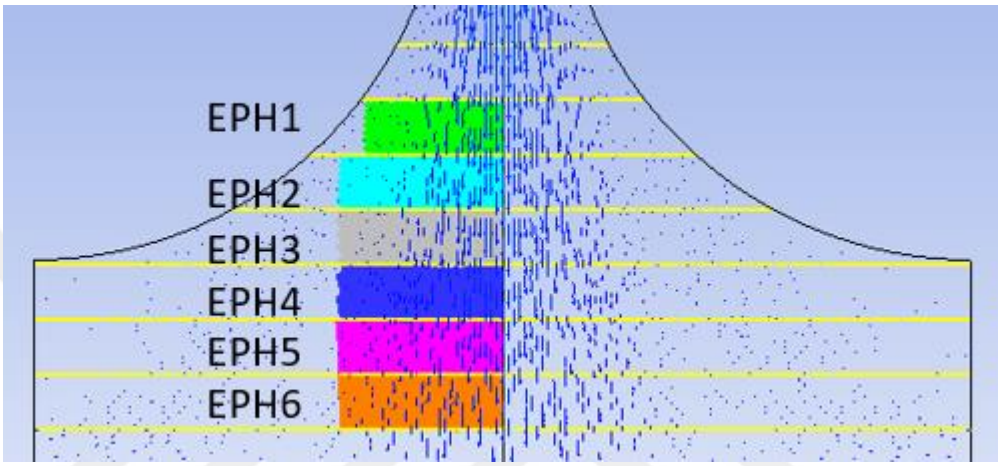


Figure 4.19 Location of flue gas outlet planes in the combustion domain

When the combustion analysis results are examined, it was observed that there were minor differences in the results of temperature, velocity, CO, and NO emissions for ST model. In Figure 4.20, variation of the temperature along the combustion domain is shown comparing current study with literature experimental study (Hinrichs et al., 2018). In the figure, the temperature profile along the dimensionless length of the combustion domain obtained from current study are compared to those attained from the experimental data of literature (Hinrichs et al., 2018). The temperature variation of the current study along the combustion chamber is in good agreement with the compared data. In the flame region, temperatures were overestimated. Temperatures are within ranges throughout the domain and some underestimation is observed in the exit region. It is predicted that this difference is due to the difference in the heat exchanger geometry. The mean temperature deviance is 6.36% between the CFD results and experimental mean data of literature (Hinrichs et al., 2018) for centerline along the combustion domain.

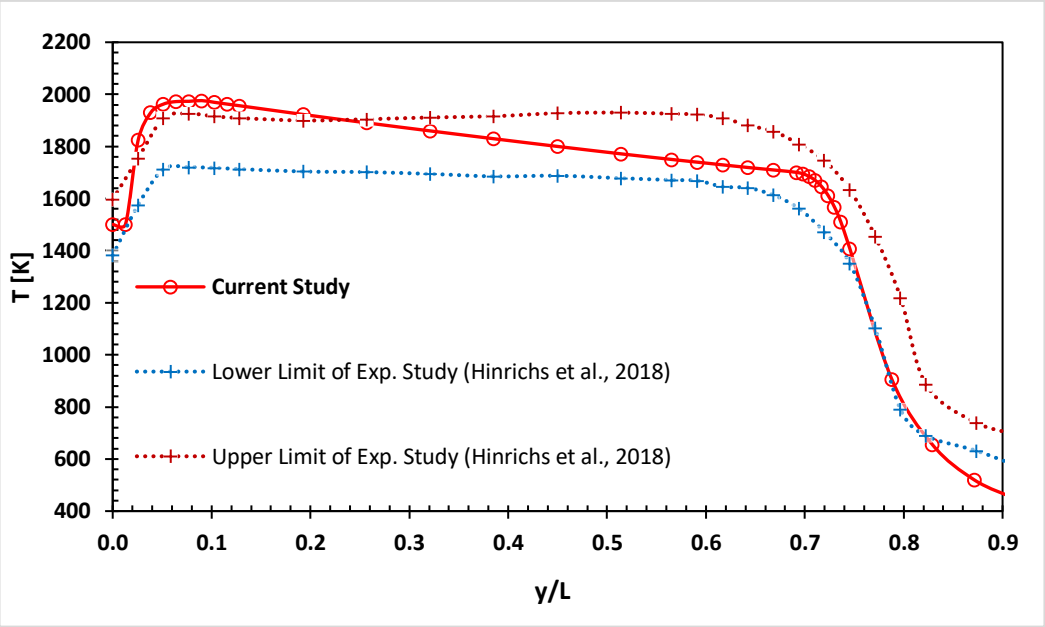


Figure 4.20 Variation of the temperature along the combustion domain comparing current study with literature experimental study (Hinrichs et al., 2018)

In similar conditions, the results of gas chromatography for CO and chemiluminescence detector (CLD) for NO in the literature study (Hinrichs et al., 2018) are compared. In the literature study, CO emissions were found in the range of 75 to 100 ppm, and NO emissions in the range of 10 to 22 ppm at the outlet region of heat exchanger. Besides, in the project studies, CO and NO emissions were obtained in the range of 50-130 ppm and 18-32 ppm, respectively. In the current study, at the same region, average CO and NO emissions are 81.6 ppm for CO and 26.8 ppm for NO, respectively. Thus, CFD model results are in reasonable agreement with the compared literature data. According to all this information obtained, CFD analyses were validated by evaluating the data.

4.5 Results

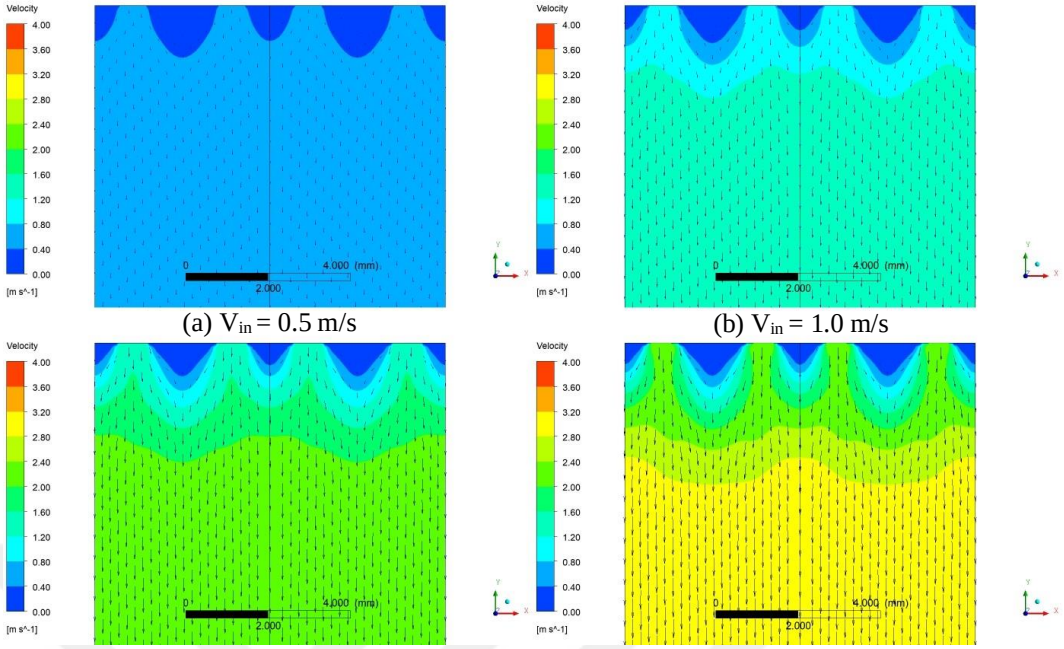
The methane-air mixture coming out of the cylindrical premix burner holes is not dispersed homogeneously. For each hole, there are differences in the air velocities depending on the location and size. In the project studies, it was determined that the flow distribution at the fan system outlet (burner inlet) was not homogeneous, and this situation could affect both the burner outlet area and the combustion characteristics. Thus, it was deemed appropriate to choose a wide range in terms of velocities in

numerical analysis. For the reasons stated, CFD analyses were performed for velocities of 0.5, 1.0, 1.5, and 2.0 m/s, respectively in the thesis.

In this section, the combustion region in the condensing boiler was investigated with ST approach. Flow and combustion characteristics including emissions were obtained for the premixed gas mixture entering the combustion region at different velocities through the holes of the burner. The contributions of premixed gas inlet velocity and temperature are shown parametrically in predicting the CO and NO emissions emerging in the combustion region. The premixed gas inlet velocity (V_{in}) interval is kept in a wide range and defined to vary between 0.5 and 2.0 m/s. Premixed gas inlet temperatures (T_{in}) are determined parametrically as 300 K, 400 K and 500 K. The case with 300 K of premix inlet temperature and 0.5 m/s of premix inlet velocity were used in the analyses to establish the baseline. In the actual boiler device, it is not possible for the fluid to come up to the burner outlet without heating due to the fan system and the internal structure of the burner.

4.5.1 Effects of Premix Inlet Velocity and Temperature on the Velocity Distribution and Flow Characteristics along the Combustion Domain

The velocity distributions are given varying between 0.5 to 2.0 m/s premix gas inlet velocity in Figure 4.21 for 500 K premixed gas inlet temperature around the burner holes and surface. As the premixed gas inlet velocity increases, the gas flow accelerates depending on the shape of the flame. Owing to the combustion over multi-holes of the burner, the velocity vectors combine after the flame is formed. As the premix gas inlet velocity rises, the combustion gas velocity advances. Flow participation occurs further at low velocities than at high velocities. This behavior indicates that velocity formation is effective in flame morphology and emission production. In addition, the velocity distribution is directly affected by the rapid acceleration of the flame tip in the entrance region (Lamioni et al., 2022a; Valiev et al., 2013).

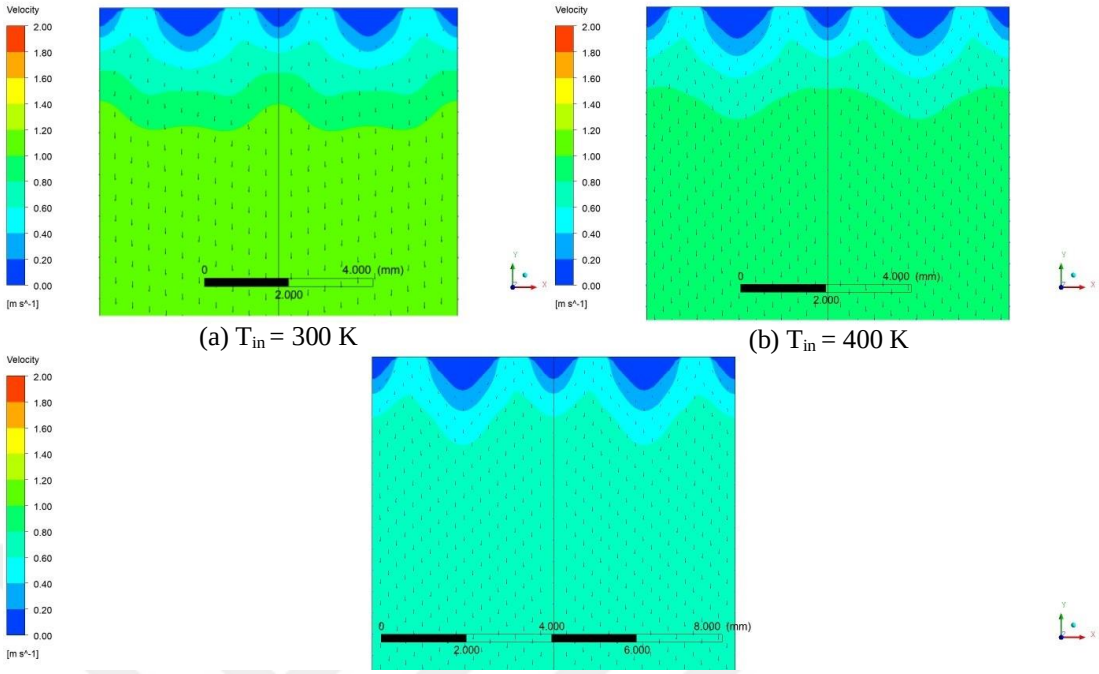


(a) V_{in} = 0.5 m/s (b) V_{in} = 1.0 m/s

(c) V_{in} = 1.5 m/s (d) V_{in} = 2.0 m/s

Figure 4.21 Velocity distributions at 500 K premixed gas inlet temperature for a) V_{in} = 0.5 m/s, b) V_{in} = 1.0 m/s, c) V_{in} = 1.5 m/s and d) V_{in} = 2.0 m/s premixed gas inlet velocities around the burner holes and surface

Velocity distributions at 0.5 m/s premix gas inlet velocity around the burner holes and surface are demonstrated in Figure 4.22 for 300 K, 400 K and 500 K premix gas inlet temperatures. It is seen that the change of premix gas inlet temperature significantly affects the flow characteristics. The flame region's flow characteristics change as the temperature rises. Species conversion is faster at higher inlet temperatures. Thus, higher velocities occur in the post flame region. As a result, these circumstances reduces residence time in the region of combustion and results in variations in emissions.



(a) T_{in} = 300 K (b) T_{in} = 400 K

(c) T_{in}= 500 K

Figure 4.22 Velocity distributions at 0.5 m/s premix gas inlet velocity for a) T_{in} = 300 K, b) T_{in} = 400 K and c) T_{in} = 500 K premix gas inlet temperatures around the burner surface

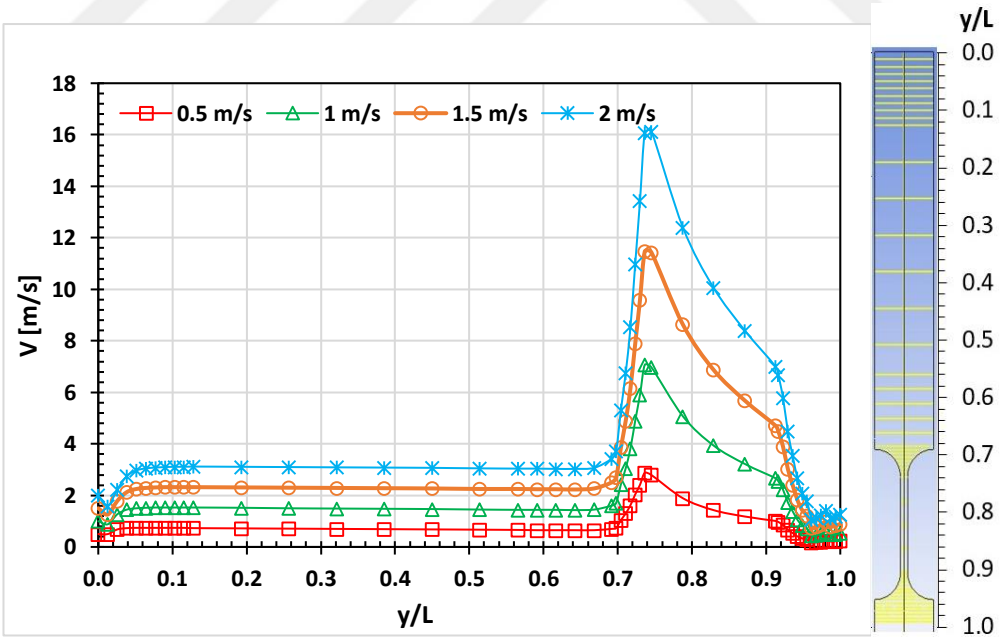


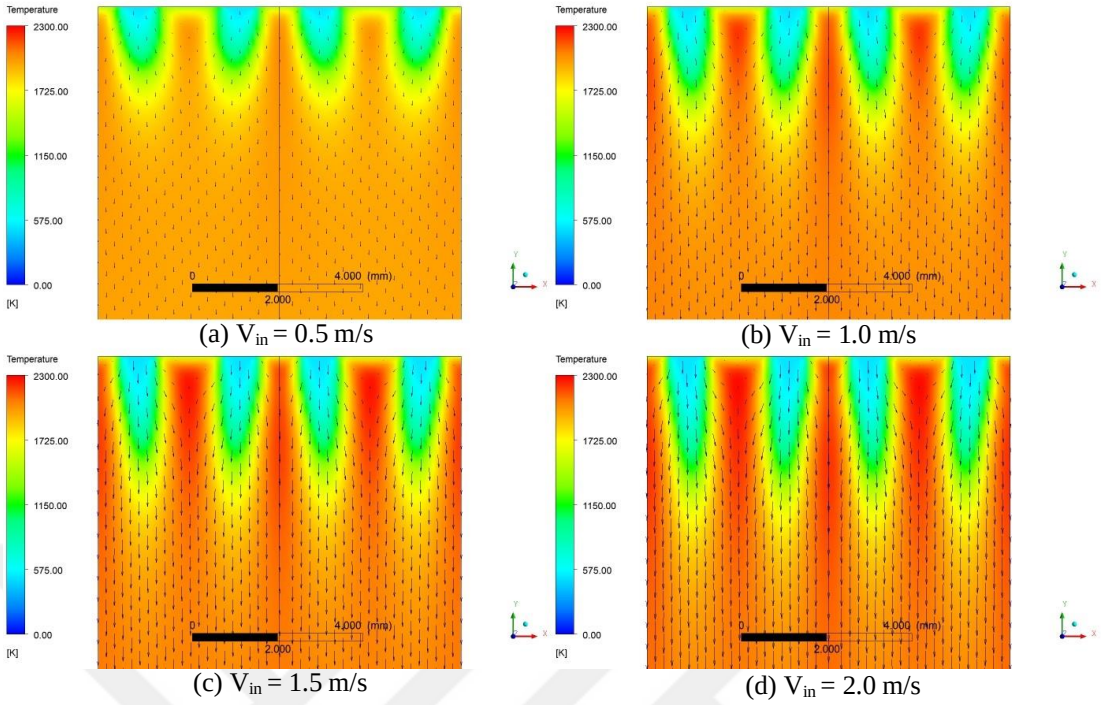
Figure 4.23 Variation of average velocities throughout the numerical domain for premixed gas inlet velocities of a) V_{in} = 0.5 m/s, b) V_{in} = 1.0 m/s, c) V_{in} = 1.5 m/s, and d) V_{in} = 2.0 m/s

Variation of average velocities throughout the numerical combustion domain for varying premixed gas inlet velocities are given in Figure 4.23.

It is clear from Figure 4.23 that the flue gas velocity remains essentially constant in the combustion region from the burner surface to the coils of the heat exchanger. A rapid increase in velocity was observed at the entrance of the coils and a sudden decrease was observed in the flue gases coming out from the coils. This acceleration is due to the shrinkage between coils of the heat exchanger. For the highest premixed gas inlet velocity, a five-fold increase was observed in the flue gas flow proportional to the incoming flow. It can be said that this situation, which has not been mentioned much in the literature, directly affects the heat transfer and the formation of emissions.

4.5.2 Effects of Premix Inlet Velocity and Temperature on the Temperature Distribution along the Combustion Domain

Temperature distributions are shown in Fig. 4.24 at 500 K premixed gas inlet temperature for premixed inlet velocities 0.5 to 2.0 m/s around the burner surface. It has been observed that the premixed gas inlet velocity directly affects the residence time and temperature in the combustion region. As seen in Figure 4.24, temperatures increases from flame downstream to upstream rapidly. As expected, the flame morphology changes with the increase in speed and the flame lengthens. Improving flame lengths causes the average temperatures around the flame to rise. This situation causes higher temperatures to be seen in the same region with the increase of premixed gas coming in higher flow rate.



(a) V_{in} = 0.5 m/s (b) V_{in} = 1.0 m/s

(c) V_{in} = 1.5 m/s (d) V_{in} = 2.0 m/s

Figure 4.24 Temperature distributions at premixed gas inlet velocities a) V_{in} = 0.5 m/s, b) V_{in} = 1.0 m/s, c) V_{in} = 1.5 m/s and d) V_{in} = 2.0 m/s at 500K premixed gas inlet temperature around the burner surface

Variation of temperature are demonstrated in Figure 4.25 throughout the numerical domain at 500 K premixed gas inlet temperature for premixed inlet velocities 0.5 m/s, 1.0 m/s, 1.5 m/s and 2.0 m/s. Temperatures decrease slightly as species conversion continues inside the combustion chamber. After the cold heat exchanger surfaces are encountered, an increase in velocities is observed due to the narrowing between the coils of the heat exchanger and temperatures have dropped radically. The rise of premixed gas inlet velocities resulted in higher temperatures throughout the combustion region. This behavior can be explained by the fact that the temperature in the flame region is higher and the transformation of the species involved in the equilibrium reactions occurs faster (Glassmann & Yetter, 2008). Additionally, residence time decreases along the combustion chamber depending on the increase in velocity and thus, flue gas enters between the heat exchanger coils at higher temperatures. There is a difference of around 300 K between the highest and the lowest velocities in the flue gas temperatures that entrain the heat exchanger coils. This behavior can be explained by the fact that the reactions take place later with the

decrease of residence time at higher velocities (Hassan et al., 2009; Hinrichs et al., 2018; Nemitallah et al., 2019).

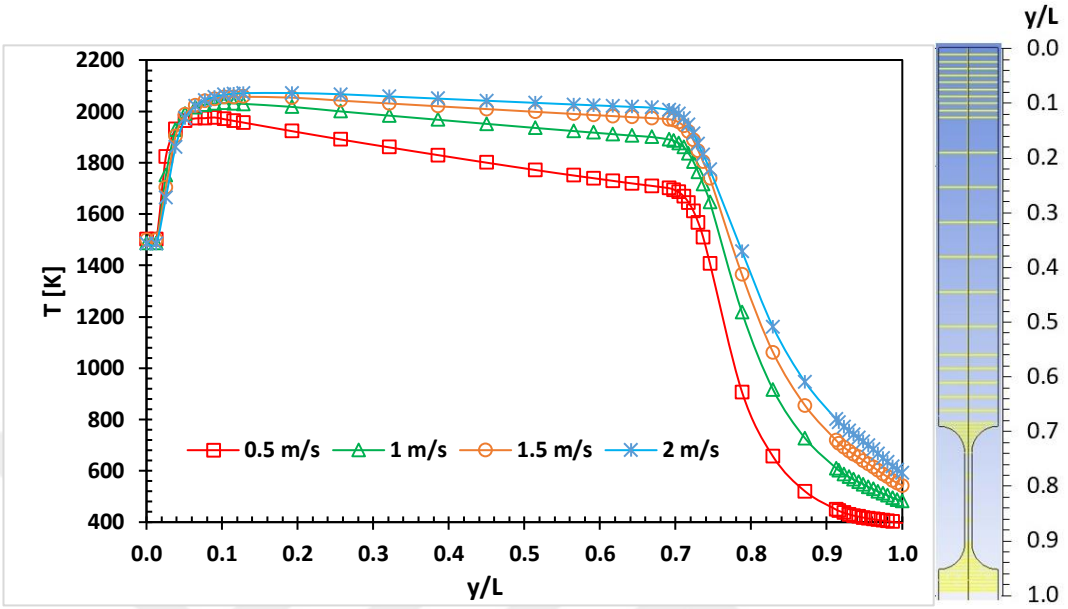
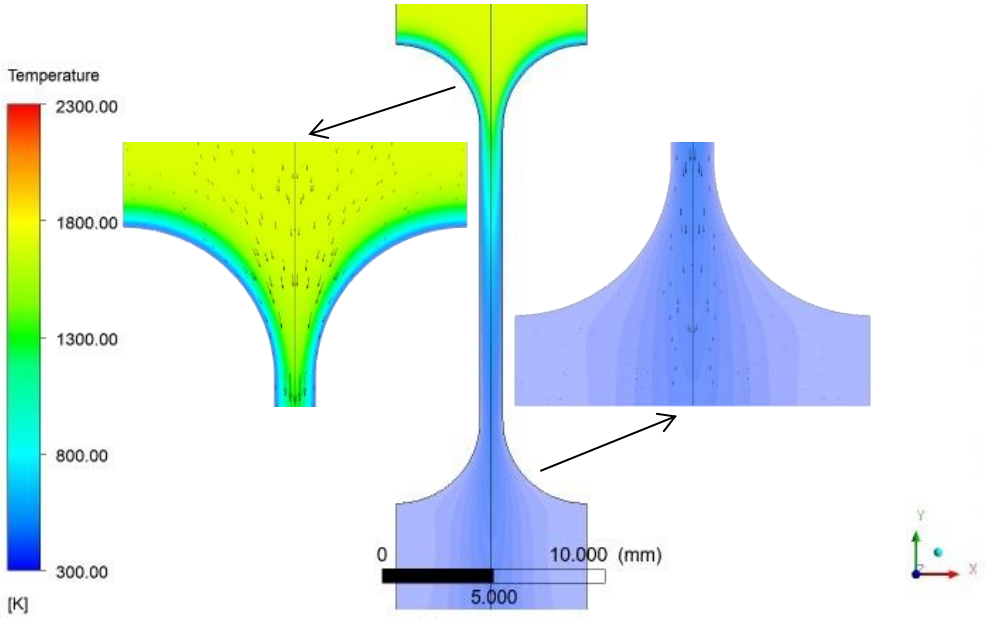
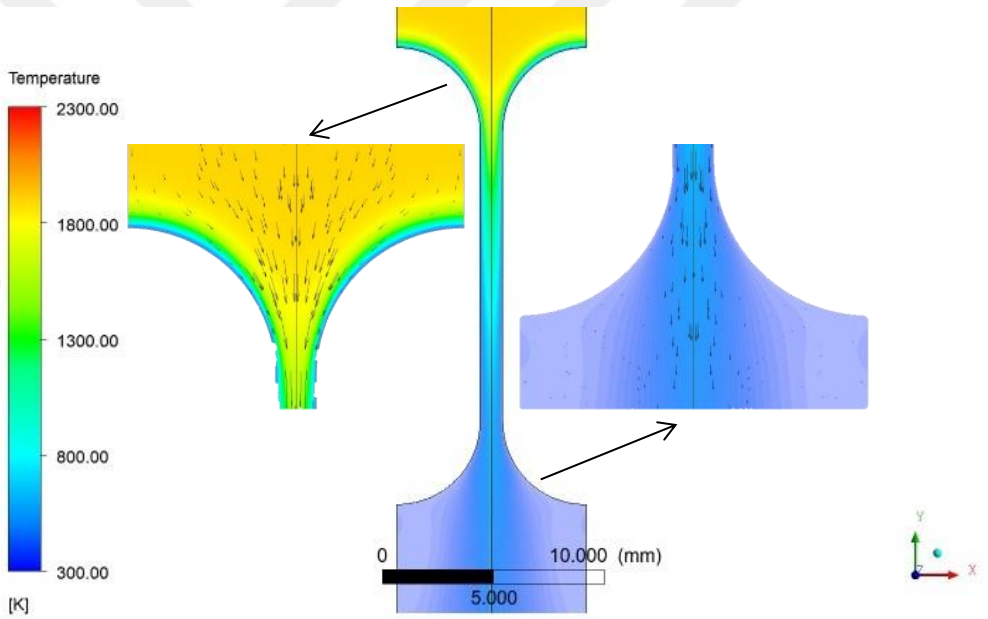


Figure 4.25 Variation of temperature throughout the numerical domain at 500 K premixed gas inlet temperature for premixed gas inlet velocities a) V_{in} = 0.5 m/s, b) V_{in} = 1.0 m/s, c) V_{in} = 1.5 m/s and d) V_{in} = 2.0 m/s

In Figure 4.26, temperature distributions are shown with velocity vectors at 500 K premixed gas inlet temperature around the heat exchanger coils for premixed inlet velocities 0.5 to 2.0 m/s around the heat exchanger coils.

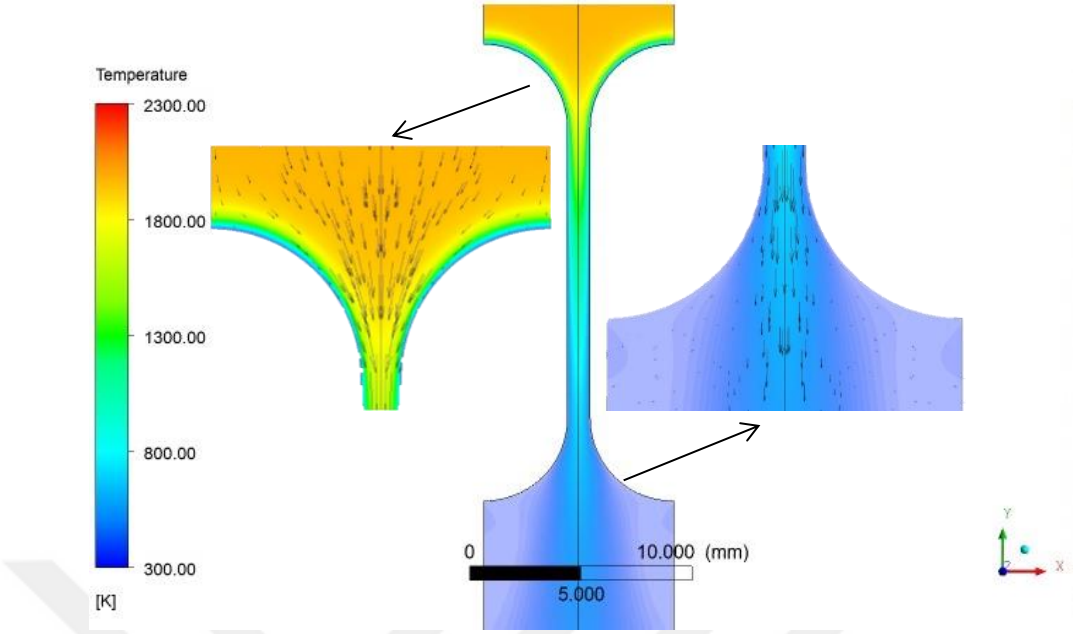


(a) V_{in} = 0.5 m/s

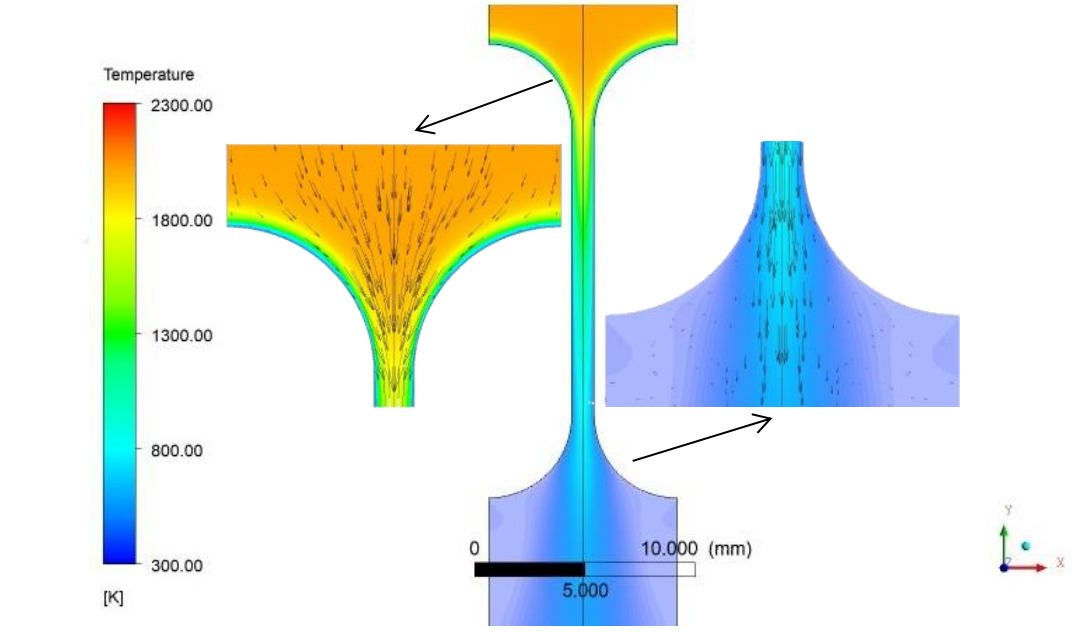


(b) V_{in} = 1.0 m/s

Figure 4.26 Temperature distributions with velocity vectors at 500 K premixed gas inlet temperature for premixed gas inlet velocities a) V_{in} = 0.5 m/s, b) V_{in} = 1.0 m/s



(c) V_{in} = 1.5 m/s

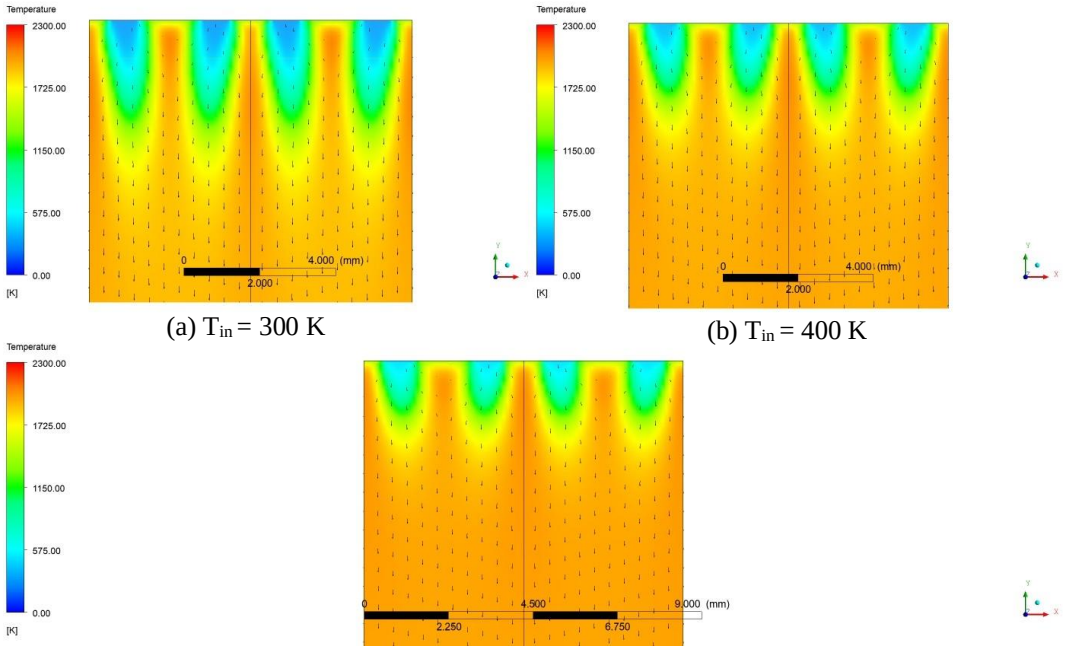


(d) V_{in} = 2.0 m/s

Figure 4.26 (cont.) Temperature distributions with velocity vectors at 500 K premixed gas inlet temperature for premixed gas inlet velocities c) V_{in} = 1.5 m/s and d) V_{in} = 2.0 m/s

It is observed that the temperature of the flue gas that encounters coils of the heat exchanger rises as the velocity of the premixed gas inflow increases. Average temperatures at the outlet rise as the emission formation region widens with flow rate. These changes in temperature and flow rate affect the variation of emissions. Temperature distributions are demonstrated with velocity vectors at 300 K, 400 K and

500 K premix gas inlet temperatures for 0.5 m/s premix gas inlet velocity around the burner surface in Figure 4.27. Variation of temperature are shown in Figure 4.28 throughout the numerical domain at 300 K, 400 K and 500 K premix gas inlet temperatures for premixed gas inlet velocity of 0.5 m/s around the burner surface. With the increase of premixed gas inlet temperatures, shortening of flame lengths is observed and simultaneously the average temperatures near the burner surface increases. This shows that combustion reactions are directly affected by the temperature of the incoming gas. The decrease in the premixed gas temperature causes the reactions to be delayed. The change of premixed gas inlet temperatures brings on different trends in the temperatures throughout the combustion region. In the case with higher inlet temperature, the flue gases enters the heat exchanger at a lower temperature. This behavior can be explained by the postponed completion of the reactions for the premixed gas with lower inlet temperature. Differences of around 150 K were observed in the mean temperatures in the outlet region of combustion chamber.



(a) T_{in} = 300 K

(b) T_{in} = 400 K

(c) T_{in} = 500 K

Figure 4.27 Temperature distributions at a) T_{in} =300 K, b) T_{in} = 400 K and c) T_{in} =500 K premix gas inlet temperatures for premixed gas inlet velocity of 0.5 m/s around the burner surface

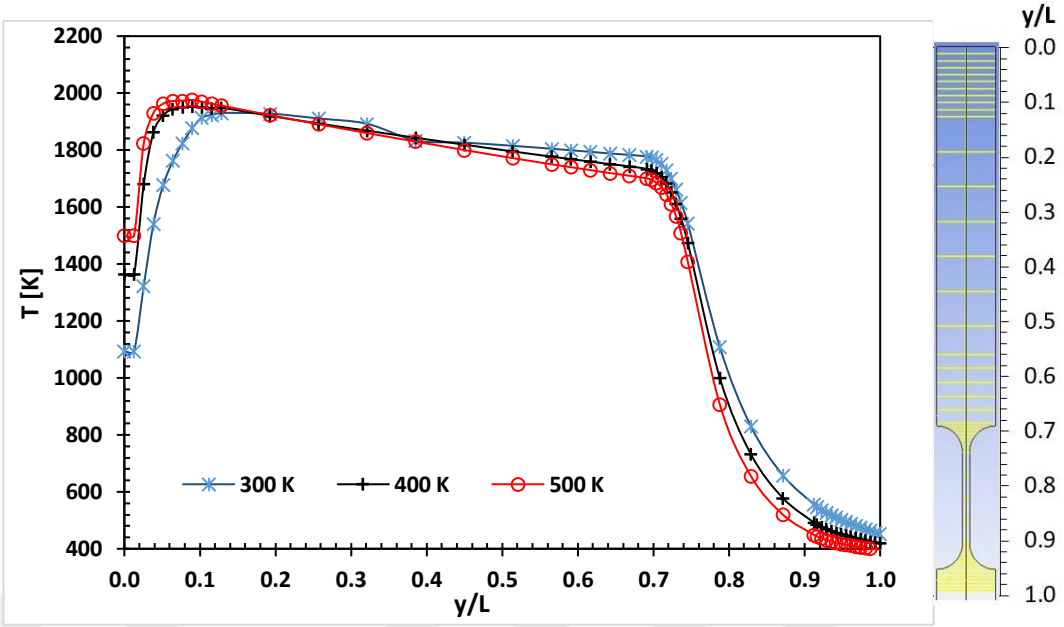
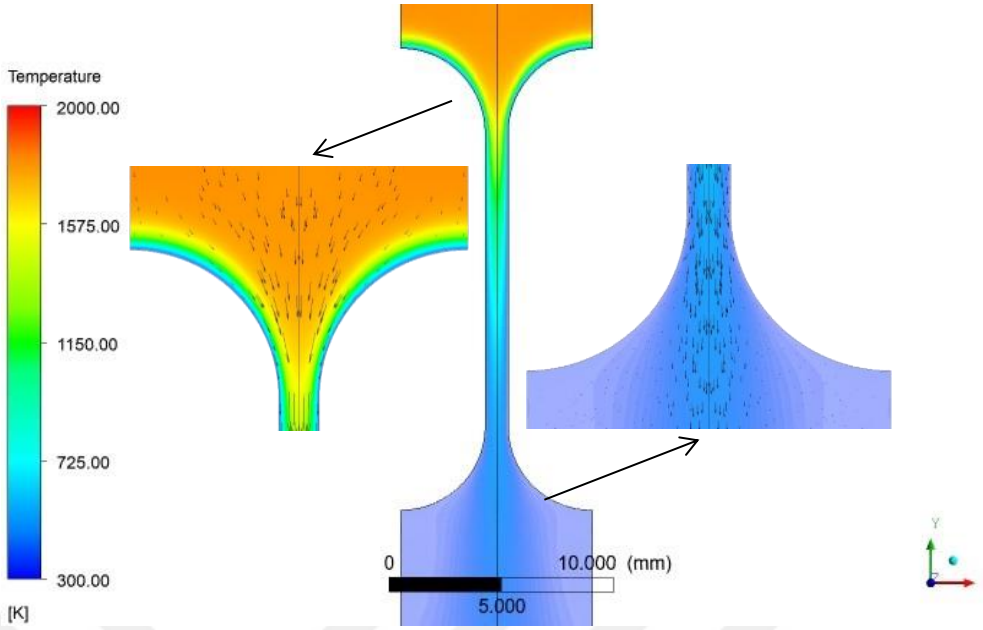
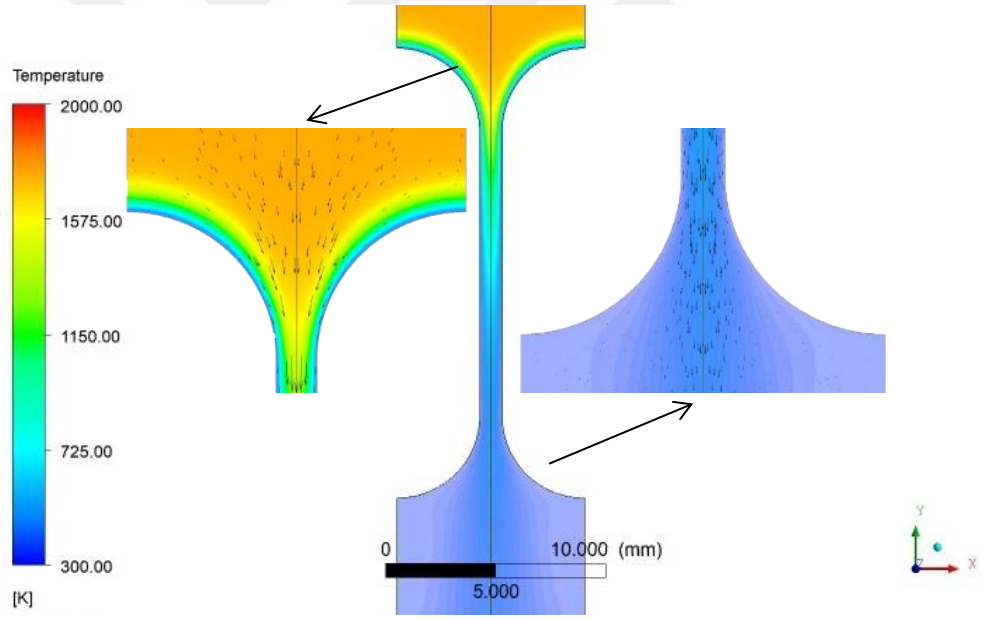


Figure 4.28 Variation of temperature throughout the numerical domain at a) T_{in} =300 K, b) T_{in} = 400 K and c) T_{in} =500 K premix gas inlet temperatures for premixed gas inlet velocity of 0.5 m/s

Temperature distributions are shown with velocity vectors at 300 K, 400 K and 500 K premix gas inlet temperatures for 0.5 m/s premix gas inlet velocity around the heat exchanger coils in Figure 4.29.

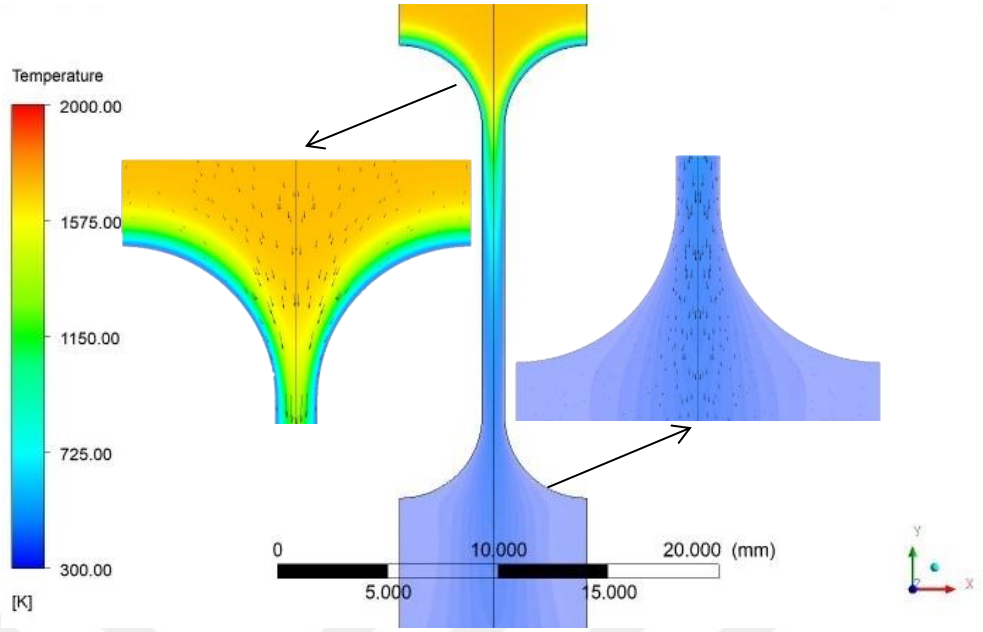


(a) T_{in} = 300 K



(b) T_{in} = 400 K

Figure 4.29 Temperature distributions with velocity vectors at a) T_{in} = 300 K, b) T_{in} = 400 K premix gas inlet temperatures for premix gas inlet velocity of 0.5 m/s around coils of the heat exchanger



(c) T_{in} = 500 K

Figure 4.29 (cont.) Temperature distributions with velocity vectors at c) T_{in} = 500 K premix gas inlet temperatures for premix gas inlet velocity of 0.5 m/s around coils of the heat exchanger

4.5.3 Effects of Premix Inlet Velocity and Temperature on CO and NO Emissions along the Combustion Domain

Figure 4.30 shows the comparison between calculated CO emissions and premixed gas inlet velocities (V_{in}) at 400 K and 500 K premixed gas inlet temperatures (T_{in}) for 350 K constant heat exchanger wall temperature (T_{wp}).

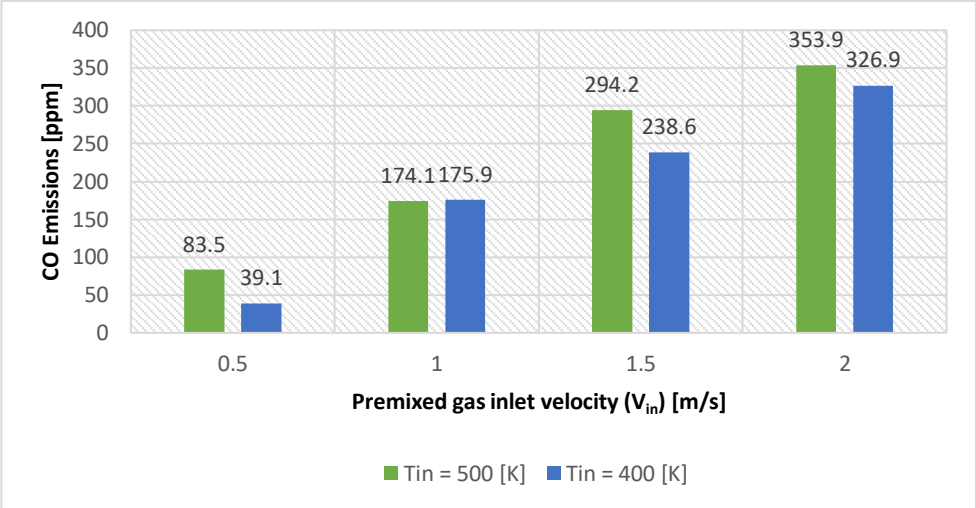


Figure 4.30 Calculated CO emissions versus premixed gas inlet velocities for 400 K and 500 K premixed gas inlet temperatures

The change of premixed gas inlet velocity directly affects the residence time and average temperature of the flue gases in the combustion region. Therefore, CO and NO emissions vary depending on these parameters. In terms of CO emissions, the premixed gas inlet velocity causes the average temperature to rise, but it also causes flue gases to reach the coils of heat exchanger faster. By the increase in premixed gas inlet velocity, CO emissions are expected to increase due to higher peak temperatures (Figure 4.26) in the flame region. As can be understand from the Figure 4.26, it has been observed that CO emissions behave similarly to the literature (Hassan et al., 2009; Hinrichs et al., 2018). In addition, the flue gas that encounters the cold heat exchanger in the outlet region freezes due to the CO oxidation freezing mechanism (Creighton, 2000; Hinrichs et al., 2018). Due to all these integrated effects, substantial escalation occur in outlet CO emissions with the rise in gas velocity. For constant velocity conditions, an increase in CO emissions is observed while the premix inlet gas temperature rises. This situation is directly related to the transformation mechanism from CO_2 to CO. Higher temperatures accelerate the conversion from CO_2 to CO (Glassmann & Yetter, 2008; Goodger, 1977; Hassan et al., 2009). Therefore, this behavior can be explained by the observation of higher peak temperatures in the flame region.

Figure 4.31 shows a comparison between calculated NO emissions and premixed gas inlet velocities (V_{in}) at 400 K and 500 K premixed gas inlet temperatures (T_{in}) for 350 K constant heat exchanger wall temperature (T_{wp}).

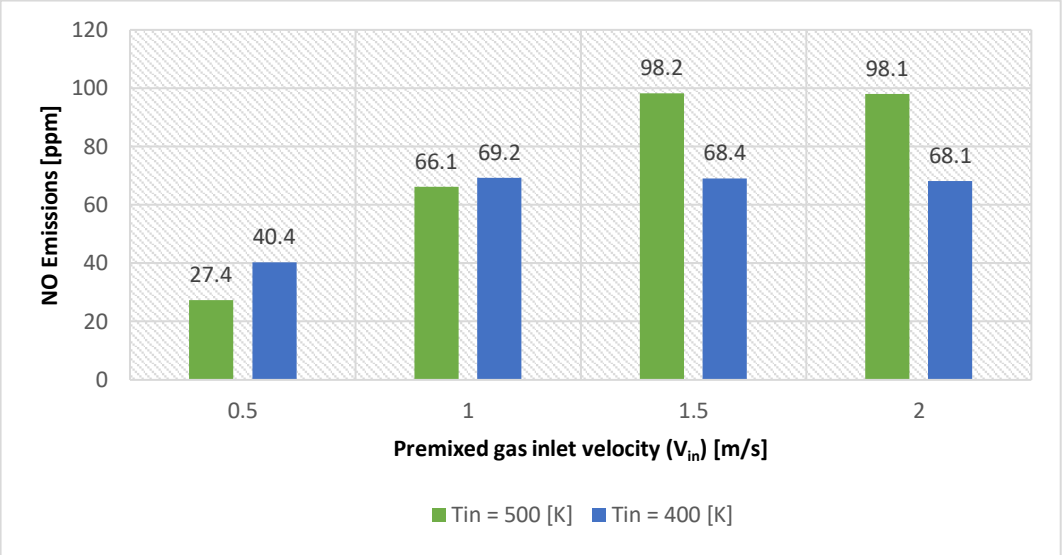


Figure 4.31 Calculated NO emissions versus premixed gas inlet velocities for 400 K and 500 K premixed gas inlet temperatures

In terms of NO emissions, the increase in premixed gas inlet velocity increased the peak temperatures in the flame region and the average temperatures in the combustion region. Thus, an increase was observed in thermal and prompt NO. By the time, NO formation is a slow chemical process (Glassmann & Yetter, 2008; van Oijen, Donini, Bastiaans, ten Thije Boonkkamp, & de Goey, 2016; Warnatz et al., 2006), as the residence time decreased, the increase in NO emissions reached equilibrium after a certain velocity. Emission increase stabilized after 1 m/s velocity for 500 K premixed inlet gas velocity and after 1.5 m/s input velocity for 400 K premix inlet gas velocity. This behavior can be explained by the increase in NO emissions with the rise in average temperatures and the decrease in NO emissions with reducing residence time.

CHAPTER FIVE
CONCLUSIONS

In the thesis, the effects of flue gases and emission characteristics were investigated on the thermal performance of a condensing boiler unit. Therefore, the chemistry, fluid mechanics, thermodynamics, and heat transfer aspects of the combustion region were extensively studied. The main aim of this study was to examine the effects of combustion gases and emission characteristics on the boiler considering with theoretical and numerical approaches.

Firstly, in accordance with the standards and regulations, the historical development, types, designs and design parameters of the components in the combustion region of a condensing boiler were evaluated. Types of flames and premix combustion mechanisms in the condensing boiler burner were investigated.

In the next section, on combustion region of the condensing boiler, investigations were performed in accordance with the determined theoretical research parameters. In the scope of the thesis, numerical codes were developed including aspects of Gibbs energy minimization and equilibrium constants methods. Theoretical investigations were carried out for standard gases as G20, G25, and NG with different equivalence ratios. The variations of adiabatic flame temperatures and gaseous emissions in respect to equivalence ratio for G20, G25, and NG fuels were investigated. Comparison of proposed models was performed with a commercial code using element potential method. When adiabatic flame temperatures were compared, predictions were made for all models with error rates below 1%. Also, while comparing emissions, minor deviations were observed in mole fractions of O_2, N_2, CO_2, H_2O, CO, and NO. In addition, CO and NO emissions, which are given importance by the standards, have been examined in detail. CO emissions tend to increase with an equivalence ratio due to quenching effect. The peak values of CO emissions are observed at $\phi = 0.9$ for all models and fuel types. Besides, NO emissions increased with the equivalence ratio due to the thermal and prompt NO mechanisms. NO emissions reach peak values at $\phi = 0.85$ for all models and fuel types. One of the important gain derived from this theoretical study is the obtained temperature and emission trends give knowledge about initial conditions of the numerical and experimental studies.

Later on, the combustion region of a commercial condensing boiler unit which has 24 kW nominal power were investigated with CFD including RANS equations in terms of combustion gases and emission characteristics. ST approach were preferred as a combustion model in the analyses. Before the analyses, the burner modelling and combustion region design was carried out. After defining the boundary conditions and analysis setup required for the numerical study, the mesh was created. Then, the mesh independency study was presented for the combustion region. Necessary reaction mechanisms were defined on designed domain and CFD analyzes were performed with different combustion models. Validation of numerical results with the literature and the experimental data of the project were accomplished according to flue gas outlet emission results. In the numerical study, velocity, temperature, pressure and emission results were obtained for the combustion region. Afterwards, extensive parametric analyzes were performed depending on different premixed gas inlet conditions including velocities and temperatures. Effects of premix inlet velocity and temperature on the flow characteristics, temperature distribution, CO and NO emission characteristics were investigated throughout the numerical combustion domain.

As a result of the validated numerical study, these conclusions were obtained as below. Combustion flue gas velocity depends on premix gas inlet velocity and temperature. It is found that flow participation emerges further at low velocities than at high velocities (Figure 4.21). This behavior shows that velocity profile is effective in flame structure (Figure 4.24) and emission production. The velocity distribution is directly affected by the rapid acceleration of the flame tip in the flame region. At the flame region, the increase in temperature changes the flow characteristics. Reactions of species are faster at higher premixed gas inlet temperatures, and higher velocities emerge in the post-flame region. Therefore, residence time diminishes in the combustion region and causes variations in the emissions.

Throughout the combustion domain, a five-fold velocity rise is realized for the highest premixed gas inlet velocity in the flue gas flow proportional to the incoming flow. It seems that this condition has direct impact on the heat transfer and the emission production. Therefore, it can be said that it is an important contribution for the literature since it is overlooked in previous studies.

Flue gas enters the heat exchanger coils at greater temperatures because residence time along the combustion chamber decreases as velocity rises. Between the highest and lowest velocities, there is a temperature difference of around 300 K in the flue gas that entrains the heat exchanger coils. The explanation for this phenomenon is that the reactions occur later with a decrease in residence time at higher velocities.

Shorter flame lengths are seen as the temperature of the premixed gas input rises, and average temperatures close to the burner surface also rise simultaneously. This demonstrates how the temperature of the incoming gas has a direct impact on combustion reactions. The flue gases enter the heat exchanger at a lower temperature when the inlet temperature is higher. This behavior can be attributed to the reactions for the premixed gas with the lower inlet temperature being delayed in their completion. Mean temperature differences of about 150 K are observed at the outlet for different premix gas inlet temperatures under constant premix gas inlet velocity.

The change in premixed gas input velocity directly impacts the average temperature and residence time of the flue gases in the combustion region. Consequently, these factors affect how much CO and NO are emitted. In terms of CO emissions, the premixed gas entry velocity raises the average temperature while also causing the flue gases to reach the heat exchanger faster. Due to greater peak temperatures in the flame region, the increased premixed gas velocity is anticipated to result in increased CO emissions. Additionally, the CO oxidation freezing mechanism causes the flue gas that comes into contact with the cold heat exchanger at the outlet to freeze. Due to all these interconnected factors, outlet CO emissions significantly increase as flow velocity increases.

In terms of NO emissions, the increase in premixed gas inlet velocity resulted in higher average combustion chamber temperatures and higher flame area peak temperatures. Therefore, thermal and prompt NO levels increased. The emission levels are balanced after 1 m/s for 500 K premixed inlet gas velocity and 1.5 m/s for 400 K premixed inlet gas velocity. This tendency can be explained by the increase in NO emissions with increasing average temperatures and the reduction in NO emissions with decreasing residence time.

When evaluated on a global scale, the use of the ST model approach provides more reasonable results for the accurate modeling of the emissions. From the emissions perspective, the major finding of the thesis is that emission characteristics of the flue gases can be easily obtained by using various fuels with the proposed models in the thesis for different combustion systems. Considering the application requirements and the design conditions demanded by the standards, the CFD model can be preferred in the estimation of flue gas velocities, temperatures and emissions.

As future studies, the temperature and velocity distributions can be examined by making improvements in the combustion region design, and the effects on the emission characteristics can be determined. By making changes on the gas mixer system and fan design before the combustion zone, positive results can be obtained in terms of temperature and emission values. In the numerical study, by using different detailed or reduced reaction mechanisms, more accurate estimations of the performance of the proposed model can be achieved.

REFERENCES

Agarwal, A. K., Pandey, A., Chaudhuri, S., & Sen, S. (2018). Modeling and Simulation of Turbulent Combustion. In *Modeling and Simulation of Turbulent Combustion*. Springer Singapore. https://doi.org/10.1007/978-981-10-7410-3

Akbari, M. H., & Riahi, P. (2010). Investigation of the structural and reactants properties on the thermal characteristics of a premixed porous burner. *Applied Energy*, *87*(4), 1433–1440. https://doi.org/10.1016/J.APENERGY.2009.08.040

Akbari, M. H., Riahi, P., & Roohi, R. (2009). Lean flammability limits for stable performance with a porous burner. *Applied Energy*, *86*(12), 2635–2643. https://doi.org/10.1016/J.APENERGY.2009.04.019

ANSYS: San Diego. (2017a). *ANSYS Chemkin-Pro Input Manual* (Issue January).

ANSYS: San Diego. (2017b). *ANSYS Chemkin-Pro Theory Manual* (Issue January).

Ansys Inc. (2021). Ansys Fluent Theory Guide. In *ANSYS Inc., USA* (Vol. 15317, Issue November).

Aste, N., Adhikari, R. S., Compostella, J., & Pero, C. Del. (2013). Energy and environmental impact of domestic heating in Italy: Evaluation of national NOx emissions. *Energy Policy*, *53*(x), 353–360. https://doi.org/10.1016/j.enpol.2012.10.064

Avci, H., Kumlutaş, D., Dutucu, M., & Kapar, A. (2015). Kombideki Isı Değiştirici Kapasitesine Tasarım Parametrelerinin Etkisi. *12. Ulusal Tesisat Mühendisliği Kongresi*, 425–437. http://www1.mmo.org.tr/resimler/dosya_ekler/ad508381377742b_ek.pdf

Bălănescu, D. T., & Homutescu, V. M. (2018). Experimental investigation on performance of a condensing boiler and economic evaluation in real operating conditions. *Applied Thermal Engineering*, *143*, 48–58. https://doi.org/10.1016/j.applthermaleng.2018.07.082

Baldi, S., Quang, T. Le, Holub, O., & Endel, P. (2017). Real-time monitoring energy efficiency and performance degradation of condensing boilers. *Energy Conversion and Management*, *136*, 329–339. https://doi.org/10.1016/J.ENCONMAN.2017.01.016

Banks, N. (2000). Socio-technical networks and the sad case of the condensing boiler. *Proceedings ACEEE Summer Study on Energy Efficiency in Buildings*, *8*, 1–12. https://doi.org/10.1007/978-3-642-56531-1_20

Basu, P., Kefa, C., & Jestin, L. (2012). *Boilers and burners: design and theory*. Springer Science & Business Media.

Baukal, C. E. J. (2003). *Industrial Burners Handbook* (Vol. 20035863). https://doi.org/10.1201/9780203488805

Bird, R. ., Stewart, E. W., & Lightfoot, N. E. (2002). *Transport Phenomena* (2nd ed.). John Wiley & Sons Inc.

Blanquart, G., Pepiot-Desjardins, P., & Pitsch, H. (2009). Chemical mechanism for high temperature combustion of engine relevant fuels with emphasis on soot precursors. *Combustion and Flame*, *156*(3), 588–607. https://doi.org/10.1016/J.COMBUSTFLAME.2008.12.007

Boggavarapu, P., Ray, B., & Ravikrishna, R. V. (2014). Thermal efficiency of LPG and PNG-fired burners: Experimental and numerical studies. *Fuel*, *116*, 709–715. https://doi.org/10.1016/j.fuel.2013.08.054

Bone, W. A., & Townend, D. T. A. (1927). *Flame and Combustion in Gases*. Longmans. https://books.google.com.tr/books?id=OQEhAAAAMAAJ

Bootsma, D., & Meijnen, A. J. (1992). Developments in Modulating Combustion Systems for Domestic Central Heating Boilers, Preprints 1992. *International Gas Research Conf., Orlando Florida*.

Boukhalfa, N. (2016). Chemical Kinetic Modeling of Methane Combustion. *Procedia Engineering*, *148*, 1130–1136.

https://doi.org/10.1016/j.proeng.2016.06.561

Bowman, C. T., Hanson, R. K., Davidson, D. F., Gardiner, W. C., Lissianski, V. V., Smith, G. P., Golden, M. D., Frenklach, M., & Goldenberg, M. (n.d.). *GRI Mech 2.11*. Retrieved November 30, 2021, from http://combustion.berkeley.edu/gri-mech/

Büyükakın, M. K. (2019). *Kare Gaz Brülör-Kazan Sistemlerinde Yanma ile Emisyon Analizleri ve Optimizasyon* (Vol. 8, Issue 5). Trakya Üniversitesi.

Çengel, Y. A., & Boles, M. A. (2015). Thermodynamics: An Engineering Approach. In *Journal of Modern Physics* (Eighth Ed.). McGraw-Hill Education.

Che, D., Liu, Y., & Gao, C. (2004). Evaluation of retrofitting a conventional natural gas fired boiler into a condensing boiler. *Energy Conversion and Management*, *45*(20), 3251–3266. https://doi.org/10.1016/j.enconman.2004.01.004

Çoban, M. T. (2015). *Numerical Thermodynamics*. Ege University. http://turhancoban.com/kitap/NUMERICAL THERMODYNAMICS.pdf

Coppalle, A., & Vervisch, P. (1983). The total emissivities of high-temperature flames. *Combustion and Flame*, *49*(1–3), 101–108. https://doi.org/10.1016/0010-2180(83)90154-2

Creighton, J. R. (2000). Dependence of CO emissions on the rate of product cooling. *Combustion and Flame*, *123*(3), 402–411. https://doi.org/10.1016/S0010-2180(00)00160-7

De Paepe, M., T'Joen, C., Huisseune, H., Van Belleghem, M., & Kessen, V. (2013). Comparison of different testing methods for gas fired domestic boiler efficiency determination. *Applied Thermal Engineering*, *50*(1), 275–281. https://doi.org/10.1016/j.applthermaleng.2012.06.027

Ding, Y., Durox, D., Darabiha, N., & Schuller, T. (2019). Chemiluminescence of Burner-Stabilized Premixed Laminar Flames. *Combustion Science and Technology*, *191*(1), 18–42. https://doi.org/10.1080/00102202.2018.1558391

Ding, Yi, Durox, D., Darabiha, N., & Schuller, T. (2019). Chemiluminescence based operating point control of domestic gas boilers with variable natural gas composition. *Applied Thermal Engineering*, *149*, 1052–1060. https://doi.org/10.1016/j.applthermaleng.2018.12.106

Dreizler, A., Pitsch, H., Scherer, V., Schulz, C., & Janicka, J. (2021). The role of combustion science and technology in low and zero impact energy transformation processes. *Applications in Energy and Combustion Science*, *7*, 100040. https://doi.org/10.1016/j.jaecs.2021.100040

EST Report CE30. (2008). *Domestic heating by gas: boiler systems*. http://bpec.org.uk/downloads/CE30 - Domestic heating by gas.pdf

European Committee for Standardization. (2003). EN 437:2018 - Test gases - Test pressures - Appliance categories- TC238. In *Official Journal of the European Union*. https://eur-lex.europa.eu/legal-content/EN/TXT/PDF/?uri=CELEX:32009L0125&from=EN

European Committee for Standardization. (2015). *EN 15502 -1:2012+A1:2015 Gas-fired heating boilers Part 1: General requirements and tests-TC109* (Issue February).

European Committee for Standardization. (2018). *EN 437:2018 - Test gases - Test pressures - Appliance categories- TC238*.

European Council. (2010). Directive 2010/75/EU Industrial Emissions. *Official Journal of the European Union*, *L334*, 17–119. https://doi.org/10.3000/17252555.L_2010.334.eng

Ferguson, C. R., & Kirkpatrick, A. T. (2016). *Internal Combustion Engines: Applied Thermosciences* (Third Ed.). Wiley & Sons Inc.

Fournel, S., Marcos, B., Godbout, S., & Heitz, M. (2015). Predicting gaseous emissions from small-scale combustion of agricultural biomass fuels. *Bioresource Technology*, *179*, 165–172. https://doi.org/10.1016/J.BIORTECH.2014.11.100

Garan, N., Dybe, S., Paschereit, C. O., & Djordjevic, N. (2023). Consistent emission correction factors applicable to novel energy carriers and conversion concepts. *Fuel*, *341*(February), 127658. https://doi.org/10.1016/j.fuel.2023.127658

Gattei, L. (2008). *A STUDY ON THE FLUID DYNAMICS OF DOMESTIC GAS BURNERS* [University of Bologna]. http://amsdottorato.unibo.it/1926/1/Lorenzo_Gattei_PhD_Thesis.pdf

Glarborg, P., Miller, J. A., Ruscic, B., & Klippenstein, S. J. (2018). Modeling nitrogen chemistry in combustion. *Progress in Energy and Combustion Science*, *67*, 31–68. https://doi.org/10.1016/j.pecs.2018.01.002

Glassmann, I., & Yetter, R. (2008). *Combustion* (4th ed.). Elsevier Inc. https://www.sciencedirect.com/science/book/9780120885732

Gonca, G. (2014). Investigation of the effects of steam injection on performance and NO emissions of a diesel engine running with ethanol–diesel blend. *Energy Conversion and Management*, *77*, 450–457. https://doi.org/10.1016/J.ENCONMAN.2013.09.031

Goodger, E. M. (1977). *Combustion calculations: theory, worked examples and problems*. Springer.

Gordon, S., & McBride, B. J. (1994). Computer Program for Calculation of Complex Chemical Equilibrium Compositions and Applications. In *NASA Reference Publication 1311* (p. 184). https://doi.org/NASA RP-1311

Gran, I. R., & Magnussen, B. F. (1996). A numerical study of a bluff-body stabilized diffusion flame. Part 2. Influence of combustion modeling and finite-rate chemistry. *Combustion Science and Technology*, *119*(1–6), 191–217. https://doi.org/10.1080/00102209608951999

Hargreaves, K. J. A., & Patterson, M. C. (1986). Advanced Combustion Systems for High Efficiency Domestic Appliance, Preprints 1986, Int. *Gas Research Conf., Toronto*.

Hassan, G., Pourkashanian, M., Ingham, D., Ma, L., & Taylor, S. (2009). Reduction in Pollutants Emissions From Domestic Boilers—Computational Fluid Dynamics Study. *Journal of Thermal Science and Engineering Applications*, *1*(1), 11007-1-11007–11009. https://doi.org/10.1115/1.3159526

Haug, J., Gebhardt, B., Weber, C., van Wees, M., Fahl, U., Adnot, J., Cauret, L., Pierru, A., Lantz, F., Bode, J.-W., Vis, J., van Wijk, A., Staniaszek, D., & Zavody, Z. (1998). Evaluation and Comparison of Utility's and Governmental DSM-Programmes for the Promotion of Condensing Boilers. In *IER Forschungsbericht. Institut für Energiewirtschaft und Rationelle Energieanwendung* (52nd ed.).

Hewson, J. C., & Bollig, M. (1996). Reduced mechanisms for NOx emissions from hydrocarbon diffusion flames. *Symposium (International) on Combustion*, *26*(2), 2171–2179. https://doi.org/10.1016/S0082-0784(96)80043-9

Hinrichs, J., Felsmann, D., Schweitzer-De Bortoli, S., Tomczak, H.-J., & Pitsch, H. (2018). Numerical and experimental investigation of pollutant formation and emissions in a full-scale cylindrical heating unit of a condensing gas boiler. *Applied Energy*, *229*, 977–989. https://doi.org/10.1016/J.APENERGY.2018.08.011

Hinrichs, J., Hellmuth, M., Meyer, F., Kruse, S., Plümke, M., & Pitsch, H. (2021). Investigation of nitric oxide formation in methane, methane/propane, and methane/hydrogen flames under condensing gas boiler conditions. *Applications in Energy and Combustion Science*, *5*, 100014. https://doi.org/10.1016/j.jaecs.2020.100014

Hinrichs, J., Schweitzer-De Bortoli, S., & Pitsch, H. (2021). 3D modeling framework and investigation of pollutant formation in a condensing gas boiler. *Fuel*, *300*, 120916. https://doi.org/10.1016/j.fuel.2021.120916

Hou, S. S., Lee, C. Y., & Lin, T. H. (2007). Efficiency and emissions of a new domestic gas burner with a swirling flame. *Energy Conversion and Management*, *48*(5), 1401–1410. https://doi.org/10.1016/j.enconman.2006.12.001

Hu, E., Li, X., Meng, X., Chen, Y., Cheng, Y., Xie, Y., & Huang, Z. (2015). Laminar flame speeds and ignition delay times of methane-air mixtures at elevated temperatures and pressures. *Fuel*, *158*, 1–10. https://doi.org/10.1016/j.fuel.2015.05.010

Jackson, R. (2012). Design of Atmospheric Gas Burners. In *PDH Center*. https://pdhonline.com/courses/m367/m367content.pd

Jannemann, T. (1996). *Kompendium Gas Brennwerttechnik* (Second Ed.). Vulkan-Verlag.

Jatoliya, A., Pandian, B., & Raghavan, V. (2012). Experimental Study of Pre-mixed Flames on a Multi-Hole Matrix Burner. *International Journal of Integrated Engineering*, *4*(1), 1–5.

Jones, H. R. . (1989). *The Application of Combustion Principles to Domestic Gas Burner Design*. British Gas plc.

Kadam, A. R., Parida, R. K., Hindasageri, V., & Kumar, G. N. (2019). Heat transfer distribution of premixed methane-air laminar flame jets impinging on ribbed surfaces. *Applied Thermal Engineering*, *163*, 114352. https://doi.org/10.1016/J.APPLTHERMALENG.2019.114352

Kayadelen, H. K. (2017). Effect of natural gas components on its flame temperature, equilibrium combustion products and thermodynamic properties. *Journal of Natural Gas Science and Engineering*, *45*, 456–473. https://doi.org/10.1016/J.JNGSE.2017.05.023

Kayadelen, H. K., & Ust, Y. (2013). Prediction of equilibrium products and thermodynamic properties in H 2O injected combustion for CαH βOγNδ type fuels. *Fuel*, *113*(x), 389–401. https://doi.org/10.1016/j.fuel.2013.05.095

Kee, R.J., Miller, J. A., & Jefferson, T, H. (1980). CHEMKIN; A General-Purpose, Problem-Independent, Transportable, Fortran Chemical Kinetics Code Package. In *Sandia Laboratries Report* (Issues SAND80-8003). https://inis.iaea.org/search/search.aspx?orig_q=RN:11548068

Kee, Robert J., Rupley, F. M., & Miller, J. A. (1989). *CHEMKIN-II: A FORTRAN CHEMICAL KINETICS PACKAGE FOR THE ANALYSIS OF GAS-PHASE CHEMICAL KINETICS* (Issue September).

Keramiotis, C., Stelzner, B., Trimis, D., & Founti, M. (2012). Porous burners for low emission combustion: An experimental investigation. *Energy*, *45*(1), 213–219. https://doi.org/10.1016/J.ENERGY.2011.12.006

Kirk, W. B. (1974). Current Activity in Appliance Design. *Proc. 3rd Conf. on Natural Gas Research and Technology, Dallas*.

Kökkülünk, G., Gonca, G., Ayhan, V., Cesur, İ., & Parlak, A. (2013). Theoretical and experimental investigation of diesel engine with steam injection system on performance and emission parameters. *Applied Thermal Engineering*, *54*(1), 161–170. https://doi.org/10.1016/J.APPLTHERMALENG.2013.01.034

Konnov, A. A., Mohammad, A., Kishore, V. R., Kim, N. Il, Prathap, C., & Kumar, S. (2018). A comprehensive review of measurements and data analysis of laminar burning velocities for various fuel+air mixtures. *Progress in Energy and Combustion Science*, *68*, 197–267. https://doi.org/10.1016/J.PECS.2018.05.003

Kuntikana, P., & Prabhu, S. V. (2018). Heat transfer investigations on impinging flame jets of a multi-port convex burner. *Applied Thermal Engineering*, *142*, 793–814. https://doi.org/10.1016/j.applthermaleng.2018.07.028

Kuo, K. (2005). *Principles of Combustion*. Wiley & Sons Inc.

Lamioni, R., Bronzoni, C., Folli, M., Tognotti, L., & Galletti, C. (2022a). Effect of slit pattern on the structure of premixed flames issuing from perforated burners in domestic condensing boilers. *Combustion Theory and Modelling*. https://doi.org/10.1080/13647830.2022.2157753

Lamioni, R., Bronzoni, C., Folli, M., Tognotti, L., & Galletti, C. (2022b). Feeding H2-admixtures to domestic condensing boilers: Numerical simulations of combustion and pollutant formation in multi-hole burners. *Applied Energy*, *309*(December 2021), 118379. https://doi.org/10.1016/j.apenergy.2021.118379

Lamioni, R., Bronzoni, C., Folli, M., Tognotti, L., & Galletti, C. (2023). Impact of H2-enriched natural gas on pollutant emissions from domestic condensing boilers: numerical simulations of the combustion chamber. *International Journal of Hydrogen Energy*, *xxxx*. https://doi.org/10.1016/j.ijhydene.2023.02.040

Law, C. K. (2006). Combustion physics. In *Combustion Physics* (Vol. 9780521870). Cambridge Univ Press. https://doi.org/10.1017/CBO9780511754517

Law, C. K. (2007). Combustion at a crossroads: Status and prospects. *Proceedings of the Combustion Institute*, *31 I*(1), 1–29. https://doi.org/10.1016/j.proci.2006.08.124

Lee, P. H., & Hwang, S. S. (2013). Formation of Lean Premixed Surface Flame Using Porous Baffle Plate and Flame Holder. *Journal of Thermal Science and Technology*, *8*(1), 178–189. https://doi.org/10.1299/jtst.8.178

Lee, S., Kim, J.-M., Kum, S.-M., & Lee, C.-E. (2010). Suggestion on the Simultaneous Reduction Method of CO and NO x in Premixed Flames for a Compact Heat Exchanger. *Energy & Fuels*, *24*(2), 821–827. https://doi.org/10.1021/ef9008554

Lee, S., Kum, S.-M., & Lee, C.-E. (2011a). Performances of a heat exchanger and pilot boiler for the development of a condensing gas boiler. *Energy*, *36*(7), 3945–3951. https://doi.org/10.1016/J.ENERGY.2011.05.018

Lee, S., Kum, S.-M. M., & Lee, C.-E. E. (2011b). An experimental study of a cylindrical multi-hole premixed burner for the development of a condensing gas boiler. *Energy*, *36*(7), 4150–4157. https://doi.org/10.1016/j.energy.2011.04.029

Lefort, B., El Bakali, A., Gasnot, L., & Pauwels, J. F. (2017). Experimental and numerical investigation of low-pressure laminar premixed synthetic natural gas flames in rich conditions. *Fuel*, *189*, 210–237. https://doi.org/10.1016/j.fuel.2016.10.043

Li, X., Grace, J. ., Watkinson, A. ., Lim, C. ., & Ergüdenler, A. (2001). Equilibrium modeling of gasification: a free energy minimization approach and its application

to a circulating fluidized bed coal gasifier. *Fuel*, *80*(2), 195–207. https://doi.org/10.1016/S0016-2361(00)00074-0

Liu, F., Zheng, L., Zhang, R., Yan, A., & Shao, M. (2020). Performance and emissions of pre-mixed and post-mixed combustion systems with a casting aluminum-silicon alloy (CASA) condensing gas boiler. *Heat and Mass Transfer*, *56*(2), 651–662. https://doi.org/10.1007/s00231-019-02708-9

Magnussen, B. F. (1981, January 12). On the structure of turbulence and a generalized eddy dissipation concept for chemical reaction in turbulent flow. *19th Aerospace Sciences Meeting*. https://doi.org/10.2514/6.1981-42

Magnussen, B. F., & Hjertager, B. H. (1977). On mathematical modeling of turbulent combustion with special emphasis on soot formation and combustion. *Symposium (International) on Combustion*, *16*(1), 719–729. https://doi.org/10.1016/S0082-0784(77)80366-4

Malalasekera, W., & Versteeg, H. K. (2007). *An Introduction to Computational Fluid Dynamics: Vol. M*. https://doi.org/10.2514/1.22547

Marcus, R. A. (2002). A Century of Chemical Dynamics Traced through the Nobel Prizes. *Journal of Chemical Education*, *79*(9).

Mathworks. (2019). *MATLAB Primer*. Mathworks Inc.

McAllister, S. (2011). *Fundamentals of Combustion Processes*. Springer. https://doi.org/10.1007/978-1-4419-7943-8

McBride, B. J., Zehe, M. J., & Gordon, S. (2002). NASA Glenn coefficients for calculating thermodynamic properties of individual species: National Aeronautics and Space Administration. *John H. Glenn Research Center at Lewis Field*, *September*. https://ntrs.nasa.gov/search.jsp?R=20020085330

Mechanical and Aerospace Engineering (Combustion Research). (2001). *San Diego Mechanism, Chemical-Kinetic Mechanisms for Combustion Applications*. University of California at San Diego.

https://web.eng.ucsd.edu/mae/groups/combustion/mechanism.html

Mitchell, P. (2008). *Central heating, installation, maintenance and repair*. WritersPrintShop.

Mlonka-Mędrala, A., Evangelopoulos, P., Sieradzka, M., Zajemska, M., & Magdziarz, A. (2021). Pyrolysis of agricultural waste biomass towards production of gas fuel and high-quality char: Experimental and numerical investigations. *Fuel*, *296*, 120611. https://doi.org/10.1016/j.fuel.2021.120611

Mohr, M., Klančišar, M., Schloen, T., Samec, N., & Kokalj, F. (2018). Numerical analysis of a non-steady state phenomenon during the ignition process in a condensing boiler. *Energy*, *158*, 623–631. https://doi.org/10.1016/J.ENERGY.2018.06.038

Nabi, M. N. (2010). Theoretical investigation of engine thermal efficiency, adiabatic flame temperature, NOxemission and combustion-related parameters for different oxygenated fuels. *Applied Thermal Engineering*, *30*(8–9), 839–844. https://doi.org/10.1016/j.applthermaleng.2009.12.015

Najarnikoo, M., Targhi, M. Z., & Pasdarshahri, H. (2019). Experimental study on the flame stability and color characterization of cylindrical premixed perforated burner of condensing boiler by image processing method. *Energy*, *189*, 116130. https://doi.org/10.1016/J.ENERGY.2019.116130

Naslund, M. (1997). *On the Design of Residential Condensing Gas Boilers*. Lund Institute of Technology.

Nemitallah, M. A., Abdelhafez, A. A., Ali, A., Mansir, I., & Habib, M. A. (2019). Frontiers in combustion techniques and burner designs for emissions control and CO2 capture: A review. *International Journal of Energy Research*, *43*(14), 7790–7822. https://doi.org/10.1002/er.4730

Néron, A., Lantagne, G., & Marcos, B. (2012). Computation of complex and constrained equilibria by minimization of the Gibbs free energy. *Chemical Engineering Science*, *82*, 260–271. https://doi.org/10.1016/J.CES.2012.07.041

Olesen, B. W., & de Carli, M. (2011). Calculation of the yearly energy performance of heating systems based on the European Building Energy Directive and related CEN standards. *Energy and Buildings*, *43*(5), 1040–1050. https://doi.org/10.1016/J.ENBUILD.2010.10.009

Olikara, C., & Borman, G. L. (1975). A computer program for calculating properties of equilibrium combustion products with some applications to I.C. engines. *SAE Technical Papers*. https://doi.org/10.4271/750468

Özdemir, B. (2017). Simulation of turbulent combustion in a self-aerated domestic gas oven. *Applied Thermal Engineering*, *113*, 160–169. https://doi.org/10.1016/j.applthermaleng.2016.10.205

Öztürk, S., & Eyriboyun, M. (2010). NOx formation in combustion of natural gases used in Turkey under different conditions. *Journal of Thermal Science and Technology*, *30*(2), 95–102. http://tibtd.org.tr/2010-2/95-102.pdf

Poinsot, T., Cnrs, D. V., Ecole, /, Paris, C., Edwards, Q., & One, T. H. . . (2001). *Theoretical and Numerical Combustion*.

Poinsot, T., & Veynante, D. (2005). Theoretical and Numerical Combustion. *Combustion and Flame*, 534. https://doi.org/6863 10.1016/j.combustflame.2007.07.002 S0010-2180(07)00176-9

Pope, S. B. (1997). Computationally efficient implementation of combustion chemistry using in situ adaptive tabulation. *Combustion Theory and Modelling*, *1*(1), 41–63. https://doi.org/10.1080/713665229

Rado, L. (1976). Die" Totale Energienutzung". 100% Wirkungsgrad? *Gaw Warme International*, *25*(7), 378–382.

Raghavan, V. (2016). Combustion Technology. In *WILEY Inc.* (1st ed.). John Wiley & Sons Ltd.

Rakopoulos, C. D., Hountalas, D. T., Tzanos, E. I., & Taklis, G. N. (1994). A fast algorithm for calculating the composition of diesel combustion products using 11

species chemical equilibrium scheme. *Advances in Engineering Software*, *19*(2), 109–119. https://doi.org/10.1016/0965-9978(94)90064-7

Rashidi, M. (1998). Calculation of equilibrium composition in combustion products. *Applied Thermal Engineering*, *18*(3–4), 103–109. https://doi.org/10.1016/S1359-4311(97)87533-3

Rayaprolu, K. (2009). *Boilers for Power and Process*. CRC Press.

Satyavada, H., & Baldi, S. (2018). Monitoring energy efficiency of condensing boilers via hybrid first-principle modelling and estimation. *Energy*, *142*, 121–129. https://doi.org/10.1016/J.ENERGY.2017.09.124

Schiro, F., Stoppato, A., & Benato, A. (2017). Gas fired boilers: Perspective for near future fuel composition and impact on burner design process. *E3S Web of Conferences*, *22*. https://doi.org/10.1051/e3sconf/20172200154

Schiro, F., Stoppato, A., & Benato, A. (2020). Modelling and analyzing the impact of Hydrogen Enriched Natural Gas on domestic gas boilers in a decarbonization perspective. *Carbon Resources Conversion*. https://doi.org/https://doi.org/10.1016/j.crcon.2020.08.001

Semenov, N. N. (1956). Some problems relating to chain reactions and to the theory of combustion. *Nobel Lecture*, 487–514.

Shohet, R., Kandil, M. S., Wang, Y., & McArthur, J. J. (2020). Fault detection for non-condensing boilers using simulated building automation system sensor data. *Advanced Engineering Informatics*, *46*, 101176. https://doi.org/10.1016/J.AEI.2020.101176

Sieradzka, M., Rajca, P., Zajemska, M., Mlonka-Mędrala, A., & Magdziarz, A. (2020). Prediction of gaseous products from refuse derived fuel pyrolysis using chemical modelling software - Ansys Chemkin-Pro. *Journal of Cleaner Production*, *248*, 119277. https://doi.org/10.1016/j.jclepro.2019.119277

Simic, K., T'Jollyn, I., Faes, W., Borrajo Bastero, J., Laverge, J., & De Paepe, M.

(2021). Modelling of a gas-fired heating boiler unit for residential buildings based on publicly available test data. *Energy and Buildings*, *253*, 111451. https://doi.org/10.1016/j.enbuild.2021.111451

Skjøth-Rasmussen, M. S., Holm-Christensen, O., Østberg, M., Christensen, T. S., Johannessen, T., Jensen, A. D., Glarborg, P., & Livbjerg, H. (2004). Post-processing of detailed chemical kinetic mechanisms onto CFD simulations. *Computers & Chemical Engineering*, *28*(11), 2351–2361. https://doi.org/10.1016/J.COMPCHEMENG.2004.05.001

Smith, G. P., Golden, M. D., Frenklach, M., Moriarty, N. W., Eiteneer, B., Goldenberg, M., Bowman, C. T., Hanson, R. K., Song, S., Gardiner Jr., W. C., Lissianski, V. V., & Qin, Z. (n.d.). *GRI Mech 3.0*. Retrieved August 20, 2023, from http://combustion.berkeley.edu/gri-mech/

Smith, M. L., & Stinson, K. W. (1952). *Fuels and combustion*. McGraw-Hill. file://catalog.hathitrust.org/Record/001115629

Soltanian, H., Targhi, M. Z., & Pasdarshahri, H. (2019). Chemiluminescence usage in finding optimum operating range of multi-hole burners. *Energy*, *180*, 398–404. https://doi.org/10.1016/j.energy.2019.05.104

Spach, A. F., & Stanford, H. W. (2019). *Analysis and Design of Heating, Ventilating, and Air-Conditioning Systems* (Second Ed.). CRC Press.

Spalding, D. B. (1971). Mixing and chemical reaction in steady confined turbulent flames. *Symposium (International) on Combustion*, *13*(1), 649–657. https://doi.org/10.1016/S0082-0784(71)80067-X

Specchia, S., & Toniato, G. (2009). Natural gas combustion catalysts for environmental-friendly domestic burners. *Catalysis Today*, *147*(SUPPL.), S99–S106. https://doi.org/10.1016/j.cattod.2009.07.033

Sreejith, C. C., Arun, P., & Muraleedharan, C. (2013). Thermochemical analysis of biomass gasification by Gibbs free energy minimization model - Part: I (Optimization of Pressure and Temperature). *International Journal of Green*

Energy, *10*(3), 231–256. https://doi.org/10.1080/15435075.2011.653846

Steele, G. (1985). *Central Heating: A Design and Installation Manual*. https://books.google.com/books?id=HAT9BAAAQBAJ&pgis=1

Sun, J., Zhang, Z., Liu, X., & Zheng, H. (2021). Reduced Methane Combustion Mechanism and Verification, Validation, and Accreditation (VV&A) in CFD for NO Emission Prediction. *Journal of Thermal Science*, *30*(2), 610–623. https://doi.org/10.1007/s11630-020-1321-3

Thomsen, D. D., Kuligowski, F. F., & Laurendeau, N. M. (1999). Modeling of NO formation in premixed, high-pressure methane flames. *Combustion and Flame*, *119*(3), 307–318. https://doi.org/10.1016/S0010-2180(99)00062-0

Trisjono, P., & Pitsch, H. (2017). A direct numerical simulation study on NO formation in lean premixed flames. *Proceedings of the Combustion Institute*, *36*(2), 2033–2043. https://doi.org/10.1016/j.proci.2016.06.130

Turns, S. R. (2000). An introduction to combustion: concepts and applications. In *Mc-Graw Hill* (Third Ed., Vol. 499). McGraw-Hill.

Valiev, D. M., Akkerman, V., Kuznetsov, M., Eriksson, L. E., Law, C. K., & Bychkov, V. (2013). Influence of gas compression on flame acceleration in the early stage of burning in tubes. *Combustion and Flame*, *160*(1), 97–111. https://doi.org/10.1016/j.combustflame.2012.09.002

Warnatz, J., Maas, U., & Dibble, R. W. (2006). Combustion: Physical and chemical fundamentals, modeling and simulation, experiments, pollutant formation. In *Springer-Verlag Berlin*. Springer Berlin Heidelberg. https://doi.org/10.1007/978-3-540-45363-5

Yılmaz, S., Kumlutaş, D., Yucekaya, U. A., & Cumbul, A. Y. (2021). Prediction of the equilibrium compositions in the combustion products of a domestic boiler. *Energy*, *233*, 121123. https://doi.org/10.1016/j.energy.2021.121123

Yu, B., Kum, S.-M., Lee, C.-E., & Lee, S. (2013). Combustion characteristics and

thermal efficiency for premixed porous-media types of burners. *Energy*, *53*, 343–350. https://doi.org/10.1016/J.ENERGY.2013.02.035

Zajemska, M., Musiał, D., & Poskart, A. (2014). Application of CHEMKIN and COMSOL programs in the calculations of chemical composition of natural gas combustion products. *Combustion Science and Technology*, *186*(2), 153–172. https://doi.org/10.1080/00102202.2013.854206

Zhang, K., Ghobadian, A., & Nouri, J. M. M. (2017). Comparative study of non-premixed and partially-premixed combustion simulations in a realistic Tay model combustor. *Applied Thermal Engineering*, *110*, 910–920. https://doi.org/10.1016/j.applthermaleng.2016.08.223

Zhang, T. H., Liu, F. G., & You, X. Y. (2014). Optimization of gas mixing system of premixed burner based on CFD analysis. *Energy Conversion and Management*, *85*, 131–139. https://doi.org/10.1016/j.enconman.2014.05.055

Zhao, D. F., Liu, F. G., You, X. Y., Zhang, R., Zhang, B. L., & He, G. L. (2015). Optimization of a premixed cylindrical burner for low pollutant emission. *Energy Conversion and Management*, *99*, 151–160. https://doi.org/10.1016/j.enconman.2015.04.039